CORRELATION AND DECAY OF TURBULENCE PRODUCED BY VARIOUS GRIDS IN A WIND TUNNEL

Thesis

by

Shoichi Atsumi

In Partial Fulfillment of the Requirements for the Degree of

Doctor of Philosophy in Aeronautical Engineering

California Institute of Technology

Pasadena, California

1939

TABLE OF CONTENTS

Appendix III

Appendix IV

Appendix V

INDEX TO TABLES

13. Correlation of Turbulence Produced by $1\frac{1}{2}$ in. Grid at U = 53.5 ft. per sec.

14. Decay of Turbulence Produced by 1 in. Grid at U = 29.9 ft./sec.

15. Decay of Turbulence Produced by 1 in. Grid at U = 42.25 ft./sec.

16. Decay of Turbulence Produced by 1 in. Grid at U = 59.7 ft./sec.

17. Correlation of Turbulence Produced by 1 in. Grid at U = 29.9 ft./sec.

18. Correlation of Turbulence Produced by 1 in. Grid at U = 42.25 ft./sec.

INDEX TO FIGURES

16. Variation of R_2 with Y for Different Values of $\frac{X}{M}$.
U = 38 ft./sec. Grid = $1\frac{1}{2}$ in.

17. Correlation curve at $\frac{X}{M}$ = 36.4. U = 38 ft./sec.

18. Correlation curve at $\frac{X}{M}$ = 50.85 . U = 38 ft./sec.

19. Correlation curve at $\frac{X}{M}$ = 66.4 . U = 38 ft./sec

20. Variation of L with $\frac{X}{M}$. U = 38 ft./sec.

21. R_2 vs $\frac{Y}{Y_{R_2=.2}}$. U = 38 ft./sec.

22. Variation of R_2 with Y for Different values of $\frac{X}{M}$.
U = 53.5 ft./sec. Grid = $1\frac{1}{2}$ in.

23. Correlation curve at $\frac{X}{M}$ = 34.7 . U = 53.5 ft./sec.

24. Correlation curve at $\frac{X}{M}$ = 50.85 . U = 53.5 ft./sec.

25. Correlation curve at $\frac{X}{M}$ = 66.2 . U = 53.5 ft./sec.

26. Variation of L with $\frac{X}{M}$. U = 53.5 ft./sec.

27. R_2 vs $\frac{Y}{Y_{R_2=.2}}$ U = 53.5 ft./sec.

28. Increase of the Scale of Turbulence with $\frac{X}{M}$.

28a. Superposition of Correlation Curve Taken at $\frac{X}{M}$ = 51.

29. Variation of $\frac{\lambda}{L}$ with $\frac{X}{M}$.

30. Decay of Turbulence Produced by 1 in. Grid

31. Variation of λ^2 with $\frac{X}{M}$.

32. Variation of Correlation Curve with $\frac{X}{M}$.
U = 29.9 ft./sec. Grid = 1 in.

33. Variation of Correlation Curve with $\frac{X}{M}$.
U = 42.25 ft./sec. Grid = 1 in.

INDEX TO PHOTOS

NOTATION

$A = \frac{u' \lambda^2}{\gamma L}$ = Constant.

$B = \frac{1}{u'} \frac{dL}{dt}$ = Constant.

B.P. = Barometer pressure.

f = Frequency of vibration.

I = Intensity of alternating current output.

$L = \int_o^\infty R \, dy$ = Scale of turbulence.

M = Mesh length of a grid.

R_1 = Longitudinal correlation factor.

R_2 = Transverse correlation factor.

$R = \frac{\overline{u_1 u_2}}{u^2}$.

R_c = Compensating resistance in ohms.

T = Temperature in degree Centigrade.

t = Time.

u = Velocity fluctuations.

u' = Root mean square of velocity fluctuations.

U = Mean stream velocity.

$\frac{u'}{U}$ = Intensity of turbulence.

X = Distance from a grid.

$Y = r$ = Distance between two hot wires.

$\alpha = \frac{\gamma t}{\lambda^2}$

$$-\frac{1}{\lambda^2} = \frac{1}{2}\left[\frac{d^2R_2}{dr^2}\right]_{r=o} = \left[\frac{d^2R_1}{dr^2}\right]_{r=o}$$

δ = Density of alcohol.

γ = Kinematic viscosity.

ρ = Density of air.

Δ = Amplitude of vibrations.

ACKNOWLEDGMENT

The author wishes to thank Drs. Th. de Karman and Clark Millikan for their constant interest and guidance in the experimental program, Drs. A. L. Klein and E. E. Sechler for their many helpful suggestions on the design of the apparatus, and Mr. Carl Thiele for his help in using the hot-wire anemometer

SUMMARY

There is a discrepancy between the assumptions made by Th. de Karman and G.I. Taylor in their Statistical Theory of Isotropic Turbulence. The present tests were undertaken to investigate the correlation and decay of the turbulence produced by the grids of various mesh lengths so that the assumptions in the theorys could be evaluated.

As no wind tunnel was suitable for this work, a new tunnel with 12 feet working section was built. The entrance was especially designed to maintain a uniform flow and to reduce an initial turbulence in the working section.

Three types of measurements were made:

1. Measurements were made with a hot wire anemometer to determine the decay of turbulence at various mean speeds of air stream.

2. Traverses were made with two hot wires to determine the scale or "average eddy size" at various positions behind the grids.

3. The initial turbulence intensities of various degrees was produced upstream of the grids of various mesh lengths. Measurements were made to determine the effect of the initial turbulence on the turbulence produced by the grids.

The results of the test gave the following facts:

1. The decay of turbulence is independent of mean speeds of air stream and is proportional to the negative -5α power of $\frac{X}{M}$.

2. The scale or "average eddy size" increases downstream. The increase of the scale is proportional to the $1-5\alpha$ power of $\frac{X}{M}$.

3. The scale at a fixed point is nearly independeent of mean speeds of air stream.

4. The quantity $\frac{u'\lambda^2}{\gamma L}$ is constant.

5. $\lambda^2 = \frac{\gamma t}{\alpha} = \frac{(5+AB)}{U} \times \gamma$

6. $\frac{1}{\alpha} = 5+AB$

7. u' is proportional to $\frac{dL}{dt}$

8. The effect of a small amount of large scale turbulence on turbulence produced by the grids was negligible.

INTRODUCTION

Turbulence involves in many engineering problems concerning a motion of fluid, namely motion of a body, dissipation of energy, mixing, evaporation, and heat transfer, yet complete solutions of these problems can only be achieved by solving first the mechanism of turbulence itself. Unfortunately the mechanism of turbulence is extremely complicated in its nature so that the mathematical treatment is very difficult. However, in recent years it became the focus of the fluid dynamicists to solve statistically the problem of isotropic turbulence.

It has been known that when air flows past a grid, a considerable amount of vortices is formed in the wake of the wires or rods of the grid and is carried downstream. At sufficiently far downstream the regular character of the vortices disappears due to the mixing and intermingling of the vortices, and velocity and velocity fluctuations appear to be uniformly distributed over the cross section of the stream. In this field of fluctuating velocity, the velocity fluctuations are statistically the same at every point over the cross section of the stream; in other words, the root mean square of the velocity

fluctuations is independent of a direction over the cross section. If an observer moves with the mean air stream, the velocity fluctuations are the same regardless of directions over the whole cross section of the stream. This type of turbulent motion is called "isotropic turbulence."

In the field of isotropic turbulence exists a definite correlation between two points separated by a known distance. Correlation factor is defined as $R_{1,2} = \frac{\overline{u_1 u_2}}{u^2}$ where R_1 is called the longitudinal correlation factor, while R_2 the transverse correlation factor, and u_1 and u_2 are velocity fluctuations. Correlation factor between two points is then a function of the distance separating them, and is a unity when two points coincide each other, and is zero when the distance is far apart so that no relation between two points exists. Correlation factor between two points in a turbulent flow can be obtained by means of a hot wire anemometer. In a strict sense, correlation factor between two short and parallel lines instead of two points is measured by means of a hot wire anemometer, since each hot wire has a finite length.

The correlation curves correspond fairly well to the error law. The width of each correlation curve gives

an idea of the average size of the eddies. Hence the comparison of correlation curves observed under different conditions give a relative measure of the "physical size" of the eddies. The average size of the eddies in the stream is called the scale of turbulence.

Statistical theories of isotropic turbulence were developed independently by G.I. Taylor, Th. de Karman, and H.L. Dryden with their own assumptions, yet a complete experimental proof of the assumptions has been lacking because of the difficulties involving in building an accurate measuring apparatus and of the difficulty in experimental technique.

The author investigated the decay and scale of turbulence produced by grids in a specially constructed tunnel by means of a hot-wire anemometer so that the experimental evaluation of the assumptions made by de Karman and Taylor could be made. The results for the decay and correlation with various mean speeds of air stream as well as the equations for the decay, scale and λ were obtained. The discussion on the validity of the assumptions made by de Karman and Taylor is also included in this thesis.

DESIGN OF APPARATUS AND EQUIPMENT

When this work was started, two design problems had to be solved: a wind tunnel and a traversing mechanism which would carry hot wires for the measurements of correlation of turbulence. A great deal of thought was given to the design of the tunnel in order to obtain constant and uniform velocity distributions with a turbulence level as low as possible and to the design of the traversing mechanism which would not cause much air disturbance around it.

With these in mind, it was decided to build a wind tunnel of Eiffel type with the working section of 12 ft. long and the cross section approximately 20 in. square. (See Fig. 1 and for detail see Appendix 1.) To take care the acceleration of air stream in the working section because of the increase in the boundary layer thickness along the inside walls, the two side walls were made adjustable. The traversing mechanism was mounted on a pair of steel rails under the tunnel, and the upper portion of the mechanism was inserted into the working section through a slot of 2 in. wide running along the bottom wall of the tunnel. The opening of the slot was closed with a movable belt made of a shim sheet which was supported by four rollers. Hence the traversing mechanism could be moved

to any desired position along the working section of the tunnel.

In order to obtain a constant and uniform flow in the working section, the design of the entrance met a great difficulty. However, by making the entrance with a contraction ratio in area of 16 to 1 and by designing the entrance in such a way that acceleration of air flow be constant, the difficulty was overcome. (For detail see Appendix 1.) At the beginning of the entrance were placed two layers of cheese cloth which served to damp out the large eddies gave a uniform flow of very fine scale turbulence which damped out before the air reached the working section. The cheese cloth caused some loss of kinetic energy, however this loss was well compensated by obtaining a steady flow with a low turbulence level in the working section. Behind the working section was placed a diffuser into which were built the vanes which served to eliminate the rotary compenent of velocity induced by the two bladed wooden propeller. The propeller was mounted directly on the shaft of a 4 h.p. D.C. motor.

The tunnel vibrations were eliminated by separating the last portion of the tunnel, where the propeller was inserted, from the rest of the tunnel. The gap was

covered with a elastic rubber band.

The various grids listed in Table 1 were used to produce turbulence. Because of slight deviation in mesh size, a mean value of the mesh size was determined and tabulated together with the maximum deviation from the mean value. The mean mesh size was used as the length characteristic of each grid.

For the measurements of correlation, the traversing mechanism to measure accurately a distance of separation of two hot wires was built. The mechanism equipped with a symmetrical airfoil to which attached two vertically extended arms each of which served to carry a hot wire. One arm could be slid along the airfoil by means of threads rotated by a handle located below the mechanism. The mechanism was designed in such ways that the distance between two hot wires was recorded on a counter, that the airfoil could be moved vertically in the working section, and that the whole mechanism could be slid along the working section.

For measurement of the correlation and decay of turbulence was used a hot wire anemometer built by D. Knoblock and C. Thiele. (For detail see Appendix II.)

VELOCITY SURVEY

As boundary layers along the walls of the working section increase in thickness, the main stream will accelerate in that section. This condition is undesirable for the present test.

The condition necessary for the stream is to have constant and uniform velocity distributions in the whole working section, so that when a grid is inserted at the beginning of the working section, isotropic turbulence can be produced in that section.

To obtain such a condition of the stream, the side walls of the working section were carefully adjusted while the pitot survey was being done. After the walls were adjusted in place, the complete velocity surveys were made at various cross sections. The results of the survey showed that the stream was quite constant and uniform except near the walls. The results are tabulated in Table 2.

The extensive velocity surveys in the region near the airfoil of the traverse mechanism were also made by means of a pitot tube and yaw meter in order to determine a best location for the hot wires. The best location for the hot wires was found to be 1.5 in. in front of the air foil and 4 in. above the chord line of the air

foil. In that location velocity distributions were uniform, and the air velocity was two percent higher than the tunnel velocity. The inclination of the stream was negligibly small. Hence that location was chosen for the hot wires to be placed for the measurements of correlation. The length and shape of the hot-wire carrying arms were designed according to the results of the velocity survey.

INFLUENCE OF INITIAL TURBULENCE

When the test was inaugurated, no reference concerning an experimental result on a superposition of two types of turbulence having different magnitudes of intensity and scale was available. Previously G.I. Taylor* mentioned the importance of an initial turbulence on the measurements of the correlation and decay of turbulence produced by a grid, however his statement was based on his intuition and not on experimental facts. It was therefore urged to investigate this problem first.

To do the investigation, at the beginning of the working section was inserted a grid for the purpose of producing an initial turbulence, the decay of which was then measured. At some distance behind the position of the first grid, was placed a second grid alone, and the decay of turbulence produced by the second grid was measured. Finally two grids were placed at their respective positions, and the measurements were made to obtain the effect of the initial turbulence on the second. Five sets of the grids were used; namely $1\frac{1}{2}$" and #4, #1 and #3, #3 and #4, and #4 and #3.

---

* Taylor, G.I., Statistical Theory of Isotropic Turbulence, Journal of the Aeronautical Sciences, Vol. 4, No. 8, page 314, June, 1937.

The results of the tests shown in Figs. 2, 3, 4, 5, and 6, illustrated interesting phonomena:

The striking feature of the results was that when the air in a wind stream had already even a large amount of large or small scale turbulence, the effect of the initial turbulence upon the turbulence produced by the grid (referred to the second grid) was negligible, provided that the intensity of the initial turbulence was lower than that of the grid. For instance, as shown in Figs. 2 and 3 the wind stream possessed larger scale turbulence than the mesh of the turbulence producing grid, yet the initial turbulence did not affect the decay of the turbulence produced by grid. The same was ture when the wind stream already had even a large amount of small scale turbulence. (See Fig. 5.) In the case when the mesh of a grid was considerably smaller than the scale of the initial turbulence, the initial turbulence even the intensity of which was high had no effect on the turbulence produced by the grid as shown in Fig. 4. By this test it was learned that the initial turbulence decayed quickly when it struck the grid due to mixing and intermingling of the eddies, however when the airstream had a higher intensity of initial turbulence than

that of the turbulence producing grid and the scale of the initial turbulence was approximately the same order of the mesh length of the grid, a portion of the initial turbulence passed through the grid as shown in Fig. 6.

The free tunnel turbulence was found to be 0.3 of one percent which was very low compared with the initial turbulence used for the test. The scale of the free tunnel turbulence was, no doubt, very small since two layers of very fine cheese cloth were used to damp out the large eddies in front of the entrance. For this reason the author expected that the effect of the initial turbulence existed in the free wind stream on the turbulence produced by the grid was negligible, and that the results of the decay and correlation of turbulence, which mentioned later, were highly reliable.

MEASUREMENTS OF CORRELATION AND DECAY OF TURBULENCE

Main objects of the measurements were to investigate the following phenomena:

1. Variation of the scale of turbulence behind the differnet turbulence producing grids.

2. Variation of the intensity of turbulence behind the differnet grids.

3. Variation of the decay of turbulence with respect to change in a mean velocity of the stream.

4. Variation of the scale of turbulence with respect to change in a mean velocity of the stream.

For these investigations two grids namely 1.5 in. grid and 1 in. grid were individsually used to produce turbulence of different scales and intensities.

Before the measurements were begun, it was necessary to calibrate each hot wire in the calibration tunnel at an air velocity exactly the same as that in the working section of the turbulence tunnel. The hot wire and holder were vibrated by means of a cross wire suspension with the known amplitudes and frequencies so that the calibration gave the output reading corresponding to a calculable level of "artificial" turbulence. (For detail see Appendix II.)

After two hot wires were carefully calibrated so that the wires gave approximately the same output readings,

they were placed at the upper edges of the arms provided on the traversing mechanism as shown in Photo 8. The hot wires were cautiously alined paralled to each other in such a way that one wire could barely pass directly behind the other. The initial gap between the wires was made as small as possible by means of the screws provided on the arms for the adjustment of the hot wire holders. The height of the traversing mechanism were adjusted such as to place the wires in the center of the working section.

At this stage the tunnel was operated at the constant mean velocity of the air stream. The hot wires with a known distance apart were then heated by means of known electric currents. Rate of cooling of each wire was caused to change by the velocity fluctuations, hence electrical resistance of the wire was changed. The change in electrical resistance of the hot wire caused the variation in the potential drop across the wire, which was properly amplified and passed through the thermocouple and then connected to the wall type galvanometer.

The output reading on the galvanometer indicated the average intensity of the square of the alternating current output, which was proportional to the mean of

the square value of the velocity flucluations. Hence the intensity of the turbulence could be computed from the output reading and the calibration data.

When two hot wires were connected by means of a switch in such a way that the change in voltages across the wires was added, the resulting output reading, M_+, was proportional to the quantity $\overline{(u_1+u_2)^2}$. When they were connected so that the voltages opposed one another, the resulting output reading, M_-, was proportional to $\overline{(u_1-u_2)^2}$. Thus

$$M_+ = K\,\overline{(u_1+u_2)^2}$$

$$M_- = K\,\overline{(u_1-u_2)^2}$$

where K is a constant of proportionality.

The measurements of M_+s and M_-s were made until the value for M_- exceeded the value for M_+ as the distance between the hot wires increased. By obtaining these values, correlation factor as a function of the distance could be computed by the relation,

$$R_z = \frac{M_+ - M_-}{M_+ + M_-} = \frac{\overline{u_1 u_2}}{u^2}$$

from which a correlation curve could be obtained.

A series of tests was repeated with the hot wire traversing mechanism being moved to various sections in the working section and then the mean velocity of the air stream being varied.

The results of the test are given in Tables 11abc, 12abc, and 13abc, and Figs. 10, 11, 12, 13, 16, 17, 18, 19, 22, 23, 24, and 25.

The measurements for the decay of turbulence were made by moving the hot wire along the longitudinal axis of the working section at the air speed corresponding to that of the correlation test. The hot wire holder was placed at the edge of a long arm especially made for the decay test. The results of the test were plotted against $\frac{X}{M}$ as shown in Figs. 7 and 30.

Among the features to be noted are: first, the decay of turbulence is not depended on varying U and, second, the width of the correlation curve increases down stream.

The absence of experimental point at the top of the correlation curves is due to two reasons: first, the initial gap between two hot wires was given to allow one hot wire move directly behind the other and, second, the hot wires introduced a mutual interference when the distance between them became short.

RESULTS AND DISCUSSION

The measurements of the decay of turbulence showed that $\frac{u'}{U}$ was independent of U and that $\frac{U}{u'}$ curves were proportional to some power of $\frac{X}{M}$. In this respect the measurements were in good agreement with those obtained by H.L. Dryden.* However, the measurements of the scale of turbulence taken by the author gave for the first time enough experimental evidences which could evaluate the assumptions in the theorys developed independently by G.I. Taylor and Th. de Karman.

The author was first concerned to evalute properly the foundamental equation for the decay of turbulence,

$$\frac{d\overline{u^2}}{dt} = -10 \frac{\nu \overline{u^2}}{\lambda^2} \quad \text{.....(1)}$$

From this equation λ^2 was solved. (For detail see Appendix IV.) The values for λ^2 was then computed from the decay curves which are shown in Figs. 7 and 30. and the computed λ^2s were plotted in Figs. 8 and 31. The evidences showed that λ^2 at a given U increased linearly with $\frac{X}{M}$ and that the increase of λ^2 was proportional to $U^{-\frac{1}{2}}$. Since the λ^2 curves were linear with $\frac{X}{M}$, the

---

* Dryden, H.L., "Measurements of Intensity and Scale of Wind Tunnel Turbulence and Their Relation to the Critical Reynolds Number of Spheres" N.A.C.A. Report No. 581.

values for $\frac{U\lambda^2}{\gamma X}$ could be computed. The result of the computation gave that $\frac{U\lambda^2}{\gamma X}$ was a constant which was designated by α. (For detail see Appendix III under "Calculation of $\frac{1}{\alpha}$.") It enabled then to obtain the equation for the decay in a form given by

$$\frac{u'}{U} = \frac{1}{C}\left(\frac{X}{M}\right)^{-5\alpha} \qquad \text{.....(2)}$$

where C is a constant. This equation was evaluated with the measured $\frac{u'}{U}$ and α. The result showed that the computed values were the same within the experimental accuracy, thus the equation (2) was proved to be satisfactory. (See Appendix III.) Therefore, the experimental results of the decay of turbulence definitely proved de Karman's assumptions that λ^2 increases proportional to the time and that $\frac{u'}{U}$ is proportional to negative 5α power of $\frac{X}{M}$.

G.I. Taylor's statement,* "The linear law for the decay can only be applied when a very definite scale can be ascribed to the turbulence. If the air in a wind stream has already a small amount of large scale turbulence when it strikes a screen of small mesh the linear law could not be expected to apply," is not fully affirmed

---

* Taylor, G.I. Statistical Theory of Isotropic Turbulence, Journal of Aeronautical Sciences, Vol. 4, No.8, Page 314, June, 1937.

by the author because the extensive research on the superposition of two types of turbulence showed that the effect of a small amount of large scale turbulence upon the turbulence produced by grids of small mesh was negligible. As was learned later, the linear law for the decay is a special case of the general equation for the decay.

The scales of the turbulence shown in Figs. 14, 20, and 26 are the graphical intergrations of the corresponding correlation curves. It was convenient to use the scale in such a form as $L = \int_0^\infty R\,dy$, which was introduced first by G.I. Taylor, because the exact "width" of each correlation curve at $R_2 = 0$ was very difficult to obtain from experiment. Among the features in the scale curves, shown in Figs. 14, 20, 26, and 28, to be noted are: first, the scale of the turbulence increases proportional to some power of X and, second, the scale is practically independent of U. The second feature agrees with that obtained by H.L. Dryden.

For the relation between u' and L, de Karman made the assumption that u' is proportional to $\frac{dL}{dt}$ so that

$$Bu' = \frac{dL}{dt} \qquad \text{.....(3)}$$

or

$$\frac{Bu'}{U} = \frac{dL}{dX}$$

where B is a constant of proportionality. The equation for L was solved after substituting equation (2) in (3). The equation thus obtained is

$$L = \frac{BC\,X^{1-5\alpha}}{1-5\alpha} \qquad \text{.....(4)}$$

where C is a constant which is the same as in the equation (2). The equation (4) was then evaluated by substituting the known quantities into the equation. (See Appendix III under "Calculation of C and B.") The result of the evaluation showed that de Karman's assumption that u' is proportional to $\frac{dL}{dt}$ gave a good agreement with the experimental fact.

It was possible at this point to evaluate the quantity

$$\frac{u'\lambda^2}{\nu L} = \text{constant A} \qquad \text{.....(5)}$$

This equation is one of important parameters which involve in the study of turbulence.

The equation (5) is held satisfactorily by both theories developed by de Karman and Taylor although their assumptions on the scale and the decay of turbulence are different. de Karman's assumption that enables to hold the equation (5) is the relationship between u' and L given in the equation (3), while Taylor's assumptions which hold the equation (5) are that the decay curve is

linear and that the scale L is constant regardless of $\frac{X}{M}$. In Taylor's case there is no relationship between u' and L.

The equations (3) and (5) were substituted in the equation (1) in order to derive the following equations:

$$\frac{U}{u'} = C_3 \frac{5+AB}{A} X^{\frac{5}{5+AB}} \quad \text{.....(6)}$$

$$L = C_1 X^{\frac{AB}{5+AB}} \quad \text{.....(7)}$$

$$\lambda^2 = \frac{5+AB}{U} \nu X \quad \text{.....(8)}$$

Comparing the equations (6) and (2) and also (7) and (4), the point of interest to be noted is that the corresponding equations are similar in their forms. The evaluations of the equations (6), (7), and (8) were then made. (For detail see Appendix III under "Calculation of L, $\frac{U}{u'}$, and λ^2 by using A and B.) The results showed that equations were completely satisfactory. The most important relationship discovered during these evaluations was that

$$\frac{1}{\alpha} = 5+AB = \frac{d \log \frac{U}{u'}}{d \left(\frac{X}{M}\right)} \quad \frac{X}{5M}$$

$$\text{or} \qquad 1-5\alpha = \frac{AB}{5+AB}$$

This relationship enabled the author to predict that the value for $\frac{1}{\alpha}$ is 5 or greater than 5 for isotropic turbulence since the value for AB never becomes negative.

Hence, the preceding results lead to conclusion that the equation (2) is identical with the equation (6), that the equation (4) is identical with the equation (7), and that the equation (8) is again identical with the equation (4) given in Appendix IV.

The point of interest was then to verify the equations (2), (4), (6), and (7) from a mathematical point of view. Since

$$\lambda^2 = \frac{5+AB}{U}\nu X = \frac{5\,M\,\nu}{U\,\dfrac{d \log \frac{U}{u'}}{d\,(\frac{X}{M})}},$$

$$\frac{d \log \frac{U}{u'}}{d\,(\frac{X}{M})} = \frac{5M}{(5+AB)\,X}$$

The integration of this equation gives

$$\frac{U}{u'} = C\,X^{\frac{5}{5+AB}} \qquad \text{.....(6a)}$$

But $\alpha = \frac{1}{5+AB}$ so that the equation (6a) becomes

$$\frac{U}{u'} = C\,X^{5\alpha} \qquad \text{.....(2)}$$

It is easily provable that the constant C in the equation (2) is the same as $C_3\frac{5+AB}{A}$ in the equation (6); therefore, the equation (2) is identical with the equation (6).

Now inserting 5+AB in place of $\frac{1}{\alpha}$ in the equation (4), the equation for L gives in the form

$$L = \frac{C_2(5+AB)}{A} X^{\frac{AB}{5+AB}}$$

But $\frac{C_2(5+AB)}{A} = C_1$, therefore

$$L = C_1 X^{\frac{AB}{5+AB}} \quad \ldots\ldots\ldots\ldots\ldots\ldots(7)$$

$$\lambda^2 = \frac{5+AB}{U} X \gamma \quad \ldots\ldots\ldots\ldots\ldots\ldots(8)$$

The equation (8) leads to conclusion that

$$\lambda^2 = \frac{\gamma t}{\alpha} \quad \ldots\ldots\ldots\ldots\ldots\ldots\ldots\ldots(9)$$

Hence all equations are consistent with one another.

The experimental evidence showed that the scale of the turbulence was nearly independent of U. (See Fig. 28.) But, as explained before, the scale definitely increased downstream from the grid, obeying the equation,

$$L = \text{const. } X^{\frac{AB}{5+AB}}$$

The superposition of three correlation curves taken at a given distance behind the 1.5 in. grid but at three different Us showed that the correlation curves

were nearly identical as shown in Fig. 28a. The curvature at the vertex of the correlation curve should have been theoretically increased as U increased, however the variation of the curvature at the vertex of the correlation curve was not obtained because of the mutual interference of two hot wires. For this reason, the curvature at the vertex of each correlation curve was drawn in such a way that the parabola which touched correlation curve met with the axis at $Y = \lambda$ where λ is calculated from the decay curve. See Figs. 11, 12, 13, 17, 18, 19, 23, 24, and 25.

The variation of the shape of the correlation curve with the increase in distance from the grid was then investigated. First, the ratios between the various widths Ys of each correlation curve and the width Y at $R_2 = .2$ were determined and, second, the ratios were plotted against the corresponding R_2 as shown in Figs. 15, 21, and 27. The striking feature of these figures is that the correlation curves are nearly the same shape, although there is very slight variation of the curvature near the vertex of the curve. The variation of the curvature near the vertex of the curve was so small that it was not well shown in the figures.

According to the experimental results, λ was proportional to $U^{-\frac{1}{2}}$ and L was constant as U varied.

Consquently $\frac{\lambda}{L}$ was proportional to $U^{\frac{1}{2}}$. The equation for $\frac{\lambda}{L}$ is

$$\frac{\lambda}{L} = C\sqrt{\frac{\nu}{\alpha U}}\, X^{5\alpha-\frac{1}{2}}$$

Since α was an order of $\frac{1}{9}$, the variation of $\frac{\lambda}{L}$ with X is very gradual as shown in Fig. 29.

Now consider the Taylor's assumptions in relation with those of de Karman. Both Taylor and de Karman made the assumption that $\frac{u'\lambda^2}{\nu L}$ = const. A, however Taylor assumed that L is a constant, while de Karman assumed that L is proportional to some power of X. These two different assumptions on L lead to an extremely interesting conclusion.

From the equation $L = \frac{u'\lambda^2}{A\nu}$, one obtains

$$L = \frac{1}{C_3}\, X^{1-\frac{5}{5+AB}} \quad \text{..... de Karman}$$

$$L = K_1 \quad \text{..... Taylor}$$

In the case of Taylor's L, AB must be zero, i.e.,

$$AB = \frac{u'\lambda^2}{\nu L}\frac{dL}{u'dt} = \frac{\lambda^2 U}{\nu L}\frac{dL}{dx} = 0$$

because $\frac{dL}{dX} = 0$ or $B = 0$.

The equations for the decay of turbulence are

$$\frac{U}{u'} = C_3 \frac{5+AB}{A} X^{\frac{5}{5+AB}} \quad \text{..... de Karman}$$

$$\frac{U}{u'} = K_2 X \quad \text{..... Taylor}$$

Solving λ^2 from the equation for the decay,

$$\frac{du'}{dt} = -5 \frac{\gamma u'}{\lambda^2} ,$$

by using Karman's $\frac{U}{u'}$, one obtains

$$\lambda^2 = \frac{(5+AB)\gamma X}{U} \quad \text{..... Karman}$$

According to Taylors

$$u' = \frac{U}{K_2 X}, \qquad U \frac{du'}{dX} = -\frac{U^2}{K_2 X^2} .$$

Putting these equation in the equation (1),

$$-\frac{U^2}{K_2 X^2} = -5 \frac{\gamma u'}{\lambda^2} = \frac{-5 \gamma U}{K_2 X \lambda^2} ,$$

$$\lambda^2 = \frac{5\gamma}{U} X \quad \text{..... Taylor}$$

Now inserting Taylor's λ^2 and L in $\frac{u' \lambda^2}{\gamma L} = A$ and solving for $\frac{u'}{U}$, one obtains

$$u' = \frac{A\gamma L}{\lambda^2} = \frac{A\gamma K_1 U}{5\gamma X} ,$$

$$\frac{u'}{U} = \frac{AK_1}{5X} = \frac{1}{K_2 X} ,$$

$$\frac{AK_1}{5} = \frac{1}{K_2}$$

where $K_1 = L$. Therefore $K_2 = \frac{5}{AL}$

Hence $\frac{U}{u'} = \frac{5}{AL} X$ ..... Taylor

Summarizing Karman's and Taylor's equations,

de Karman	Taylor
$L = \frac{1}{C_3} X^{1 - \frac{5}{5+AB}}$	$L = K_1$
$\lambda^2 = \frac{(5+AB)}{U} \gamma X$	$\lambda^2 = \frac{5\gamma}{U} X$
$\frac{U}{u'} = C_3 \frac{(5+AB)}{A} X^{\frac{5}{5+AB}}$	$\frac{U}{u'} = \frac{5}{K_1 A} X$

The comparison of the corresponding equations give definitely that the Taylor's theory is a special case of the general theory developed by de Karman.

CONCLUSION

As far as the author knows, the present investigation is the first to reveal the following facts:

1. The decay of the turbulence is proportional to the negative 5 α power of $\frac{X}{M}$.

2. The scale or "average eddy size" increases downstream. The increase of the scale is proportional to the negative 1-5 α power of $\frac{X}{M}$.

3. The scale at a fixed point is nearly independent of U.

4. The quantity of $\frac{u'\lambda^2}{\gamma L}$ is constant.

5. u' is proportional to $\frac{dL}{dt}$.

6. $\lambda^2 = \frac{\gamma t}{\alpha} = \frac{(5+AB)}{U} \gamma X$

7. $\frac{1}{\alpha} = 5+AB$ or $\alpha = \frac{1}{5} - \frac{X}{5L} \frac{dL}{dX}$

8. The effect of a small amount of initial turbulence on the decay of turbulence produced by the grids is negligible.

9. de Karman's assumptions related to (1) to (7) inclusive are completely satisfied by the experimental results.

APPENDIX I. DETAIL DESCRIPTION OF THE VARIOUS PARTS OF THE WIND TUNNEL.

ENTRANCE (See Fig. 1 and photo 1)

Three important and necessary requirements for a wind tunnel are:

(1) Constant and parallel direction of air flow.

(2) Constant and uniform velocity distributions across the working sections.

(3) Minimum amount of turbulence in air flow.

To satisfy these requirements the author found a simple method to design a proper entrance. The satisfactory way for an entrance design is to maintain airflow in such a way to have uniform acceleration. With this in mind, the ratio of air velocities at the two extreme edges of the entrance are first determined; needless to say that the ratio is the same as the contraction ratios of areas. The intermediate velocities are then obtained by a straight line variation. By using $Q = VA = \text{constant}$, the area at any section can be determined, from which the curvature is easily obtained. Q is the quantity of air, V is the velocity, and A is the cross section area.

This method was used to design the entrance. The forward end of the entrance was 80 in. by 80 in. in area and contracted to 20 in. square over the distance of 9 ft.

The inner walls were made of 22 gage galvanized steel sheets which were nailed against a number of wooden ribs and frames. Yet the surface of the walls were kept as smooth as possible. The joints of the walls were soldered together and made air tight. At the rear end of the entrance a straight plywood section 2 ft. long was added.

Two layers of cheese cloth with mesh size of about .016 in. square were placed at the beginning of the entrance in order to damp out the motion of large eddies in the incoming air.

WORKING SECTION (See Fig. 1. and photo 2)

The working section was 12 feet long with a cross section being approximately 20 in. square. The top and bottom walls consisted of .75 in. plywood stiffened by 2 in. by 4 in. lumber. Each of the side walls consisted of three plywoods 3 ft. long, the end of which being hinged together, was made adjustable in or out in order to obtain constant and uniform air flow along the working section. Each side wall was equipped with observation sindows, and was stiffened with 2 in. by 3 in. angle iron which was connected to the top and bottom walls by means of wooden screws. The bottom wall was equipped with a slot 2 in. wide along its entire length for the movement

of the traversing mechanism. The slot was closed by a shim sheet of .0005 in. thick. The sheet was rolled around four rollers of 6 in. in diameter, so it could be moved with the traversing mechanism. The whole working section was made rigid by 4 in. by 4 in. wooden columms and frames.

EXIT DIFFUSER

The exit diffuser was added to the rear end of the working section. The diffuser was built in such a way as to transform a rectangular section 20 in. by 21 in. to the cylindrical section 30 in. diameter over the distance of 5 ft. 2 in. Consideration was given for the design in order to avoid separation of air flow from the walls. It was made of 20 gauge galvanized steel sheets stiffened by angle iron and the center lines of the walls. A rectangular frame made of angle iron and an iron ring were rivetted to the extreme edges of the diffuser.

A circular cylinder 30 in. diam. was added to the rear end of the diffuser with a gap of 1 in. The cylinder was made of 16 gauge steel sheet reinforced by two steel rings at the edges of the cylinder.

A counter propeller consisted of four sheet metal vanes, placed in the cylinder, served to eliminate the

rotary component of velocity induced by the propeller.

PROPELLER AND MOTOR (See photo 4.)

The propeller consisted of two wooden blades, mounted directly on the shaft of 4 h.p. D.C. shunt motor The propeller 29 in. diameter was inserted about 5 in. into the cylinder as shown in Fig. 1.

APPENDIX II. HOT WIRE ANEMOMETER AND ELECTRICAL EQUIPMENT

The hot wire anemometer is a wire of small diameter through which is heated by passing an electric current through it. Two types of wires may be used: first, pure platinum wire of about .0005 in. in diameter and, second, Wollaston wire which is platinum wire of .0005 in. in diameter with a .0045 in silver covering. Wollaston wire is generally used for a hot wire because of two advantages: the wire is easily handled and the silver coating may be etched to obtain any desirable length of the platinum wire. The Wollaston wire is soldered to two spindles, made of sewing needles, which form the tips of the holder. The silver coating is etched away for a short length in the center of the Wollaston wire. When the hot wire is heated, velocity fluctuations cause changes in the rate of cooling of the wire, hence in its temperture and in its resistance. The resulting variations in the potential drop across the wire may then be amplified and passed through a thermocouple and applied to a wall type galvanometer which indicates the intensity of square of the alternating current output. The variation of the wires temperature is mainly affected by the component of the velocity fluctuation parallel to the direction of mean

flow, the other components producing only second order affects. If the velocity fluctuations are low, the output reading is proportional to the mean-square of the velocity fluctuations.

The instrument in this form is not applicable when velocity fluctuations become rapid because the electric current is not able to supply sufficient energy to raise the temperature of wire fast enough to correspond to the equilibrium temperature. The theoretical study of this problem shows that a sinusoidal fluctuation of frequency f has its amplitude diminished in the ratio $\frac{1}{\sqrt{1+(2\pi f)^2 M^2}}$ where M is a time constant depending on the physical properties of the wire and the mean temperature and heating at which it is operated. In order to resotre the amplitude and compensate for the lag the method adopted by D. Knoblock and C. Thiele was to insert in the amplifier circuit a voltage divider consisting of an inductance and adjustable resistance in series. The amplifier then amplifies the high frequencies more than the low frequencies. If the ratio of inductance to adjustable resistance is made equal to the time constant of the wire, a sinusoidal fluctuation of frequency f has its amplitude increased proportional to $\sqrt{1+(2\pi f)^2 M^2}$, so that with this arrangement the amplifier compensates for the lag of the wire

up to frequencies at which the unavoidable distributed capacity of the inductance begins to short circuit the voltage divider. The lower and upper frequency limit in the equipment used for the turbulence test is 5 and 8000 cycles per sec. respectively.

The maximum sensitivity of the apparatus is that $\frac{1}{10,000}$ of a volt gives full scale reading on the wall type galvanometer.

The amplifiers and input circuit for correlation amplifier are shown in Figs. 35, 36, and 37.

HOT-WIRE TECHNIQUE

The hot wire is made of .005 in. Wollaston wire which is a .0005 in. platinum wire with a .0045 in. silver covering. The wire was soldered to two spindles made of sewing needles by means of soft solder. While soldering, the spindles were pressed slighty inward so when released, the spindles sprang and gave a slight tension to the wire. The slight tension in the wire was necessary to prevent warpage of the wire when it was heated during the test. After the wire was soldered in place, about 2 mm. of silver in the center was etched off by means of a bubble of 60 percent diluted nitric acid formed at the end of a capillary tube.

For etching silver off a valuable point of technique was discovered. The best result was obtained by the aid of electric current. The Wollaston wire was connected to the positive terminal of one-volt dry cell and the negative terminal was connected to a carbon rod which was dipped into the nitric acid. When the wire was placed in the bubble of the nitric acid, electric current began to flow through the acid. Thus etching of silver was made very quickly. It took approximately two minutes to etch 2 mm. of silver by this method, while without the aid of the dry cell, it might have taken as long as two hours.

APPENDIX III

Calculation of $\lambda^2 = \dfrac{5\,M\,\gamma}{U\,\dfrac{d\,\log\frac{U}{u'}}{d\,(\frac{X}{M})}}$

$\frac{X}{M}$	$\frac{d\,\log\frac{U}{u'}}{d\,(\frac{X}{M})}$	U = 29.7 ft./sec. λ^2(sq. in.)	U = 38 ft./sec. λ^2(sq. in.)
26.09	.0220	.0221	.01736
34.10	.0164	.02965	.0233
42.10	.0131	.0372	.0292
50.06	.0110	.04425	.0347
58.10	.0095	.05125	.04025
66.08	.0084	.0579	.0455

$\frac{X}{M}$	$\frac{d\,\log\frac{U}{u'}}{d\,(\frac{X}{M})}$	U = 53.5 ft./sec. λ^2
26.09	.0220	.01250
34.10	.0164	.01676
42.10	.0131	.02100
50.06	.0110	.02500
58.10	.0095	.02896
66.08	.0084	.03270

Calculation of $\frac{1}{\alpha}$

1.5 in. grid ($\frac{1}{2}$ in. dowel)

$$\lambda^2 = \frac{\gamma}{\alpha}\frac{MX}{M}, \quad \frac{1}{\alpha} = \frac{U}{M\,\frac{X}{M}}$$

U = 29.8 ft./sec. γ = .0231 sq. in./sec.

$$\frac{1}{\alpha} = \frac{356 \quad \lambda^2}{(1.5)(.0231)\,\frac{X}{M}} = \frac{(356) \quad (.05275)}{(1.5)(.0231)(60)} = 9.025$$

U = 38 ft./sec. γ = .02322 sq. in./sec.

$$\frac{1}{\alpha} = \frac{(456) \quad (.0413)}{(1.5)(.02322)(60)} = 9.01$$

U 53.5 ft./sec. γ = .02354 sq. in./sec.

$$\frac{1}{\alpha} = \frac{(642.5) \quad (.02985)}{(1.5)(.02354\ (60)} = 9.06$$

Calculation of coefficient, C, in $\frac{U}{u'} = C \left(\frac{X}{M}\right)^{5\alpha}$

U = 29.8 ft./sec. $\qquad \frac{U}{u'} = C \left(\frac{X}{M}\right)^{.554}$

$\frac{X}{M}$	$\left(\frac{X}{M}\right)^{.554}$	$\frac{U}{u'}$ (from exp.)	C
35	7.14	37.5	5.25
40	7.71	40.3	5.23
45	8.20	43.0	5.24
50	8.70	45.5	5.23
55	9.175	48.0	5.235
60	9.63	50.5	5.24
65	10.06	52.8	5.25

Average 5.24

U = 38 ft./sec. $\qquad \frac{U}{u'} = C \left(\frac{X}{M}\right)^{.555}$

$\frac{X}{M}$	$\left(\frac{X}{M}\right)^{.555}$	$\frac{U}{u'}$ (from exp.)	C
35	7.19	37.5	5.22
40	7.76	40.3	5.2
45	8.27	43	5.2
50	8.77	45.5	5.19
55	9.25	48	5.19
60	9.72	50.5	5.2
65	10.14	52.8	5.21

Average 5.21

U = 53.5 ft./sec. $\qquad \frac{U}{u'} = C \left(\frac{X}{M}\right)^{.5425}$

$\frac{X}{M}$	$\left(\frac{X}{M}\right)^{.5425}$	$\frac{U}{u'}$ (from exp.)	C
35	7.125	37.5	5.265
40	7.675	40.3	5.260
45	8.180	43	5.260
50	8.670	45.5	5.250
55	9.160	48	5.240
60	9.600	50.5	5.265
65	10.050	52.8	5.260

Average 5.26

Calculation of Coefficient, B, in $L = \frac{BC_2 X^{1-5a}}{(1-5a)}$

1.5 in. grid ($\frac{1}{2}$ in. dowel) U = 29.8 ft./sec.

$L = B\frac{.239}{.446} X^{.446} = B(.526) X^{.446}$

$\frac{X}{M}$	X	$.526X^{.446}$	L (from exp.)	B
40.0	60	3.26	.5575	.171
46.7	70	3.495	.605	.173
53.3	80	3.71	.641	.1726
60.0	90	3.92	.670	.171
66.7	100	4.10	.695	.1695
			Average	.1714

$L = (.1714)(526) X^{.446} = .0902 X^{.446}$ .0905

U = 38 ft./sec. $L = .54 B X^{.445}$

X	$.54 X^{.445}$	L (from exp.)	B
60	3.34	.574	.172
70	3.58	.616	.172
80	3.80	.652	.1715
90	4.005	.683	.1705
100	4.19	.716	.1705
		Average	.1713

$L = .0925 X^{.445}$ .0925

U = 53.5 ft./sec. $L = .532 B X^{.445}$

X	$.532X^{.4475}$	L (from exp.)	B
60	3.316	.557	.1678
70	3.640	.600	.1650
80	3.770	.634	.1680
90	3.948	.661	.1674
100	4.175	.680	.1630
		Average	.166

$L = .08825 X^{.4475}$ .0885

Calculation of A and B

1.5 in. grid (.5 in. dowel) $U = 29.8$ ft./sec.

$A = \frac{u'\lambda^2}{\gamma L}, \quad \lambda^2 = \frac{X}{U}\frac{\gamma}{\alpha}$

$u' = (.239)\, U X^{-5\alpha}$

$L = (.1714)(.526)\, X^{1-5\alpha}$

$A = \frac{(.0902)(.446)}{.0902} = 239$ 250

$\frac{dL}{dt} = Bu' = B(.239)U\, X^{-.554} = U\frac{dL}{dX} = U\,(.0902)(.446)\, X^{-.554}$

$B = \frac{(.0902)(.446)}{.239} = .1683$

$U = 38$ ft./sec.

$u' = (.2404)\, U\, X^{-.555}$

$L = (.0925)\, X^{.445}$

$A = \frac{(.2404)(9.01)}{.0925} = 23.4$

$\frac{dL}{dt} = B\, U\, (.2404) X^{-.555} = (.0925)(.445)\, U\, X^{-.555}$

$B = \frac{(.0925)(.445)}{.2404} = .1713$

$U = 53.5$ ft./sec.

$u' = (.238)\, U\, X^{-.5525}$

$L = (.166)(.532)\, X^{.4475}$

$A = \frac{(.238)(9.06)}{(.166)(.532)} = 24.4$

$\frac{dL}{dt} = B\, U\, (.238)\, X^{-.5525} = (.116)(.532)(.4475)\, U\, X^{-.5525}$

$B = .166$

Calculation of L, $\frac{U}{u'}$, and λ^2 using A and B

$1\frac{1}{2}$ in. grid ($\frac{1}{2}$ in. dowel)

U = 29.8 ft./sec. A = 23.9 B = .1683 AB = 4.025

$L = C_1 X^{\frac{AB}{5+AB}} = C_1 X^{.446}$ $C_1 = .0902$

$\frac{U}{u'} = C_3 \frac{5+AB}{A} X^{\frac{5}{5+AB}} = C_3 \frac{9.025}{23.9} X^{.554} = .3775\, C_3 X^{.554}$ $C_3 = 11.08$

$\lambda^2 = \frac{(5+AB)\gamma X}{U} = \frac{(9.025)(.0231)}{356} X = .000586X$

U = 38 ft./sec. A = 23.4 B = .1713 AB = 4.01

$L = C_1 X^{\frac{AB}{5+AB}} = C_1 X^{.445}$ $C_1 = .0925$

$\frac{U}{u'} = C_3 \frac{5+AB}{A} X^{\frac{5}{5+AB}} = .385 C_3 X^{.555}$ $C_3 = 10.8$

$\lambda^2 = \frac{(5+AB)\gamma X}{U} = .000459X$

U = 53.5 ft./sec. A = 24.4 B = .166 AB = 4.06

$L = C_1 X^{\frac{AB}{5+AB}} = C_1 X^{.4475}$ $C_1 = .08825$

$\frac{U}{u'} = C_3 \frac{5+AB}{A} X^{\frac{5}{5+AB}} = .371 C_3 X^{.5525}$ $C_3 = 11.32$

$\lambda^2 = \frac{(5+AB)\gamma X}{U} = .000332X$

Calculation of $\lambda^2 = \dfrac{5 M \gamma}{U \dfrac{d \log \frac{U}{u}'}{d(\frac{X}{M})}}$

Grid = 1 in.

$\frac{X}{M}$	$\frac{d \log \frac{U}{u}'}{d(\frac{X}{M})}$	U = 29.9 ft./sec λ^2 (sq.in.)	U = 42.25 ft/sec. λ^2
35	3.893	.018	.01272
40	3.98	.01995	.0141
45	4.06	.0228	.01615
50	4.125	.02645	.0187
60	4.24	.03175	.0229
70	4.325	.0377	.0266
80	4.41	.0421	.0298
90	4.49	.04625	.0327

$\frac{X}{M}$	$\frac{d \log \frac{U}{u}'}{d(\frac{X}{M})}$	U = 59.7 ft./sec. λ^2
35	3.893	.01084
40	3.98	.012
45	4.06	.01375
50	4.125	.0159
60	4.24	.0191
70	4.325	.0227
80	4.41	.0253
90	4.49	.0279

Calculation of $\frac{1}{\alpha} = \frac{\nu X}{U \lambda^2}$

Grid = 1 in.

U = 29.9 ft./sec.

$$\frac{1}{\alpha} = \frac{29.9 \times 12}{.02324} \times \frac{.0445}{85} = 8.08$$

U = 42.25 ft./sec.

$$\frac{1}{\alpha} = \frac{42.25 \times 12}{.02324} \frac{.0335}{90} = 8.125$$

Calculation of C in $\frac{U}{u'} = C \left(\frac{X}{M}\right)^{5\alpha}$

Grid = 1 in.

U = 29.9 ft./sec.

$\frac{U}{u'} = C \left(\frac{X}{M}\right)^{\frac{5}{8.08}}$

$\frac{X}{M}$	$\left(\frac{X}{M}\right)^{.619}$	$\frac{U}{u'}$ (actual)	C
35	9.035	48.75	5.39
40	9.825	53.25	5.425
45	10.60	57.20	5.39
50	11.27	61.30	5.44
60	12.60	69.00	5.475
70	13.90	75.25	5.410
80	15.07	81.30	5.40
90	16.20	88.50	5.46
		Average	5.41

Calculation of B from $L = \frac{BC_2 X^{1-5\alpha}}{(1-5\alpha)}$

Grid = 1 in.

$L = B\ .485\ X^{.381}$

$\frac{X}{M}$	$.485\ X^{.381}$	L (actual)	B
40	1.98	.3525	.178
50	2.15	.383	.178
60	2.31	.412	.178
70	2.45	.436	.178
80	2.575	.456	.177
90	2.695	.476	.165
100	2.805	.495	.166
		Average	.177

$L = (.117)(.485)\ X^{.381} = .0858\ X^{.381}$

Calculation of A

Grid = 1 in.

$$A = \frac{u'\lambda^2}{\gamma L}$$

where $u' = .185\ U\ X^{-.619}$

$L = .0858\ X^{.381}$

$\lambda^2 = \frac{\gamma X}{\alpha U}$

$$A = \frac{.185 \times 8.08}{.0858} = 17.4$$

Calculation of C in $L = C_1 X^{\frac{AB}{5+AB}}$

$AB = 17.4 \times 1.77 = 3.08$

$L = C_1 X^{\frac{AB}{5+AB}} = C_1 X^{.381}$

Therefore $C_1 = .0858$

Calculation of C in $\frac{U}{u'} = \frac{5+AB}{A} C_3 X^{\frac{5}{5+AB}}$

$\frac{U}{u'} = C_3 .4645\ X^{.619} = 5.41\ X^{.619}$

Therefore $C_3 = 11.65$

Calculation of λ^2

$$\lambda^2 = \frac{(5+AB)}{U} \gamma X = .000522\ X$$

where $\gamma = .02324$ sq. in./sec.

APPENDIX IV.

EQUATION FOR DETERMINING λ^2

de Karman's equation for the decay of energy of turbulence is in the form:

$$\frac{d\overline{u^2}}{dt} = -10\gamma\frac{\overline{u^2}}{\lambda^2} \quad \text{.....(1)}$$

If the condition downstream of a grid in the wind tunnel is $t = \frac{X}{U}$,

$$\frac{d\overline{u^2}}{dt} = U\ \frac{d\overline{u^2}}{dx} = -10\gamma\frac{\overline{u^2}}{\lambda^2} \quad \text{.....(1a)}$$

or

$$U\frac{du'}{dx} = -5\gamma\frac{u'}{\lambda^2} \quad \text{.....(1a)}$$

$$\frac{1}{\lambda^2} = -\frac{U}{5\gamma u'}\frac{du'}{dx} \quad \text{.....(2)}$$

For more convenient form, let $\frac{U}{u'} = y$, then

$$\log U = \log u' + \log y$$

By differentiating with respect to X,

$$\frac{d\ \log U}{dx} = \frac{d\ \log u'}{dx} + \frac{d\ \log y}{dx}$$

But $$\frac{d\ \log U}{dx} = 0,$$

$$\frac{d\ \log u'}{dx} = -\frac{d\ \log y}{dx} \quad \text{.....(3)}$$

Substituting the equation (3) in (2),

$$\frac{1}{\lambda^2} = \frac{U}{5\gamma M}\frac{d\ \log\frac{U}{u'}}{d(\frac{X}{M})}$$

$$\lambda = \sqrt{\frac{5\,M\,\gamma}{U\,\dfrac{d\,\log\frac{U}{u'}}{d\,(\frac{X}{M})}}} \qquad \ldots\ldots\ldots\ldots\ldots(4)$$

which is the equation for λ, introduced as a length for a smallest eddy by G.I. Taylor.

EQUATION FOR DETERMINING α FOR THE DECAY OF TURBULENCE

$$\frac{d\overline{u^2}}{dt} = -10\,\gamma\,\frac{\overline{u^2}}{\lambda^2} = -10\,\frac{\overline{u^2}\,\alpha}{t} \qquad \ldots\ldots\ldots(5)$$

Hence

$$\lambda^2 = \frac{\gamma t}{\alpha} \qquad \ldots\ldots\ldots\ldots\ldots(5a)$$

$$\alpha = \frac{\gamma t}{\lambda^2} = \frac{\gamma M}{U\lambda^2}\frac{X}{M} \qquad \ldots\ldots\ldots\ldots\ldots(6)$$

EQUATION FOR $\frac{U}{u'}$

From the equation (4),

$$\frac{5\gamma M}{U\lambda^2} = \frac{d\,\log\frac{U}{u'}}{d\,(\frac{X}{M})} \qquad \ldots\ldots\ldots\ldots\ldots(7)$$

Substituting the equation (6) in (7),

$$\frac{d\,\log\frac{U}{u'}}{d\,(\frac{X}{M})} = \frac{5\alpha}{\frac{X}{M}} \qquad \ldots\ldots\ldots\ldots\ldots(8)$$

Intergrating the equation (8),

$$\frac{U}{u'} = C\,(\frac{X}{M})^{5\alpha} \qquad \ldots\ldots\ldots\ldots\ldots(9)$$

where C is a numerical constant for a given grid.

EQUATION FOR SCALE OF TURBULENCE

$\frac{dL}{dt}$ is proportional to u'

Hence $$\frac{dL}{dt} = Bu'$$

where B is a numerical constant.

From the equation (9) $$u' = C_2 U X^{-5\alpha}$$

$$\frac{dL}{dt} = BC_2 UX^{-5\alpha} = U \frac{dL}{dX} \quad \text{.....(10)}$$

$$L = \frac{BC_2}{1-5\alpha} X^{1-5\alpha} \quad \text{.....(11)}$$

where B can be determined from the measurements of L and the decay of turbulence.

POSSIBLE SOLUTION FOR LARGE REYNOLDS NUMBERS.

de Karman derived the equation for the propagation of the correlation:

$$\frac{\partial(f\bar{u}^2)}{\partial t} + 2(\bar{u}^2)^{\frac{3}{2}}\left(\frac{\partial h}{\partial r} + \frac{4h}{r}\right) = 2\nu\bar{u}^2\left(\frac{\partial^2 f}{\partial r^2} + \frac{4}{r}\frac{\partial f}{\partial r}\right) \quad \cdots\cdots (12)$$

For large Reynolds numbers the assumptions were made that the correlation functions would preserve their shapes and only their scale would charge. These assumptions mean that both f (r, t) and h (r, t) are functions of one variable $\psi = \frac{r}{L}$ only where L is a function of M and Ut.

By introducing f (ψ) and h (ψ) in equation (12) de Karman obtained the expression:

$$-\frac{df}{d\psi}\psi\frac{\bar{u}^2}{L}\frac{dL}{dt} + f\frac{d\bar{u}^2}{dt} + 2\frac{(\bar{u}^2)^{\frac{3}{2}}}{L}\left(\frac{dh}{d\psi} + \frac{4h}{\psi}\right) = 2\nu\frac{\bar{u}^2}{L^2}\left(\frac{d^2 f}{d\psi^2} + \frac{4}{\psi}\frac{df}{d\psi}\right) \cdots (13)$$

For large Reynolds number, $\frac{u'L}{\nu}$, the term of the right side vanishes.

$$\text{Hence } -\frac{df}{d\psi}\psi\frac{\bar{u}^2}{L}\frac{dL}{dt} - f\frac{10\nu\bar{u}^2}{\lambda^2} + \left(\frac{dh}{d\psi} + 4\frac{h}{\psi}\right)2\frac{(\bar{u}^2)^{\frac{3}{2}}}{L} = 0 \quad \cdots\cdots (14)$$

$$\text{or} \quad -\frac{df}{d\psi}\psi\left(\frac{1}{2u'}\frac{dL}{dt}\right) - f\left(\frac{5\nu L}{u'\lambda^2}\right) + \frac{dh}{d\psi} + 4\frac{h}{\psi} = 0$$

The equation (14) can be satisfied if the coefficients which are function of t without being functions of ψ are constants. Hence de Karman obtained the relationships:

$$\frac{u'\lambda^2}{L\nu} = A \quad \cdots\cdots\cdots\cdots\cdots (15)$$

$$\frac{dL}{dt} = Bu' \qquad \text{.....(16)}$$

where A and B are numerical constants.

By eliminating u' from the equation (15) and (16) the differential equation for L (t) is

$$L \frac{d^2L}{dt^2} = - \frac{5}{AB} \left(\frac{dL}{dt}\right)^2 \qquad \text{.....(17)}$$

or when $t = \frac{X}{U}$,

$$L \frac{d^2L}{dt^2} = - \frac{5}{AB} \left(\frac{dL}{dX}\right)^2 \qquad \text{.....(18)}$$

The solution of the equation (18) is

$$L = C X^{\frac{AB}{5+AB}} \qquad \text{.....(19)}$$

where C is a numerical constant.

Introducing the equation (19) in (16)

$$\frac{U}{u'} = C_3 \frac{5+AB}{A} X^{\frac{5}{5+AB}} \qquad \text{.....(20)}$$

Substituting the expression (20) in (1a)

$$\lambda^2 = \frac{(5+AB)}{U} \gamma X \qquad \text{.....(21)}$$

It is interesting to notice that the equations (19) and (20), and (21) with $\alpha = \frac{1}{5+AB}$ are indentical with the corresponding equations (9), (5a) and (11), for the case of small Reynolds number.

APPENDIX V. EFFECT OF HOT-WIRE LENGTH

The author investigated experimentally the effect of hot-wire length on the measurements of $\frac{u'}{U}$ at a fixed point from the grids. The hot wire from 1 to 5 mm. long were used. The results were plotted in Fig. 38. $\frac{u'}{U}$ increased to its maximum value as the wire length decreased down to about 2 mm., and the $\frac{u'}{U}$ decreased slightly as the wire length decreased to 1 mm. At the wire length of 1 mm. there existed a high temperature gradient over the wire so that it was difficult to compensate the amplifier for the lag of the wire. For this reason, it was decided to use the wire length of 2 mm. for the measurements of the correlation and decay of turbulence.

It has been known that the variation of correlation with distance across the stream makes some error in hot-wire results due to the lack of complete correlation over the length of the wire. The theoretical correlation for this effect was done by W.C. Mock, Jr.* By using Mock's correction formula, the error in the correlation readings in the present research was less than 5 percent in any case.

---

* Mock, Jr., W.C. "The Effect of Wire Length in Measurements of Intensity and Scale of Turbulence By The Hot-Wire Method." N.A.C.A. Report 581, 1937.

TABLE 1

DIMENSIONS OF GRIDS FOR PRODUCING TURBULENCE

No.	Nominal mesh length, in.	Average measured mesh length, in.	Deviation of individual meshes from average, in.	Average measured wire diameter, in.	Material
1	.50	.4956	.0156	.23	Iron wire
2	.50	.50		.105	Iron wire
3	.50	.507	.031 .035	.084	Iron wire
4	.125	.125	.006 .003	.054	Iron wire
	1.5	1.5		.50	Wooden dowel
	1.0	1.0		.25	Wooden dowel

TABLE 2

SURVEY OF DYNAMIC PRESSURE IN THE WORKING SECTION

Pos.	6 in.	4 in.	2 in.	C.L.	2 in.	4 in.	6 in.
			q (cm.) alcohol				
6 in.	4.324	4.341	4.340	4.338	4.338	4.342	4.353
5 in.	4.339	4.346	4.355	4.358	4.355	4.342	4.362
4 in.	4.345	4.360	4.355	4.358	4.355	4.360	4.362
3 in.	4.345	4.360	4.355	4.358	4.355	4.360	4.370
2 in.	4.345	4.360	4.360	4.360	4.360	4.360	4.370
1 in.	4.345	4.360	4.360	4.360	4.360	4.360	4.370
C.L.	4.345	4.360	4.360	4.360	4.360	4.360	4.370
1 in.	4.356	4.365	4.365	4.360	4.363	4.365	4.385
2 in.	4.356	4.370	4.370	4.365	4.370	4.375	4.385
3 in.	4.356	4.371	4.371	4.365	4.370	4.380	4.385
4 in.	4.367	4.384	4.389	4.380	4.384	4.386	4.392
5 in.	4.367	4.390	4.395	4.392	4.393	4.397	4.399
6 in.	4.373	4.400	4.394	4.407	4.409	4.400	4.410

Pos. = Position

C.L. = Center line

TABLE 2a

SURVEY OF DYNAMIC PRESSURE IN THE WORKING SECTION

Pos.	6 in.	4 in.	2 in.	C.L.	2 in.	4 in.	6 in.
			q (cm.) alcohol				
6 in.	4.310	4.31	4.306	4.315	4.317	4.318	4.313
5 in.	4.334		4.330	4.327	4.321		4.324
4 in.	4.337	4.335	4.340	4.340	4.336	4.335	4.333
3 in.	4.340		4.340	4.345	4.343		4.345
2 in.	4.343	4.336	4.340	4.345	4.343	4.345	4.346
1 in.	4.345		4.345	4.345	4.350		4.346
C.L.	4.355	4.340	4.340	4.350	4.350	4.350	4.350
1 in.	4.355		4.345	4.345	4.354		4.350
2 in.	4.355	4.345	4.350	4.355	4.360	4.356	4.350
3 in.	4.363		4.355	4.355	4.366		4.355
4 in.	4.365	4.356	4.365	4.365	4.366	4.362	4.360
5 in.	4.368		4.371	4.370	4.366		4.365
6 in.	4.373	4.363	4.371	4.380	4.372	4.374	4.365

Pos. = Position

C.L. = Center line

TABLE 2b

SURVEY OF DYNAMIC PRESSURE IN THE WORKING SECTION

Pos.	6 in.	4 in.	2 in.	C.L.	2 in.	4 in.	6 in.
				q (cm.) alcohol			
6 in.	4.305	4.300	4.305	4.305	4.310	4.305	4.310
5 in.	4.310	4.300	4.315	4.315	4.320	4.315	4.320
4 in.	4.320	4.305	4.315	4.320	4.320	4.320	4.330
3 in.	4.320	4.310	4.320	4.325	4.325	4.325	4.330
2 in.	4.325	4.315	4.325	4.330	4.330	4.325	4.330
1 in.	4.325	4.320	4.325	4.330	4.330	4.325	4.330
C.L.	4.325	4.320	4.330	4.330	4.330	4.325	4.330
1 in.	4.325	4.320	4.330	4.335	4.330	4.325	4.330
2 in.	4.327	4.320	4.330	4.335	4.335	4.330	4.340
3 in.	4.335	4.325	4.330	4.340	4.345	4.335	4.345
4 in.	4.340	4.330	4.335	4.340	4.350	4.340	4.350
5 in.	4.345	4.335	4.340	4.350	4.350	4.345	4.360
6 in.	4.345	4.335	4.350	4.350	4.360	4.350	4.360

C.L. = Center Line

Pos. = Position

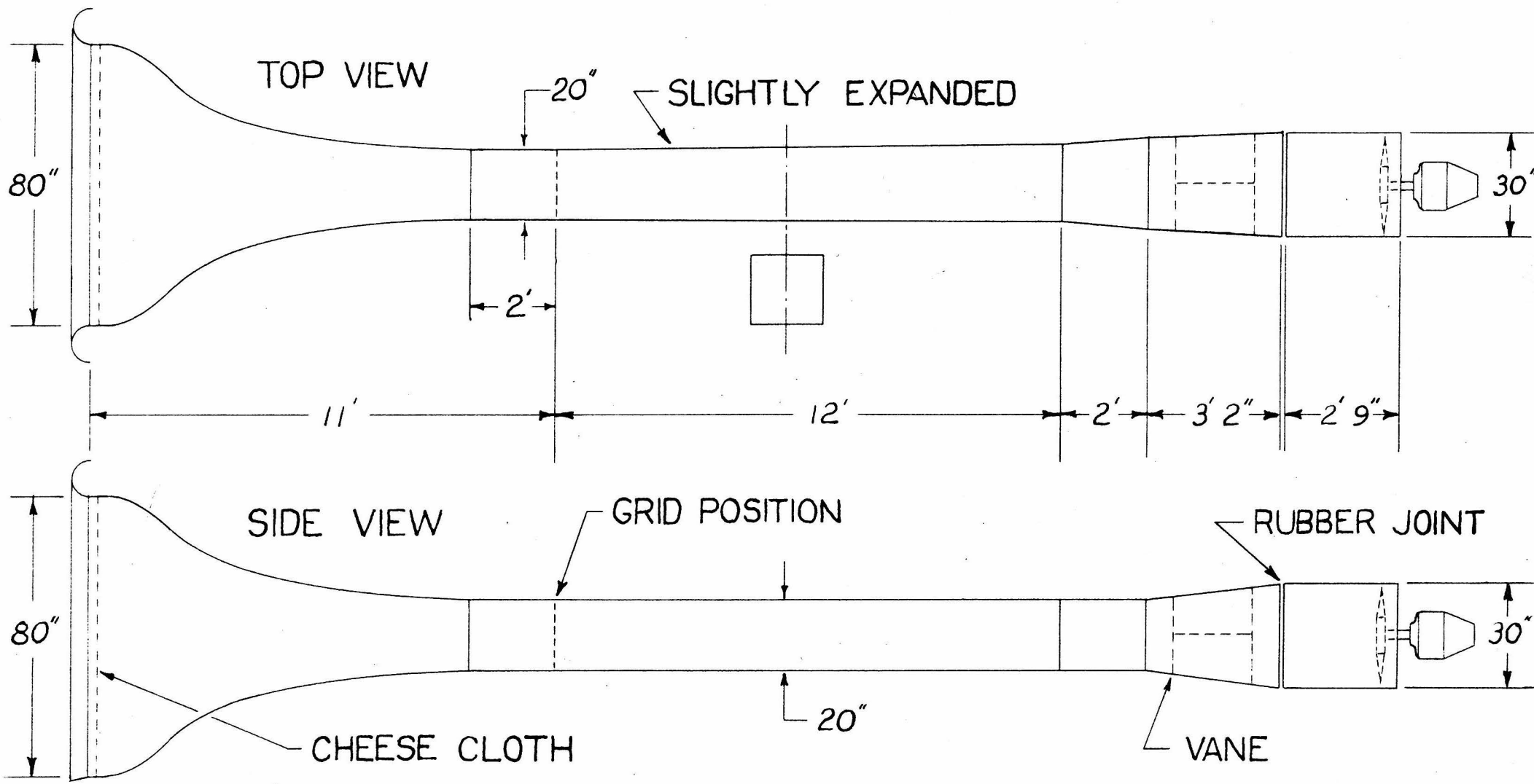

FIG. 1 SCHEMATIC DIAGRAM OF THE WIND TUNNEL

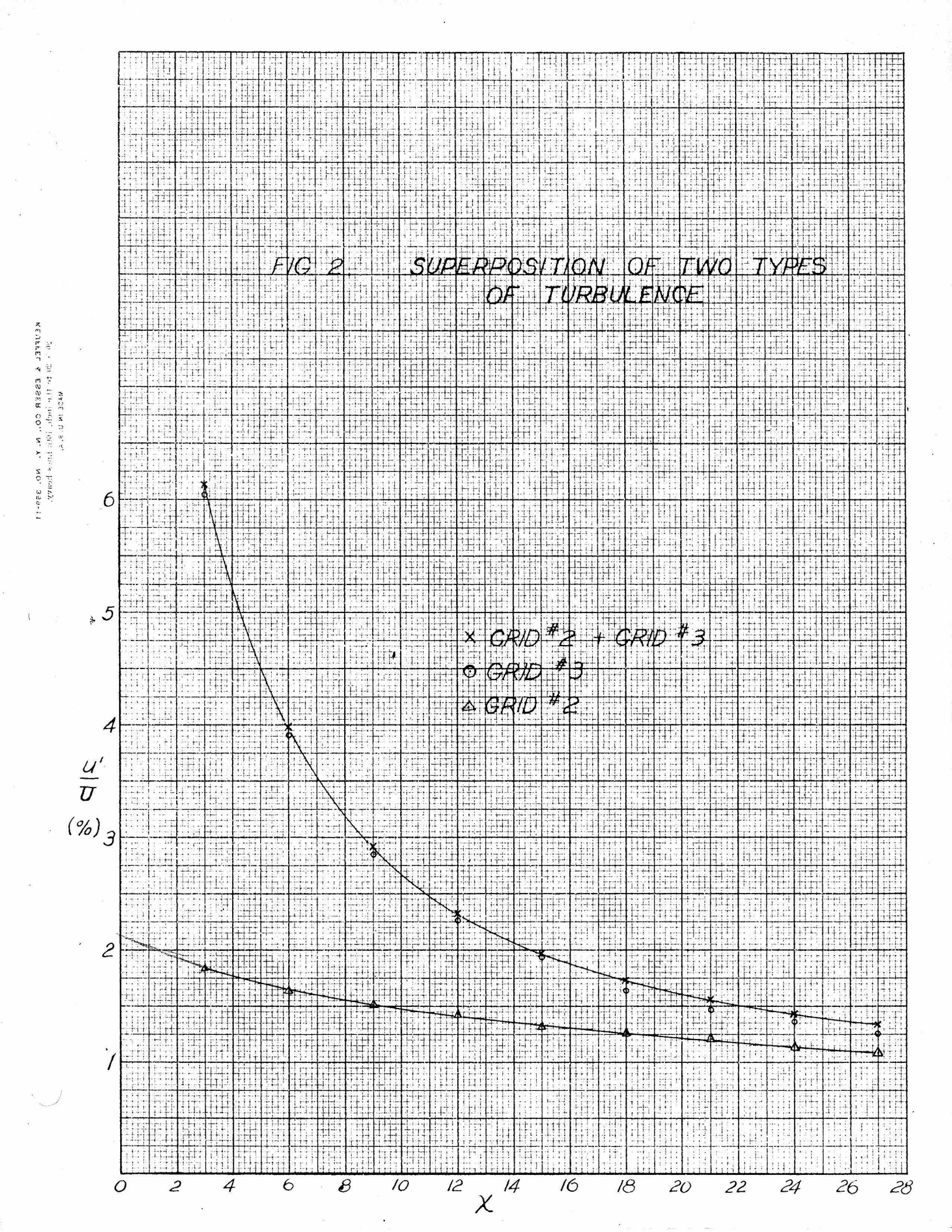
FIG 2 SUPERPOSITION OF TWO TYPES OF TURBULENCE
× GRID #2 + GRID #3
○ GRID #3
△ GRID #2
u'/U (%)
1
2
3
4
5
6
0
2
4
6
8
10
12
14
16
18
20
22
24
26
28
X

TABLE 3a

SUPERPOSITON OF TWO TYPES OF TURBULENCE

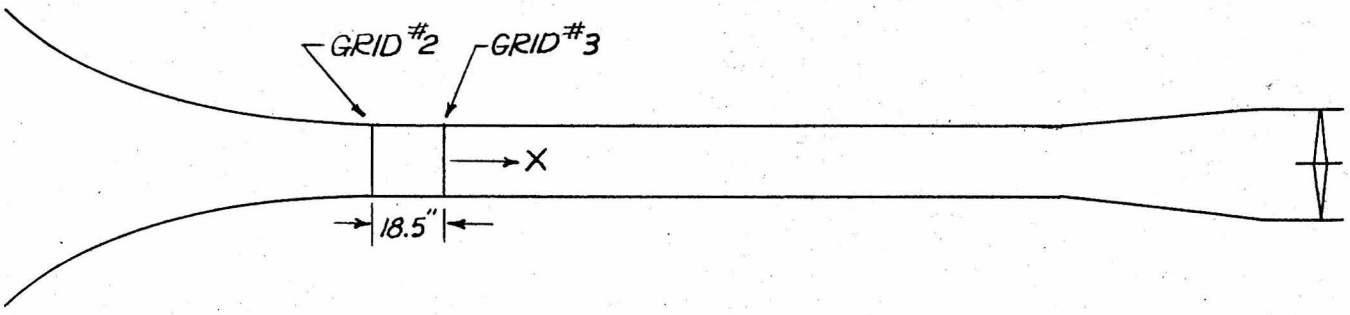

B = 745.3 mm. T = 22 deg. C. ζ=.794

H.W. length ~ 3.5 mm.(.0005 in. diam.)

X (in.)	u'/U (percent)
3	6.13
6	3.98
9	2.92
12	2.32
15	.197
18	1.73
21	1.57
24	1.44
27	1.34

TABLE 36

SUPERPOSITON OF TWO TYPES OF TURBULENCE

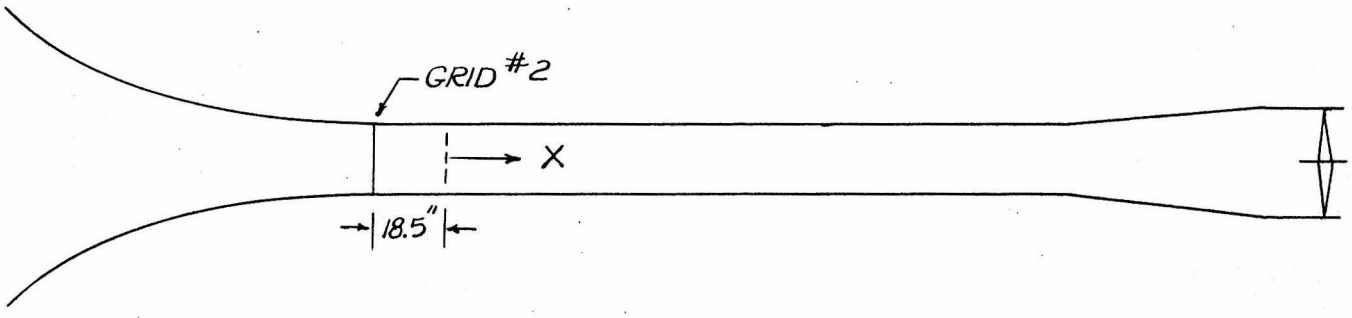

B = 745.3 mm. T = 22 deg. C. δ=.794

H.W. length ~ 3.5 mm.(.0005 in. diam.)

X (in.)	u'/U (percent)
3	1.84
6	1.63
9	1.51
12	1.43
15	1.32
18	1.27
21	1.21
24	1.13
27	1.08

TABLE 3.c

SUPERPOSITON OF TWO TYPES OF TURBULENCE

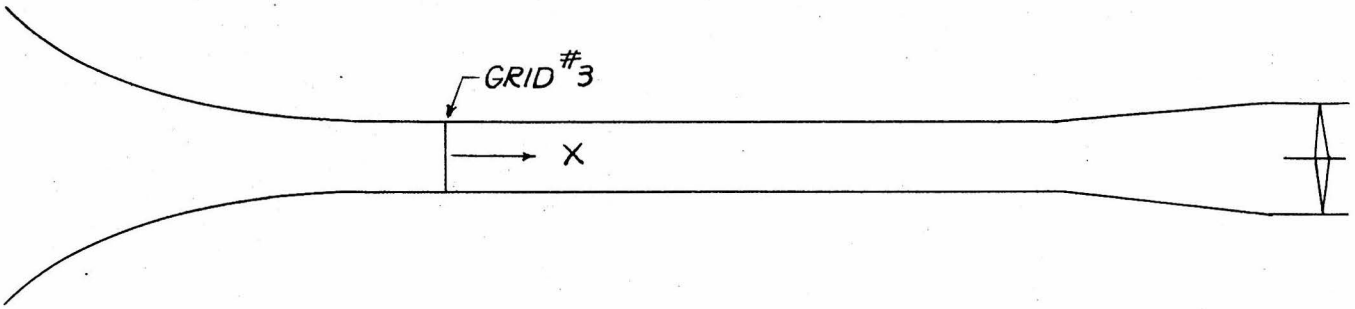

B = 745.3 mm. T = 22 deg. C. δ = .794

H.W. length ~ 3.5 mm. (.0005 in. diam.)

X (in.)	u'/U (percent)
3	6.04
6	3.91
9	2.85
12	2.26
15	1.94
18	1.64
21	1.47
24	1.36
27	1.26

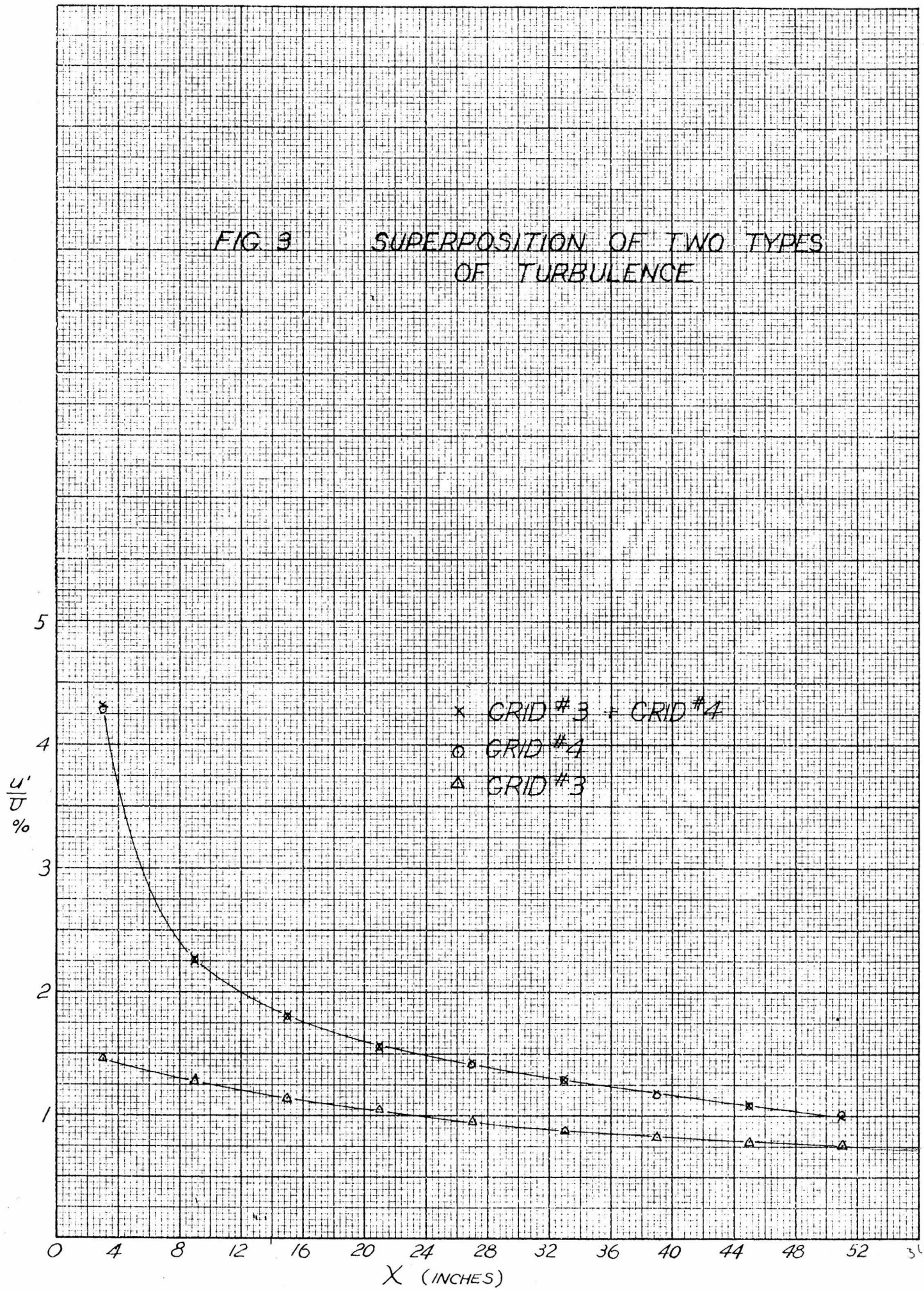
FIG. 3 SUPERPOSITION OF TWO TYPES OF TURBULENCE
× GRID #3 + GRID #4
○ GRID #4
△ GRID #3
u'/U %
5
4
3
2
1
0
4
8
12
16
20
24
28
32
36
40
44
48
52
X (INCHES)

TABLE 4a

SUPERPOSITON OF TWO TYPES OF TURBULENCE

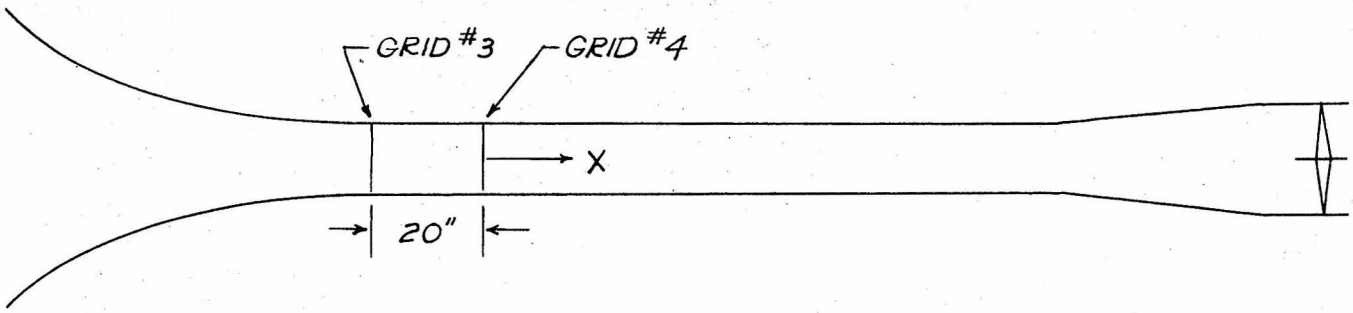

B = 744.5 mm. T = 25 deg. C. δ = .793 ρ = .118

H.W. length ~ 3 mm.(.0005 diam.) U = 11.6 m/s.

X (in.)	u'/U (percent)
3	4.31
9	2.26
15	1.81
21	1.56
27	1.44
33	1.29
39	1.19
45	1.09
51	.999

TABLE 4 b

SUPERPOSITON OF TWO TYPES OF TURBULENCE

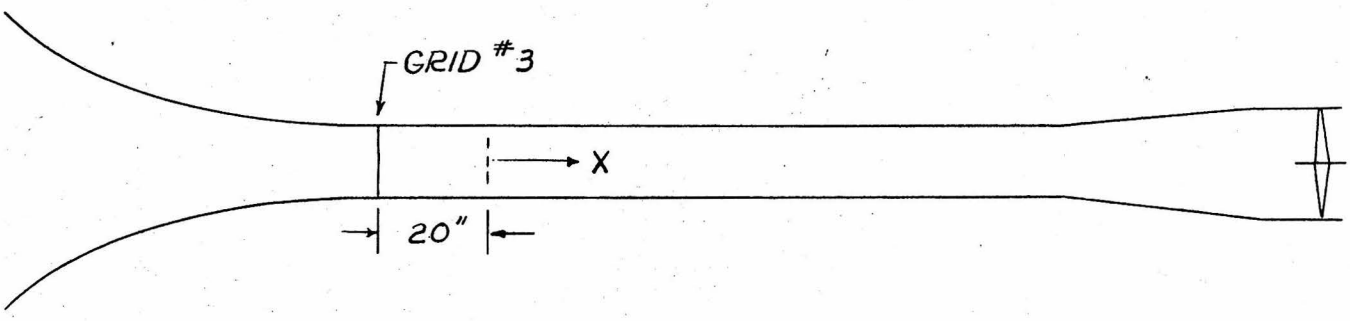

B = 744.5 mm. T = 25 deg. C. δ=.793 ρ=.118

H.W. length ~ 3 mm.(.0005 diam.) U =11.6 m/s.

X (in.)	u'/U (percent)
3	1.47
9	1.28
15	1.14
21	1.05
27	.95
33	.878
39	.828
45	.796
51	.765

TABLE 4c

SUPERPOSITON OF TWO TYPES OF TURBULENCE

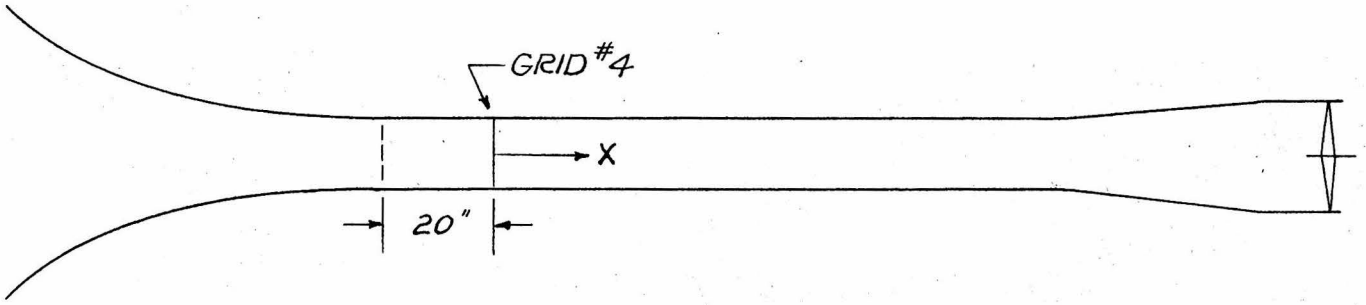

B = 744.5 mm. T = 25 deg. C. δ = .793 ρ = .118

H.W. length ~ 3 mm. (.0005 diam.) U = 11.6 m/s.

X (in.)	u'/U (percent)
3	4.28
9	2.27
15	1.81
21	1.56
27	1.41
33	1.29
39	1.17
45	1.095
51	1.02

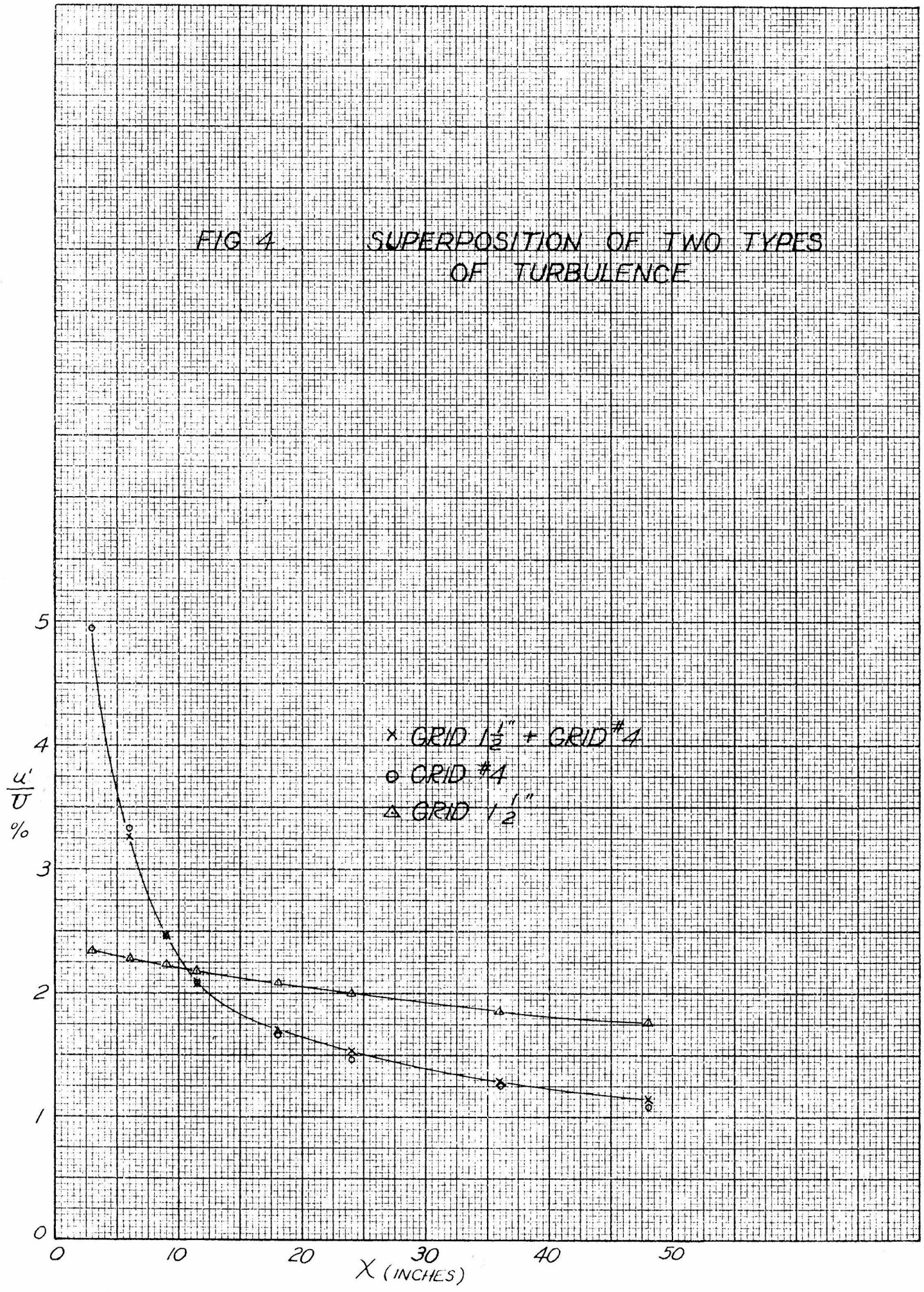
FIG 4. SUPERPOSITION OF TWO TYPES OF TURBULENCE
× GRID 1½" + GRID #4
○ GRID #4
△ GRID 1½"
u'/U %
0
1
2
3
4
5
0
10
20
30
40
50
X (INCHES)

TABLE 5a

SUPERPOSITON OF TWO TYPES OF TURBULENCE

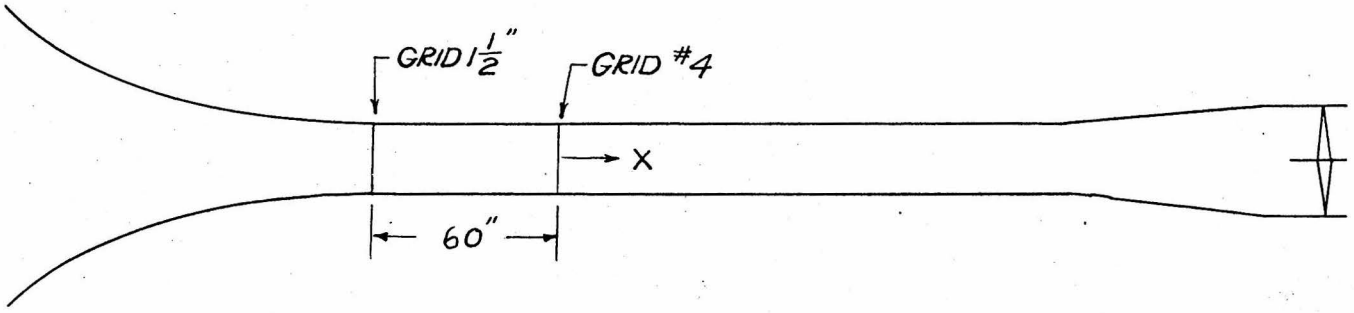

B = 746.4 T = 23.5 deg. C. δ = .795 ρ = .11875

H.W. length ~ 3 mm. (.0005 in. diam.) U = 11.56 m/s.

X (in.)	u'/U (percent)
3	4.95
6	3.26
9	2.46
12	2.09
18	1.71
24	1.54
36	1.29
48	1.15

TABLE 5b

SUPERPOSITON OF TWO TYPES OF TURBULENCE

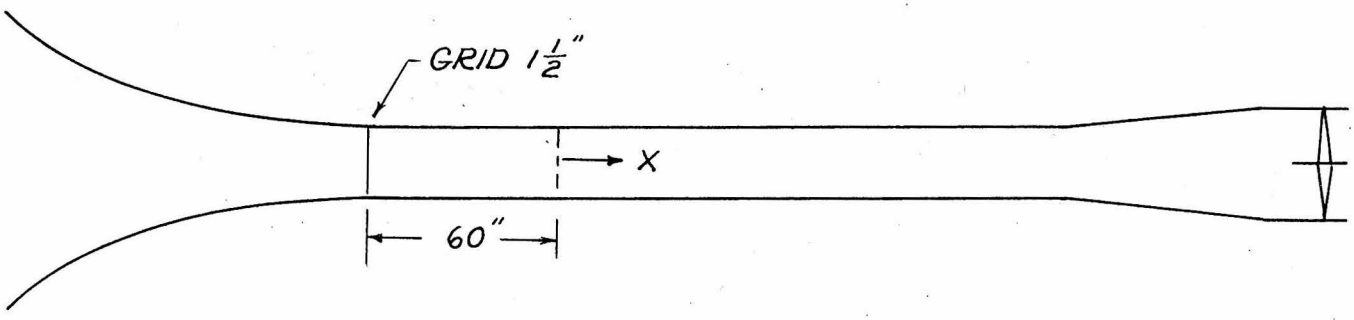

B = 746.4 T = 23.5 deg. C. δ = .795 ρ = .11875

H.W. length ~ 3 mm.(.0005 in. diam.) U = 11.56 m/s.

X (in.)	u'/U (percent)
3	2.35
6	2.28
9	2.24
12	2.18
18	2.08
24	2.00
36	1.85
48	1.77

TABLE 5c

SUPERPOSITON OF TWO TYPES OF TURBULENCE

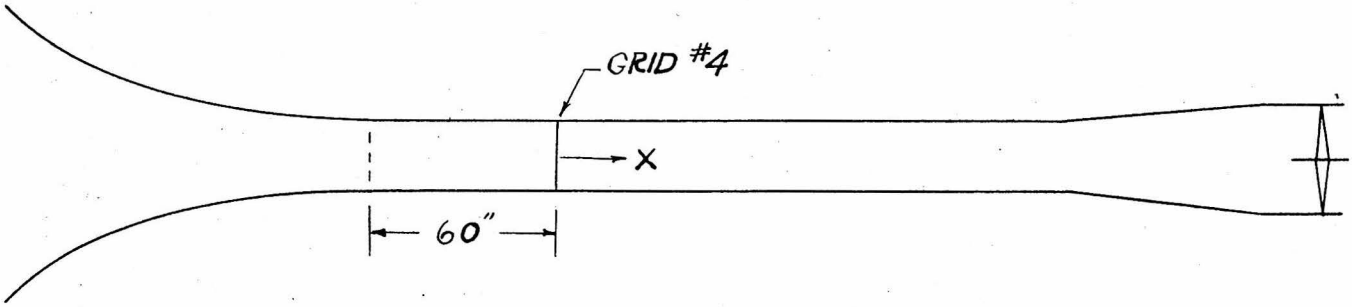

B = 746.4 T = 23.5 deg. C. δ = .795 ρ = .11875

H.W. length ~ 3 mm.(.0005 in. diam.) U 11.56 m/s.

X (in.)	u'/U (percent)
3	4.95
6	3.33
9	2.45
12	2.07
18	1.66
24	1.46
36	1.25
48	1.085

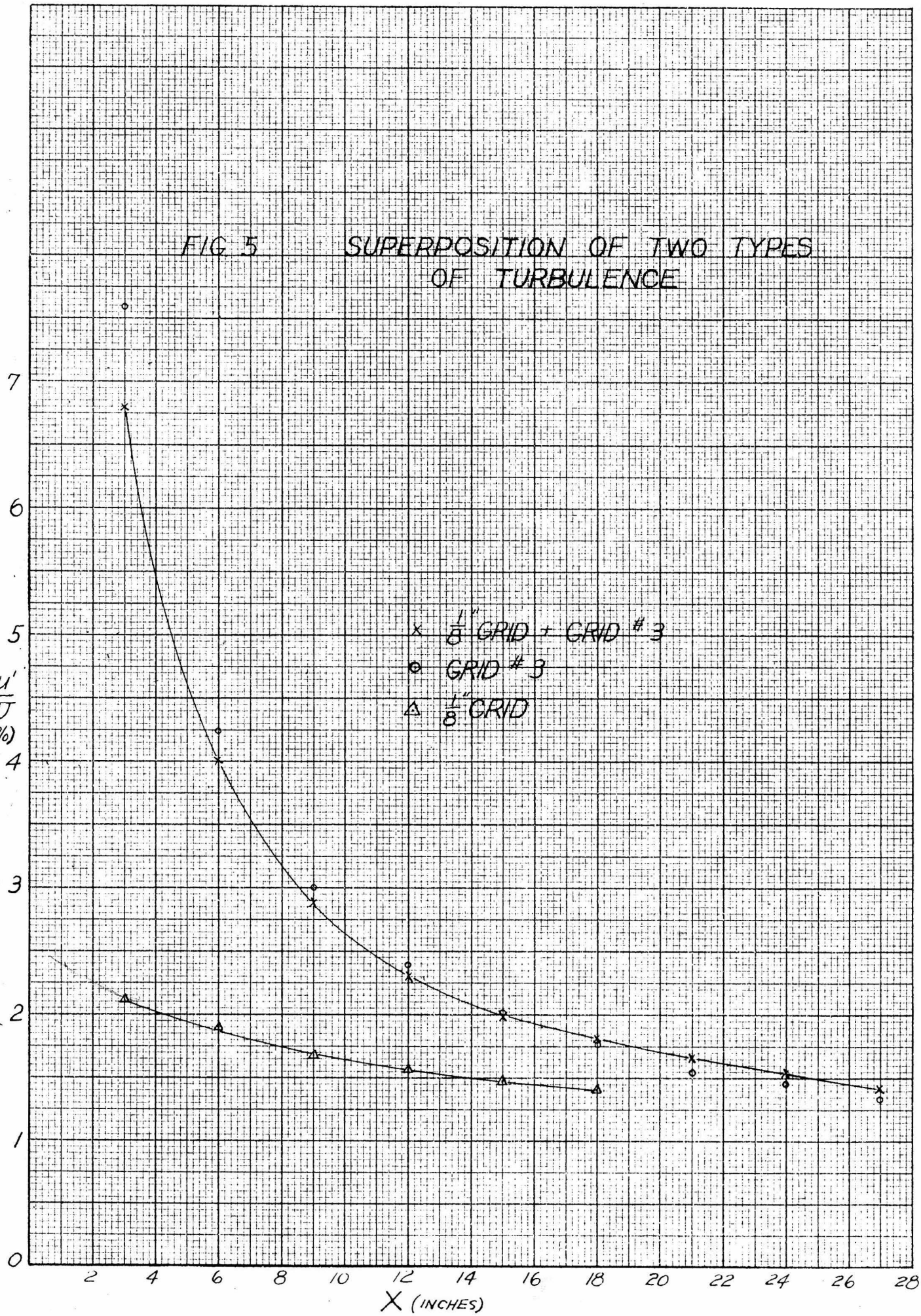
FIG 5 SUPERPOSITION OF TWO TYPES OF TURBULENCE
× 1/8" GRID + GRID # 3
⊙ GRID # 3
△ 1/8" GRID
u'/U (%)
X (INCHES)
0
1
2
3
4
5
6
7
2
4
6
8
10
12
14
16
18
20
22
24
26
28

TABLE 6a

SUPERPOSITON OF TWO TYPES OF TURBULENCE

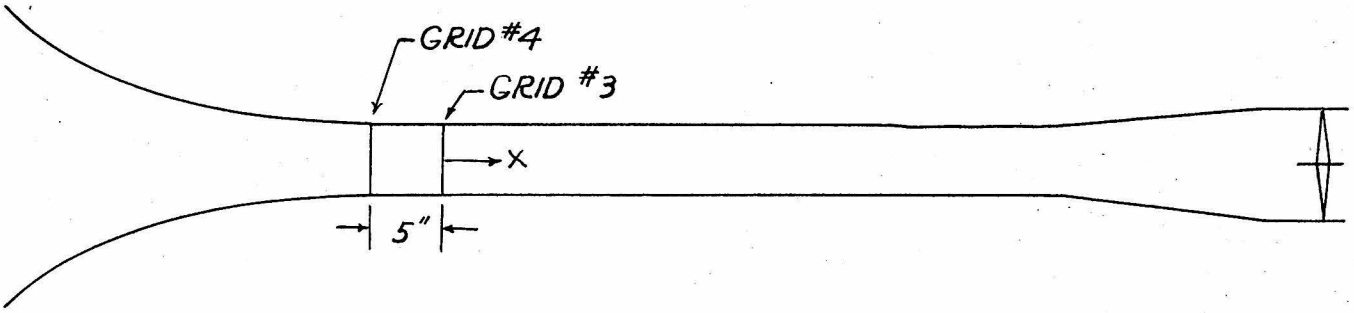

B = 742.4 mm. T = 26 deg. C. δ = .794 ρ = .117

H.W. length ~ 3 mm.(.0005 in. diam.)

X (in.)	u'/U (percent)
3	6.8
6	4
9	2.88
12	2.30
15	2
18	1.81
21	1.66
24	1.55
27	1.41

TABLE 6b

SUPERPOSITON OF TWO TYPES OF TURBULENCE

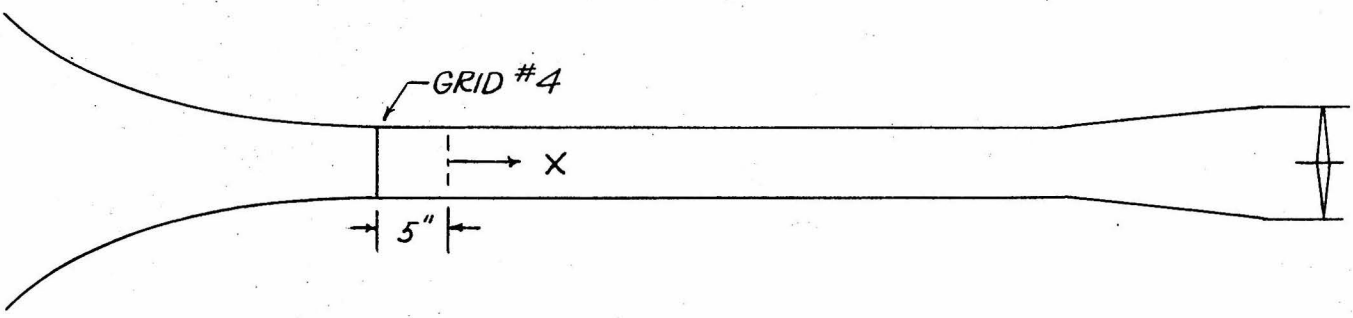

B = 742.4 mm. T = 26 deg. C. δ=.794 ρ=.117

H.W. length ~ 3 mm.(.0005 in. diam.)

X (in.)	u'/U (percent)
3	2.12
6	1.9
9	1.68
12	1.57
15	1.48
18	1.42

TABLE 6c

SUPERPOSITON OF TWO TYPES OF TURBULENCE

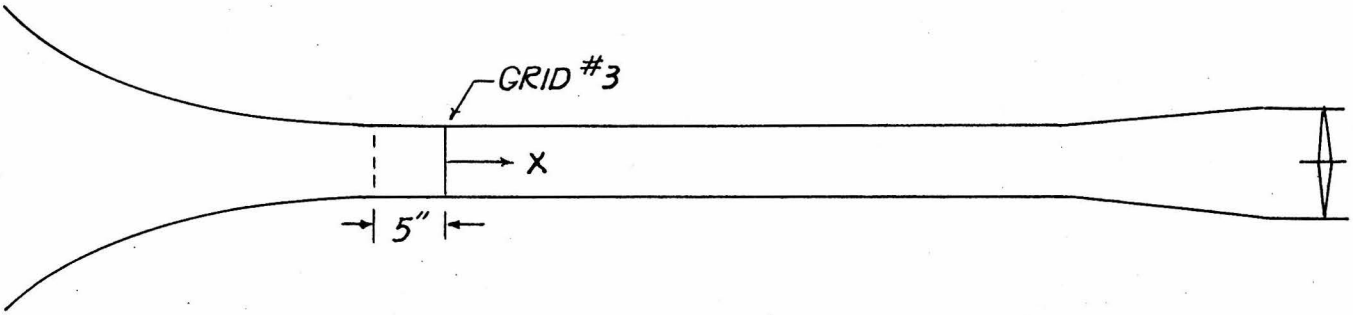

B = 742.4 mm. T = 26 deg. C. σ=.794 ρ=.117

H.W. length ~3 mm.(.0005 in. diam.)

X (in.)	u'/U (percent)
3	7.6
6	4.25
9	3.01
12	2.39
15	2.02
18	1.77
21	1.55
24	1.46
27	1.34

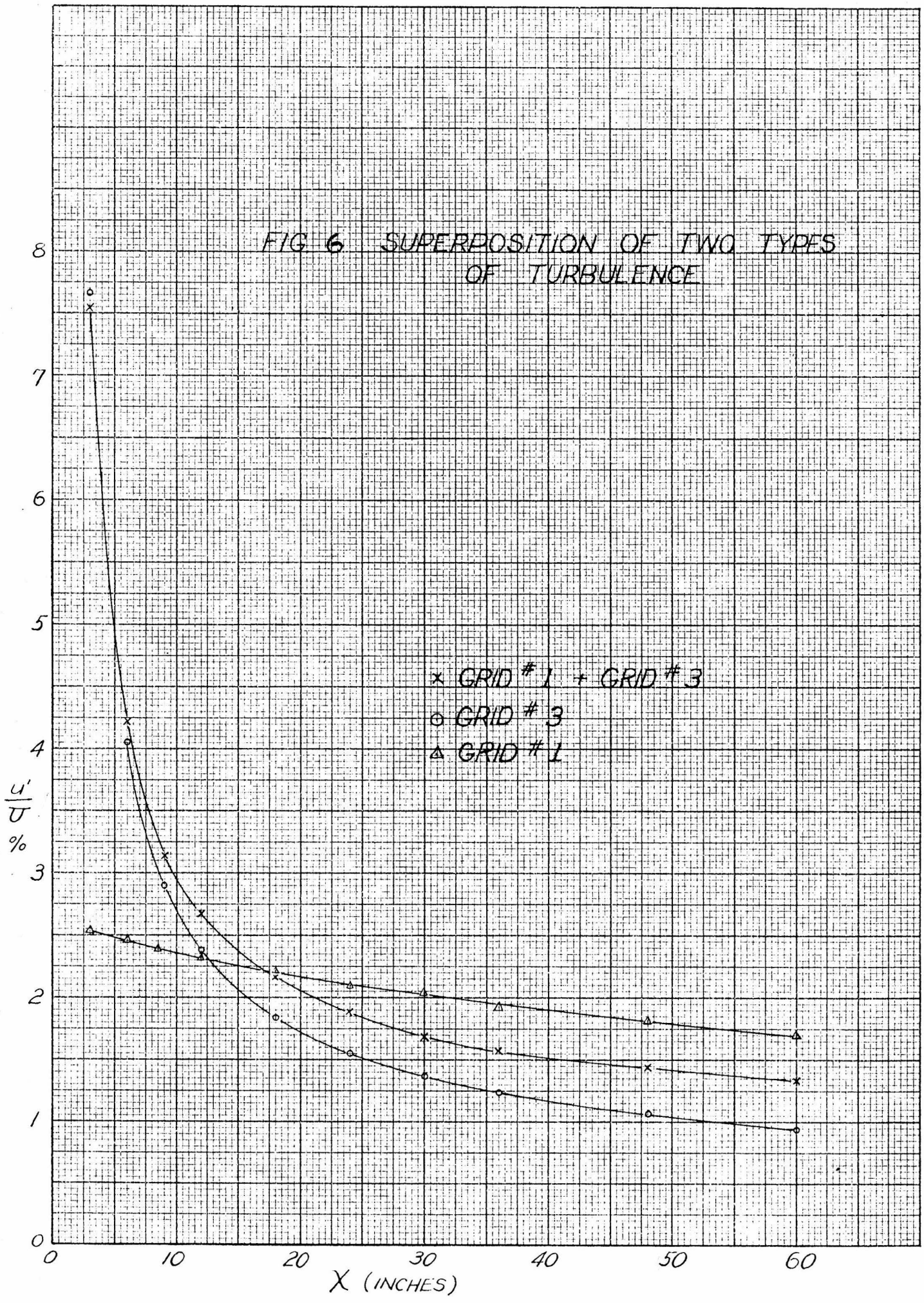
FIG 6 SUPERPOSITION OF TWO TYPES OF TURBULENCE
× GRID # 1 + GRID # 3
○ GRID # 3
△ GRID # 1
u'/U %
X (INCHES)
0
1
2
3
4
5
6
7
8
0
10
20
30
40
50
60

TABLE 7a

SUPERPOSITION OF TWO TYPES OF TURBULENCE

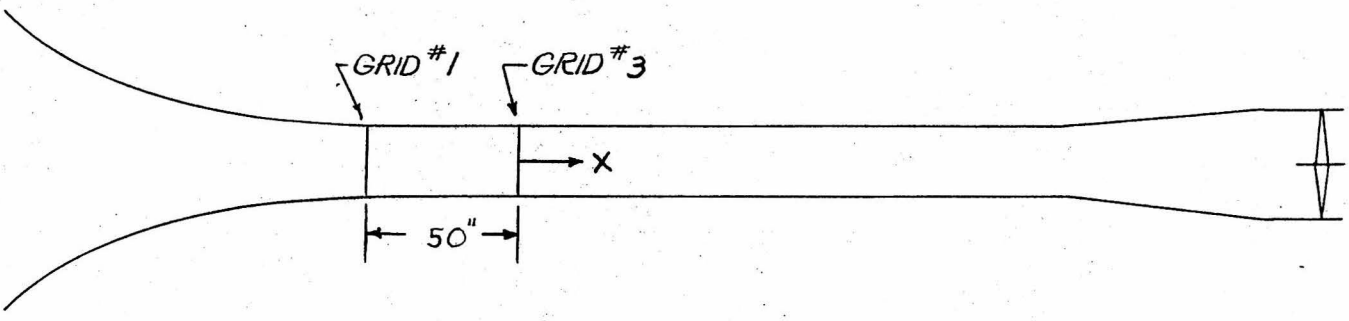

B = 747.8 T = 25 deg. C. δ = .795 ρ = .1185

H.W. length ~ 3 mm.(.0005 diam.) U = 11.6 m/s.

X (in.)	u'/U (percent)
3	7.53
6	4.22
9	3.14
12	2.66
18	2.16
24	1.88
30	1.68
36	1.57
48	1.43
60	1.33

TABLE 76

SUPERPOSITON OF TWO TYPES OF TURBULENCE

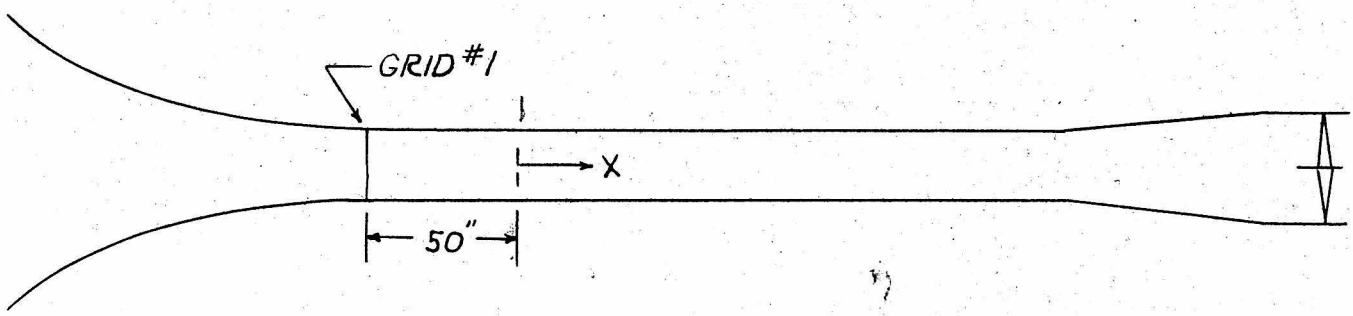

B = 747.8 T = 25 deg. C. δ = .795 ρ = .1185

H.W. length ~ 3 mm.(.0005 diam.) U = 11.6 m/s.

X (in.)	u'/U (percent)
3	2.53
6	2.46
9	2.39
12	2.32
18	2.22
24	2.10
30	2.04
36	1.92
48	1.82
60	1.70

TABLE 7c

SUPERPOSITON OF TWO TYPES OF TURBULENCE

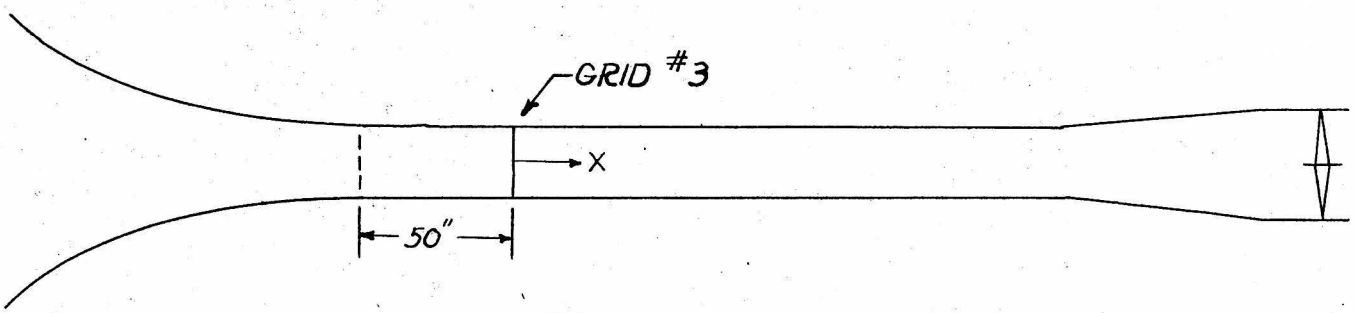

B = 747.8 T = 25 deg. C. δ=.795 ρ=.1185

M.M. length ~ 3 mm.(.0005 diam.) U = 11.6 m/s.

X (in.)	u'/U (percent)
3	7.62
6	4.06
9	2.90
12	2.38
18	1.84
24	1.55
30	1.36
36	1.24
48	1.07
60	.935

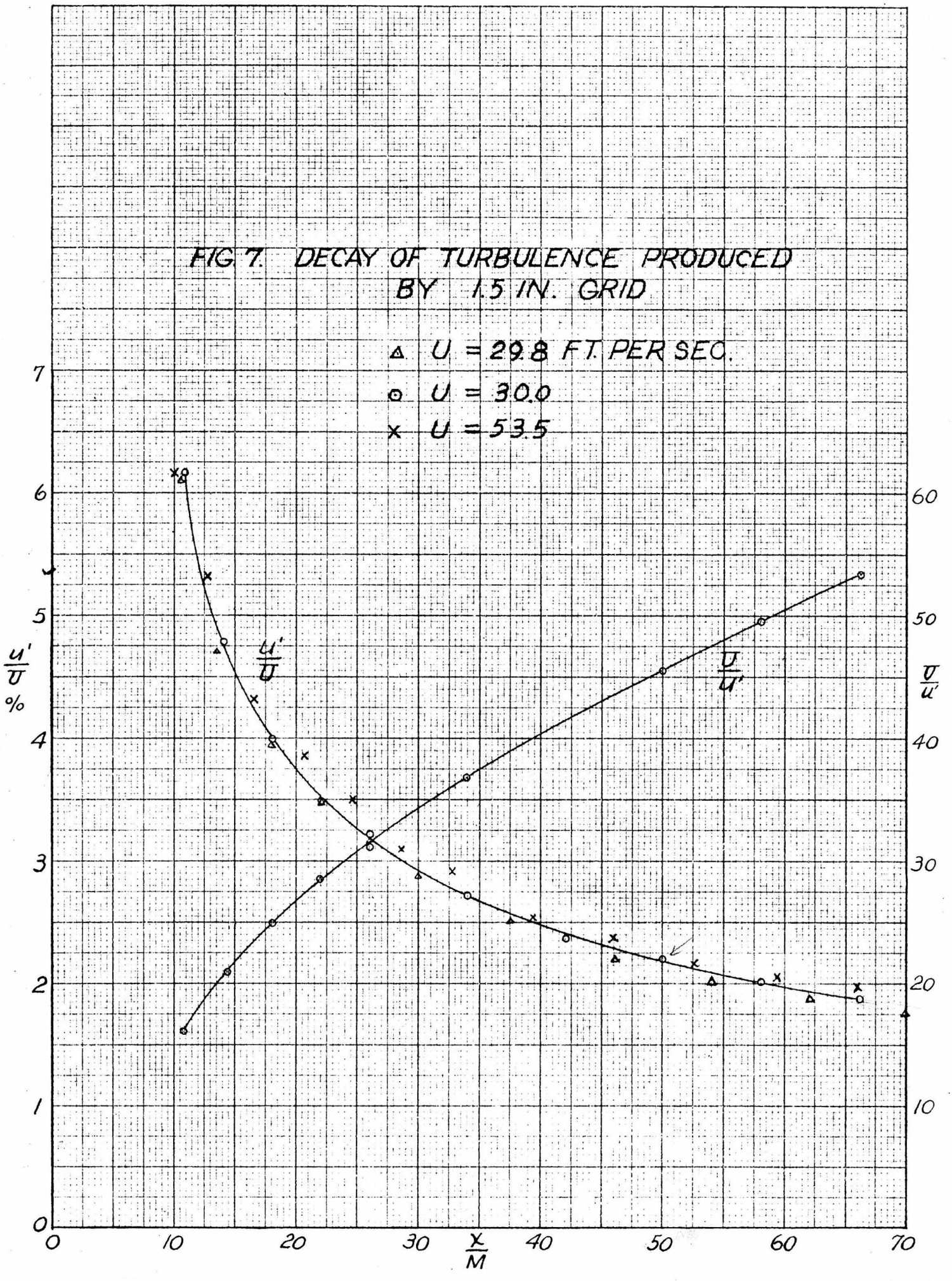
FIG 7. DECAY OF TURBULENCE PRODUCED BY 1.5 IN. GRID
△ U = 29.8 FT. PER SEC.
⊙ U = 30.0
× U = 53.5
u'/U %
U/u'
x/M
0
1
2
3
4
5
6
7
10
20
30
40
50
60
70

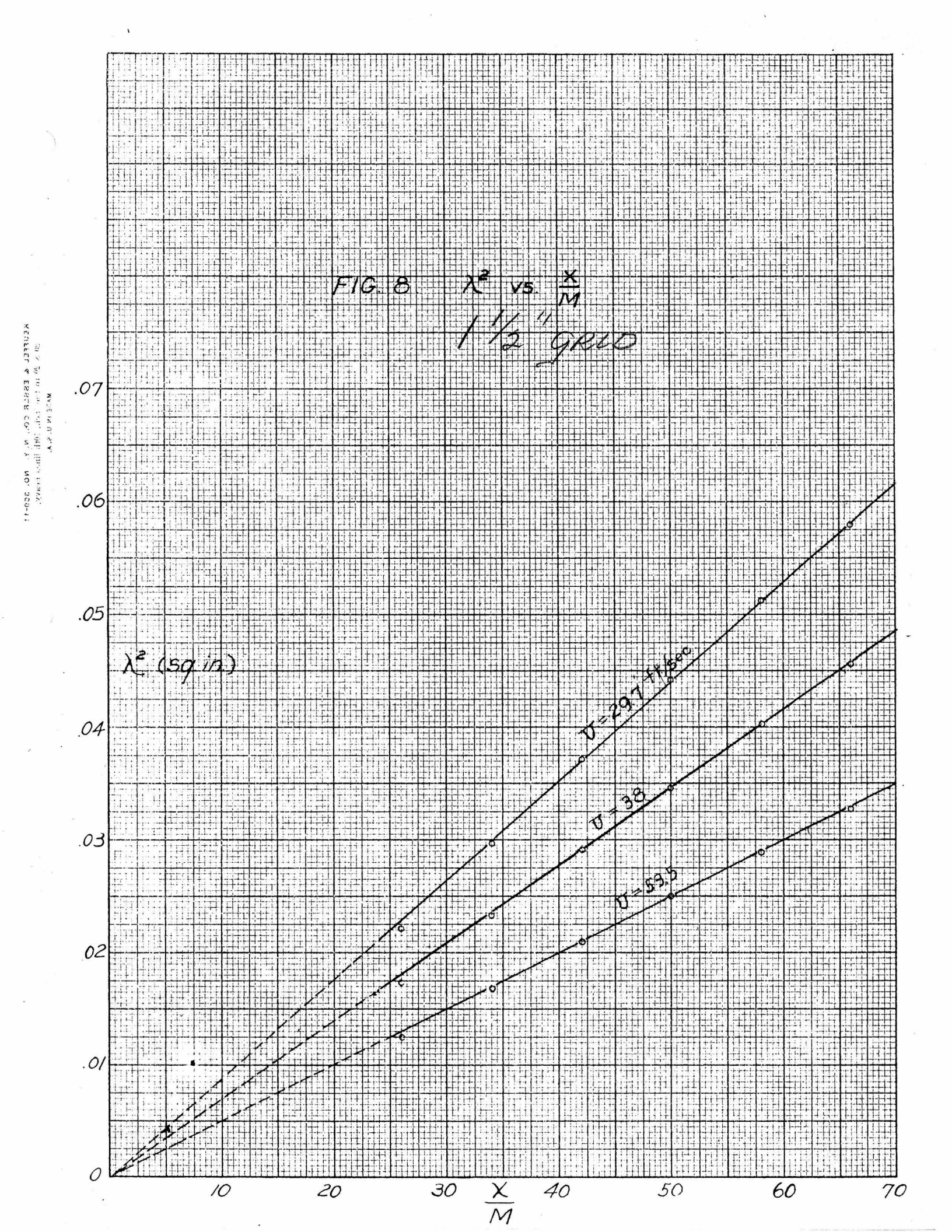
FIG. 8 λ^2 vs. $\frac{X}{M}$
1 1/2" GRID
λ^2 (sq in)
.07
.06
.05
.04
.03
.02
.01
0
10
20
30
40
50
60
70
$\frac{X}{M}$
V = 29.7 ft/sec
V = 38
V = 53.5

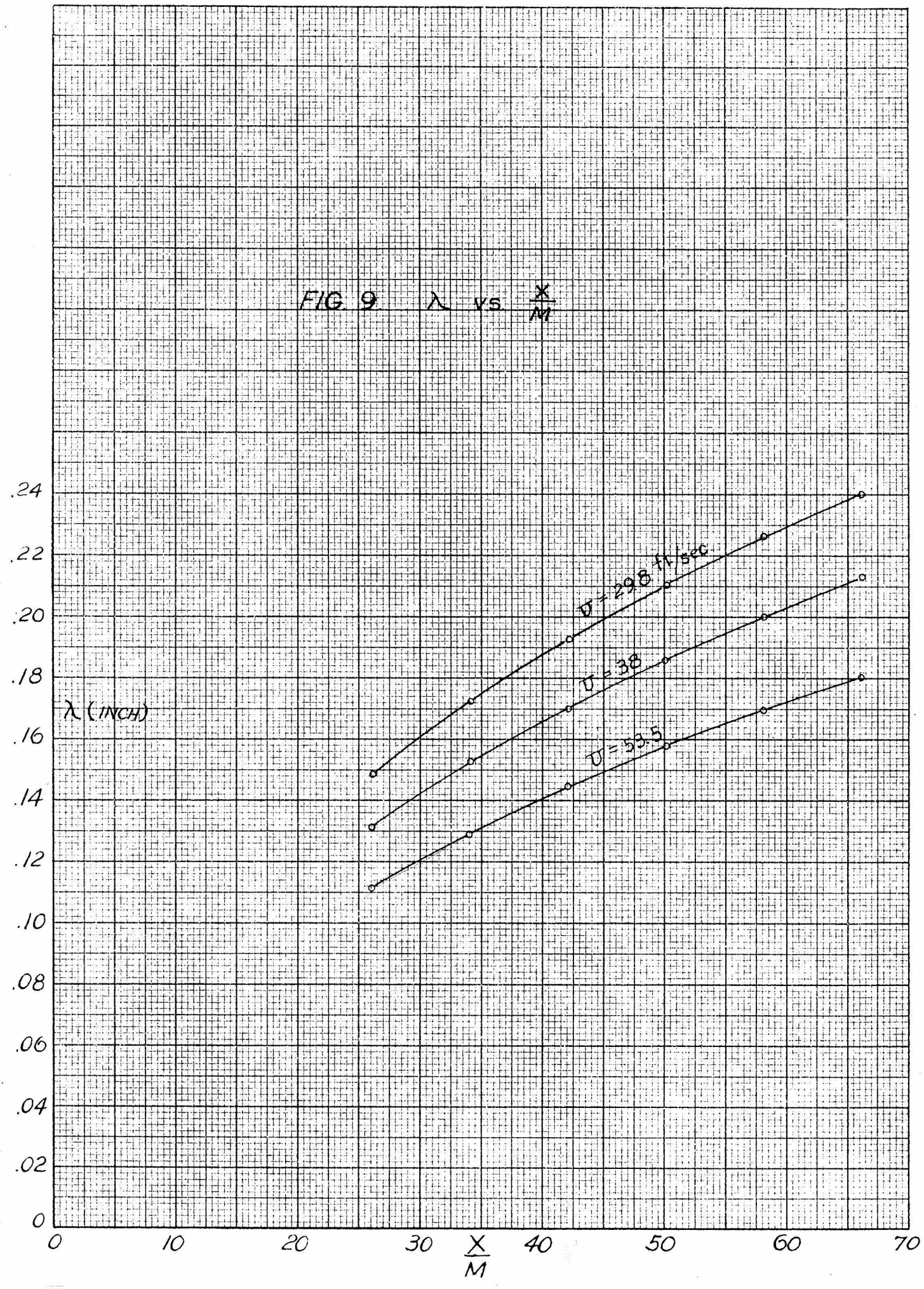
FIG. 9 λ vs X/M
λ (INCH)
.24
.22
.20
.18
.16
.14
.12
.10
.08
.06
.04
.02
0
0
10
20
30
40
50
60
70
X/M
U = 29.8 ft/sec
U = 38
U = 53.5

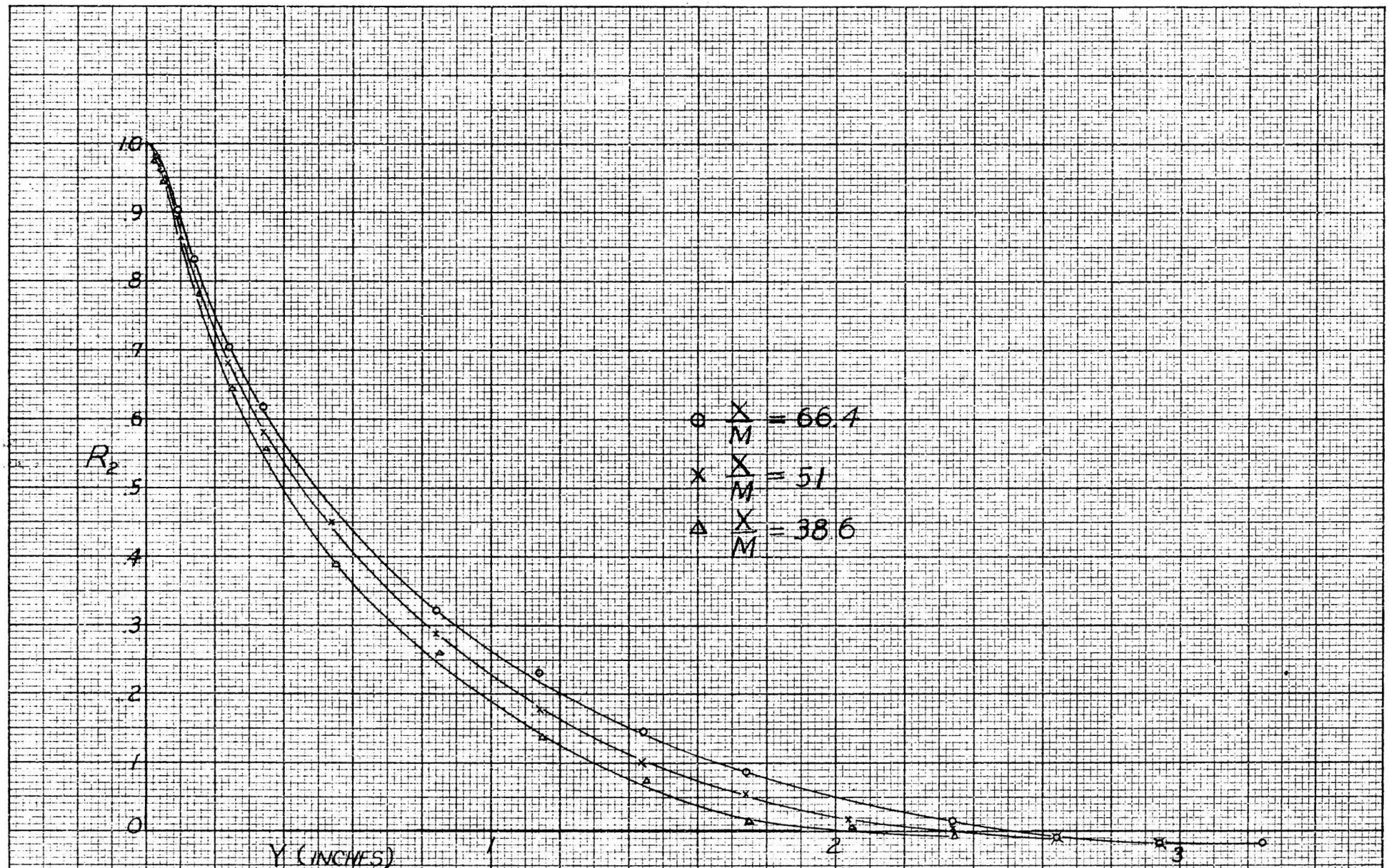

FIG. 10. VARIATION OF R_2 WITH Y FOR DIFFERENT VALUES OF $\frac{X}{M}$
WIND SPEED = 29.8 ft/sec GRID SIZE = 1.5 INCHES

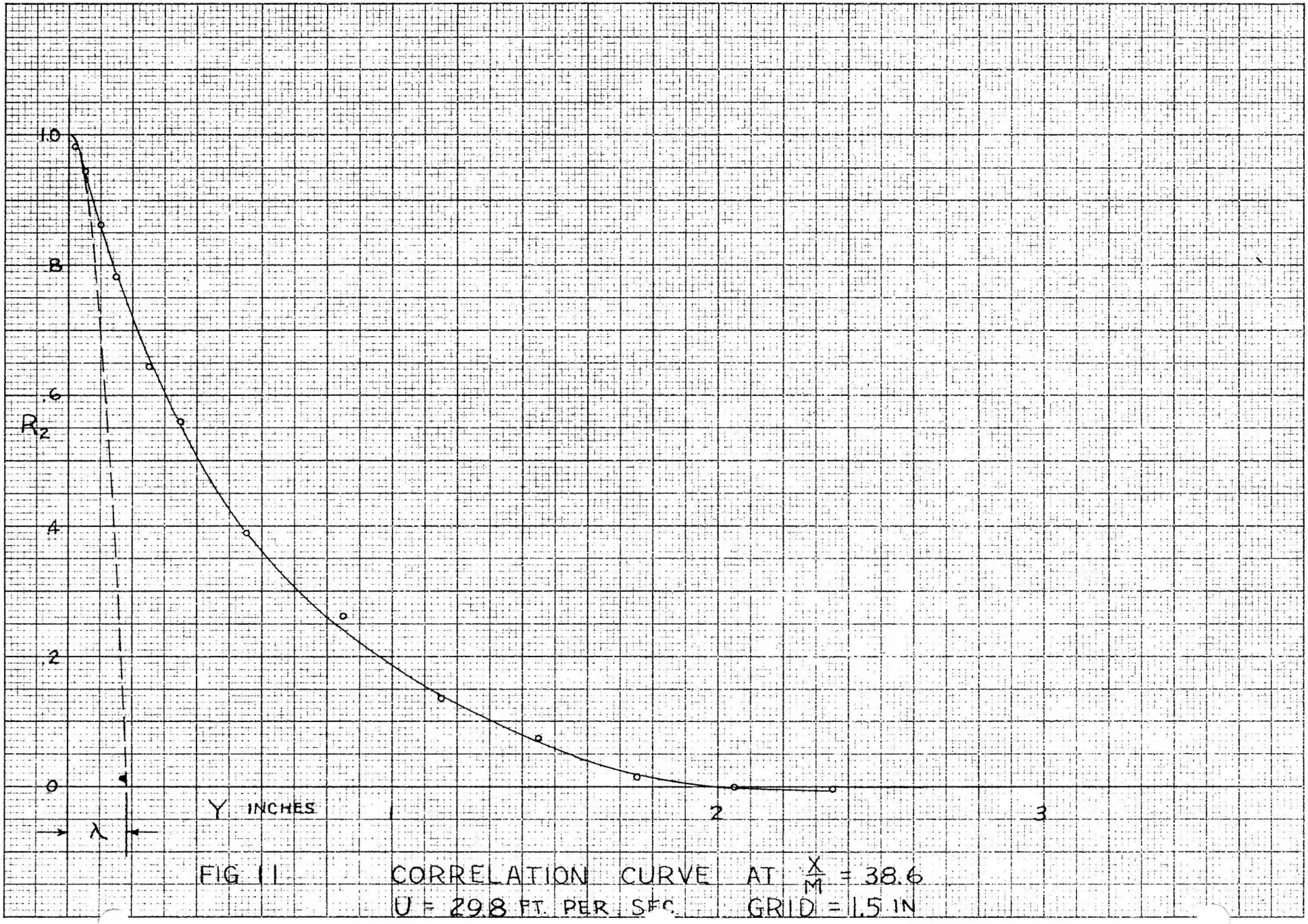

FIG 11 CORRELATION CURVE AT $\frac{X}{M}$ = 38.6
U = 29.8 FT. PER SEC. GRID = 1.5 IN

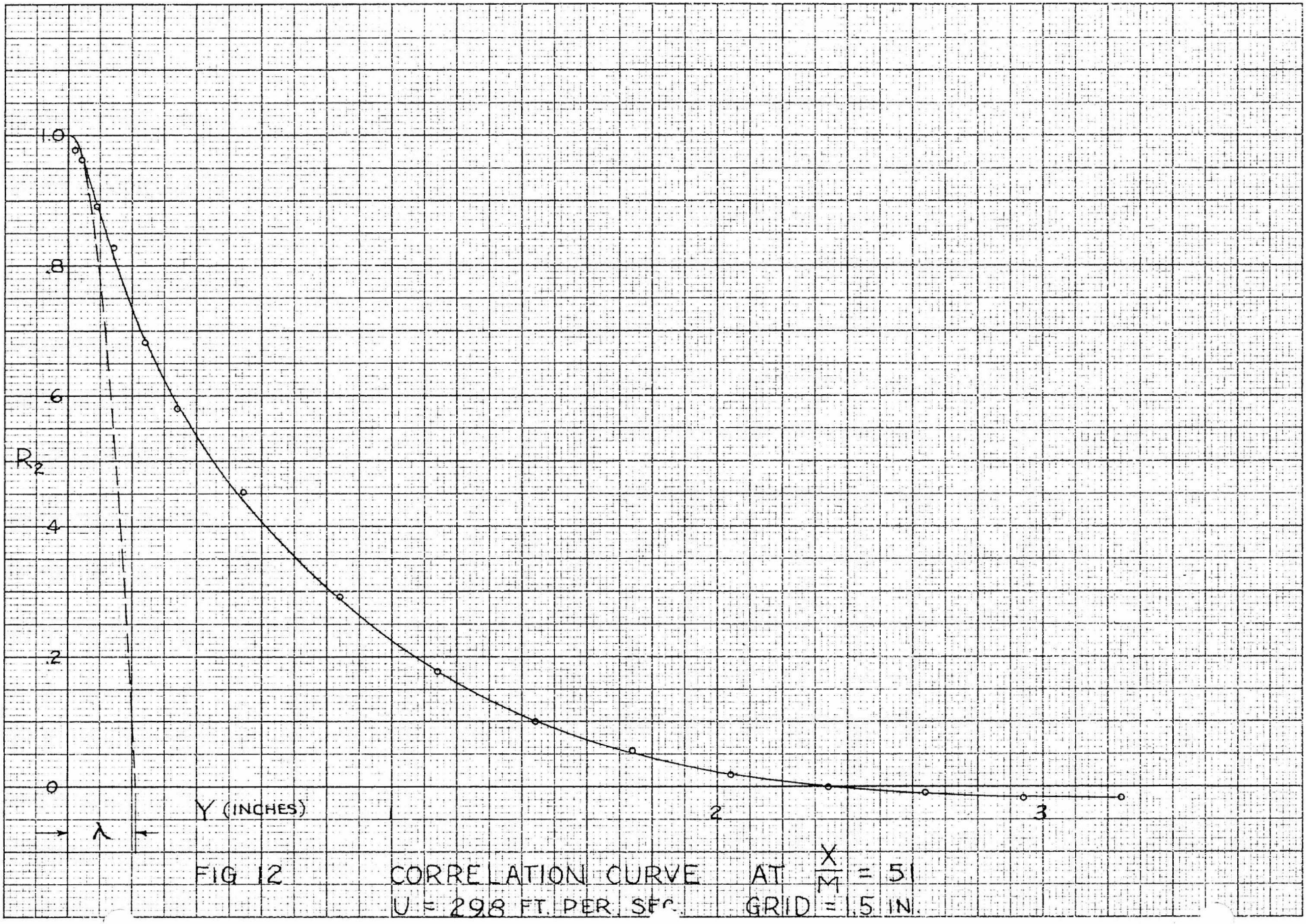

FIG 12 CORRELATION CURVE AT $\frac{X}{M} = 51$
U = 298 FT. PER SEC. GRID = .5 IN.

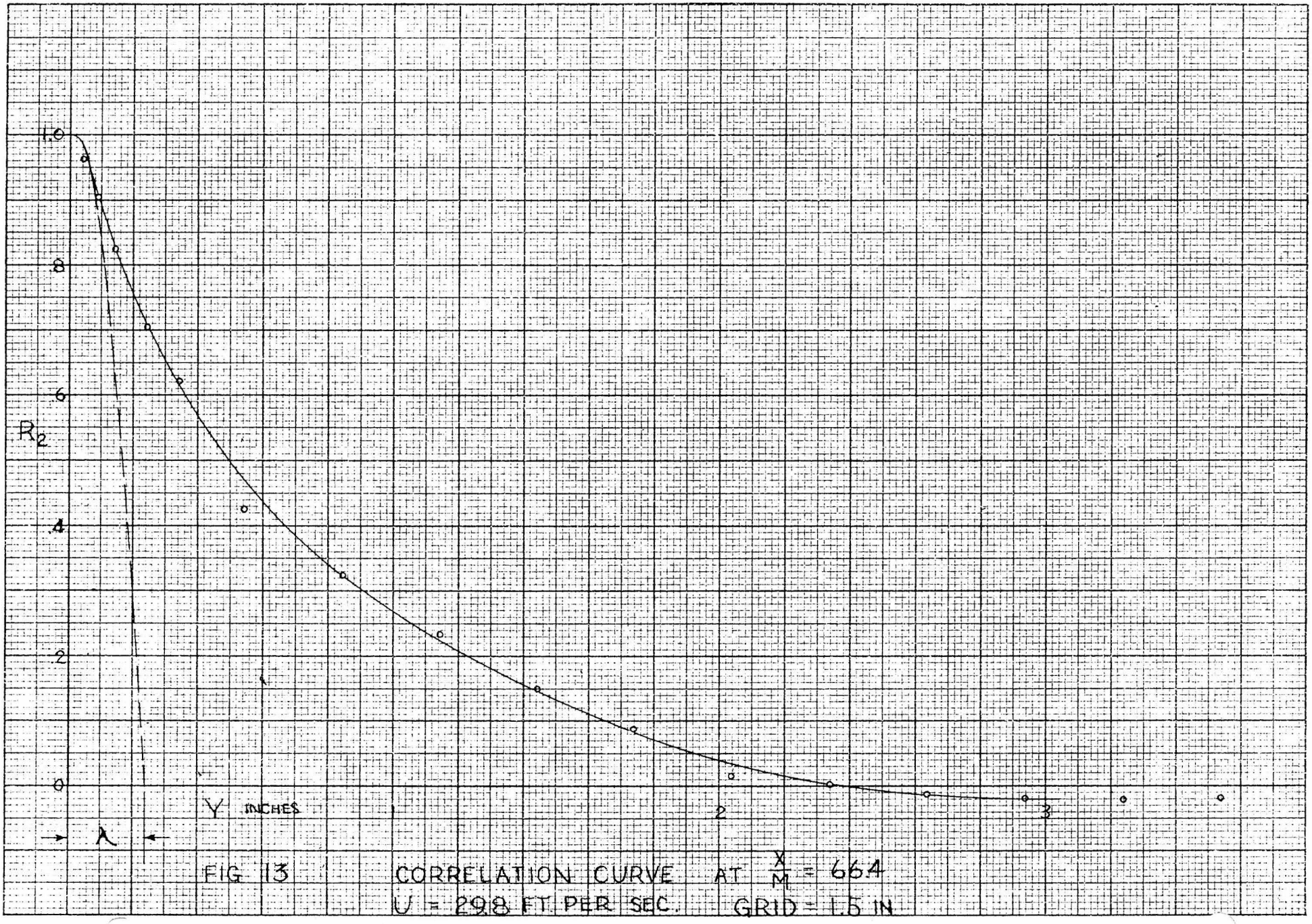

FIG 13 CORRELATION CURVE AT $\frac{X}{M} = 66.4$
U = 298 FT PER SEC. GRID = 1.5 IN

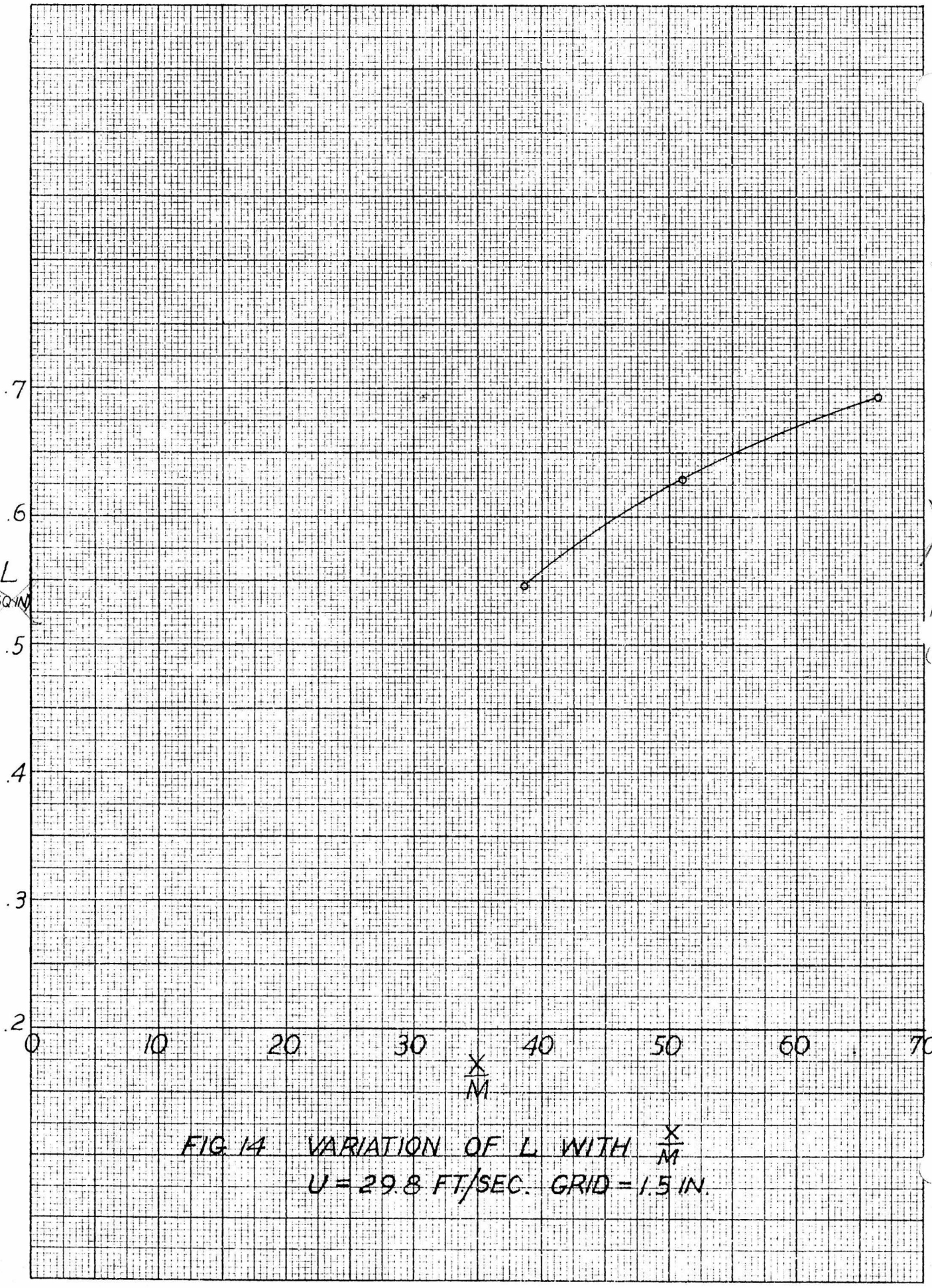

FIG. 14 VARIATION OF L WITH $\frac{X}{M}$
U = 29.8 FT/SEC. GRID = 1.5 IN.

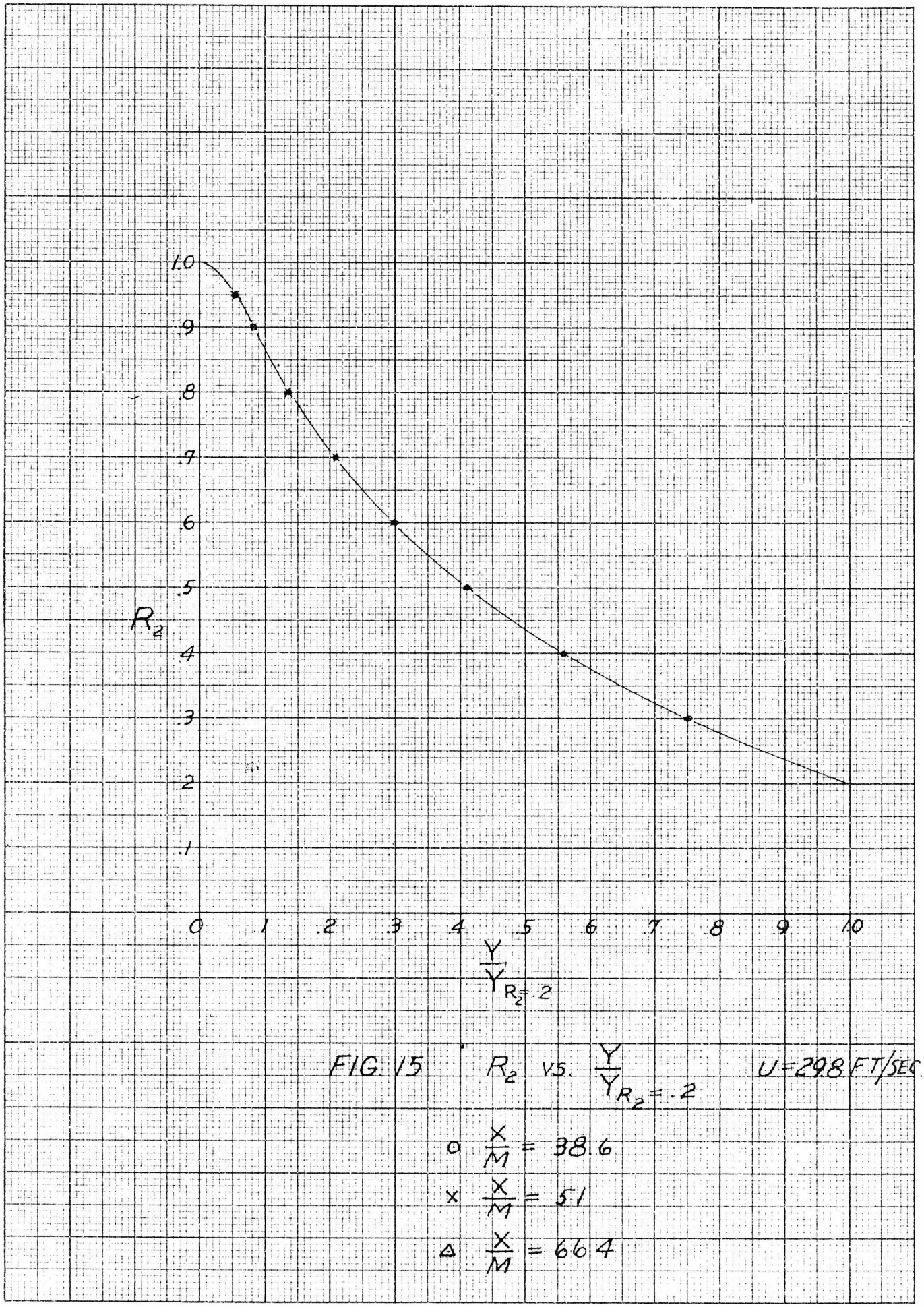

FIG 15 R_2 VS. $\frac{Y}{Y_{R_2=.2}}$ U=298 FT/SEC

○ $\frac{X}{M} = 38.6$

× $\frac{X}{M} = 51$

△ $\frac{X}{M} = 66.4$

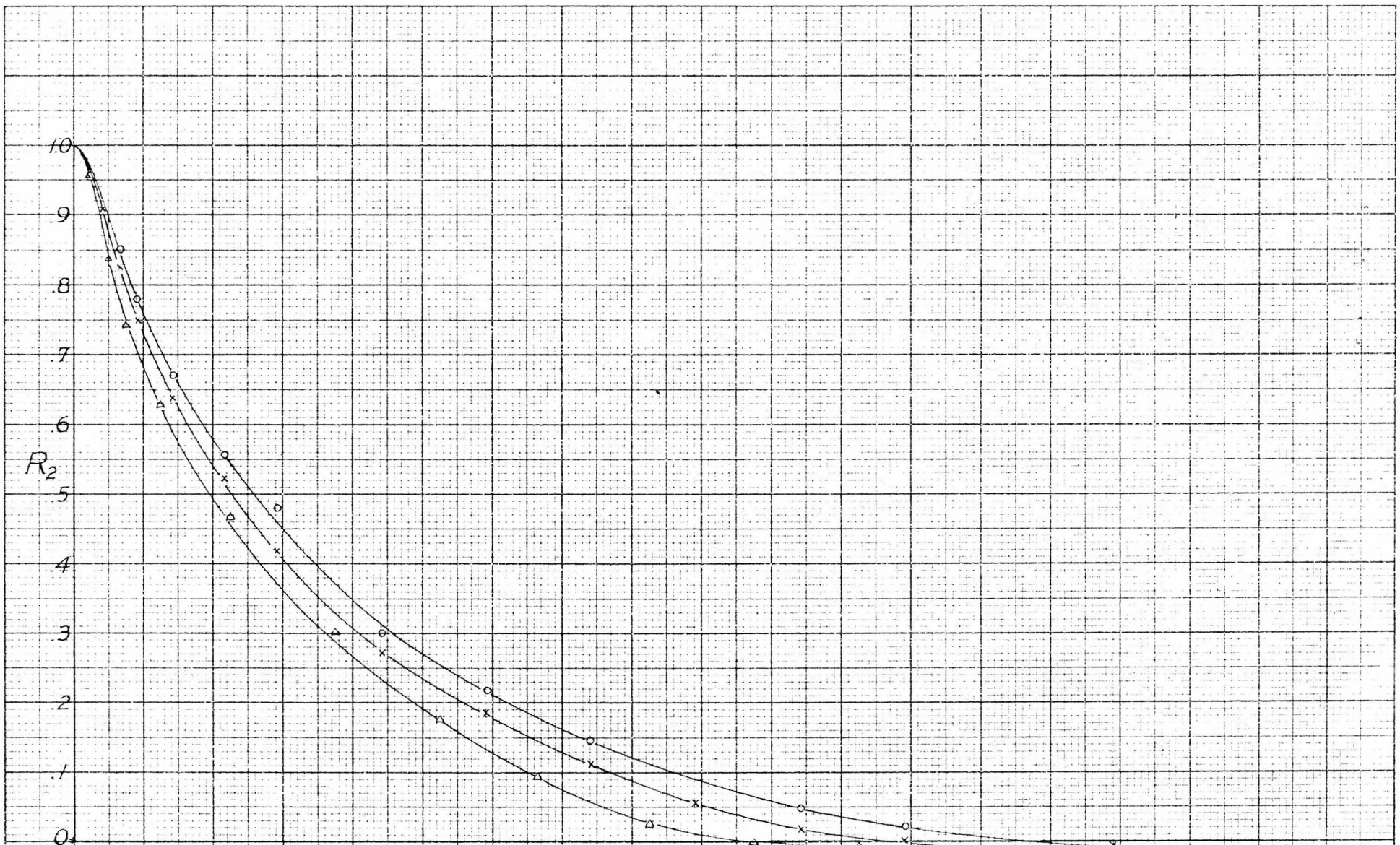

FIG. 16. VARIATION OF R_2 WITH Y FOR DIFFERENT VALUES OF $\frac{X}{M}$
WIND SPEED = 38 FT./SEC GRID SIZE = 1.5 IN.

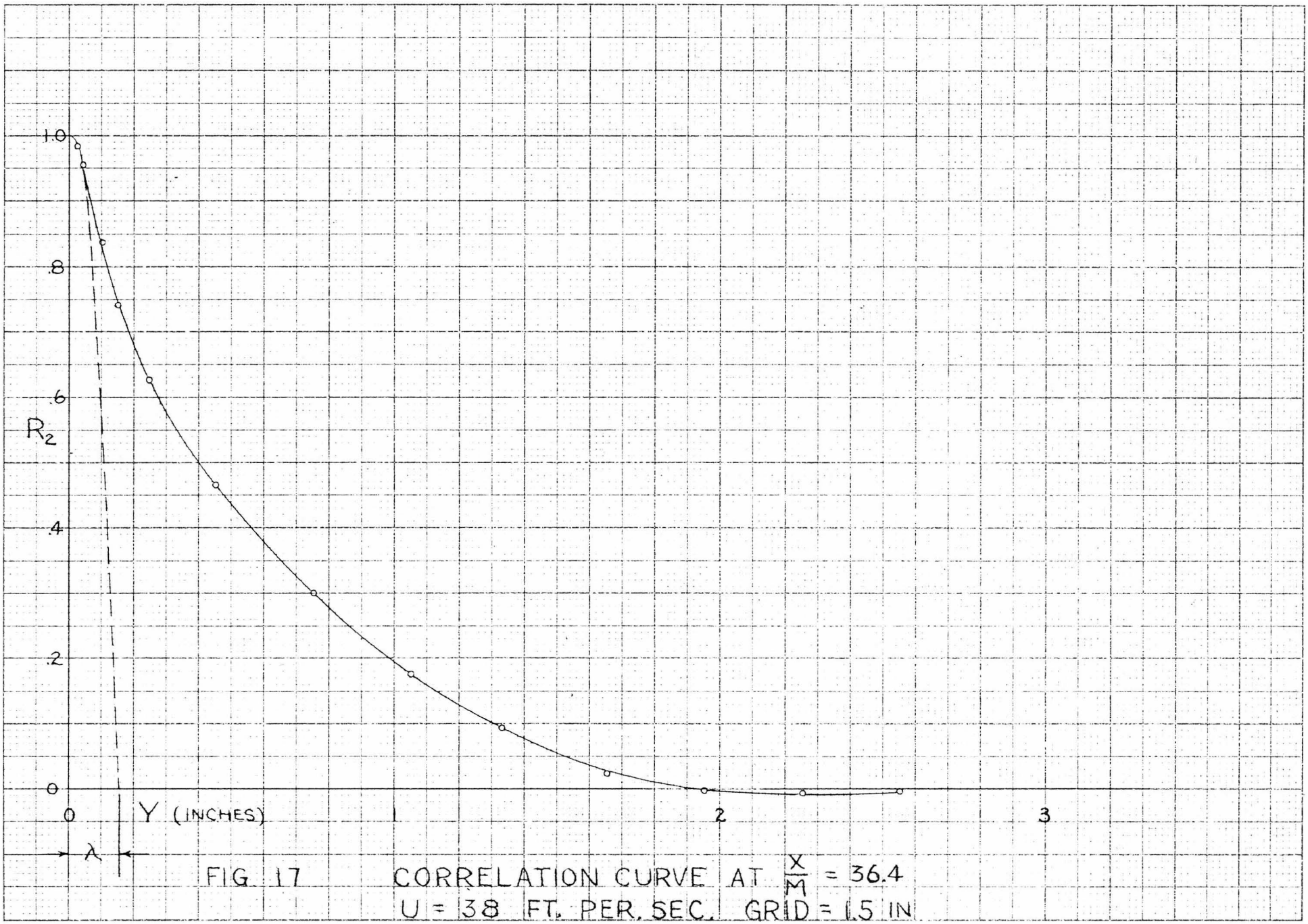

FIG. 17 CORRELATION CURVE AT $\frac{X}{M} = 36.4$
U = 38 FT. PER. SEC. GRID = 1.5 IN

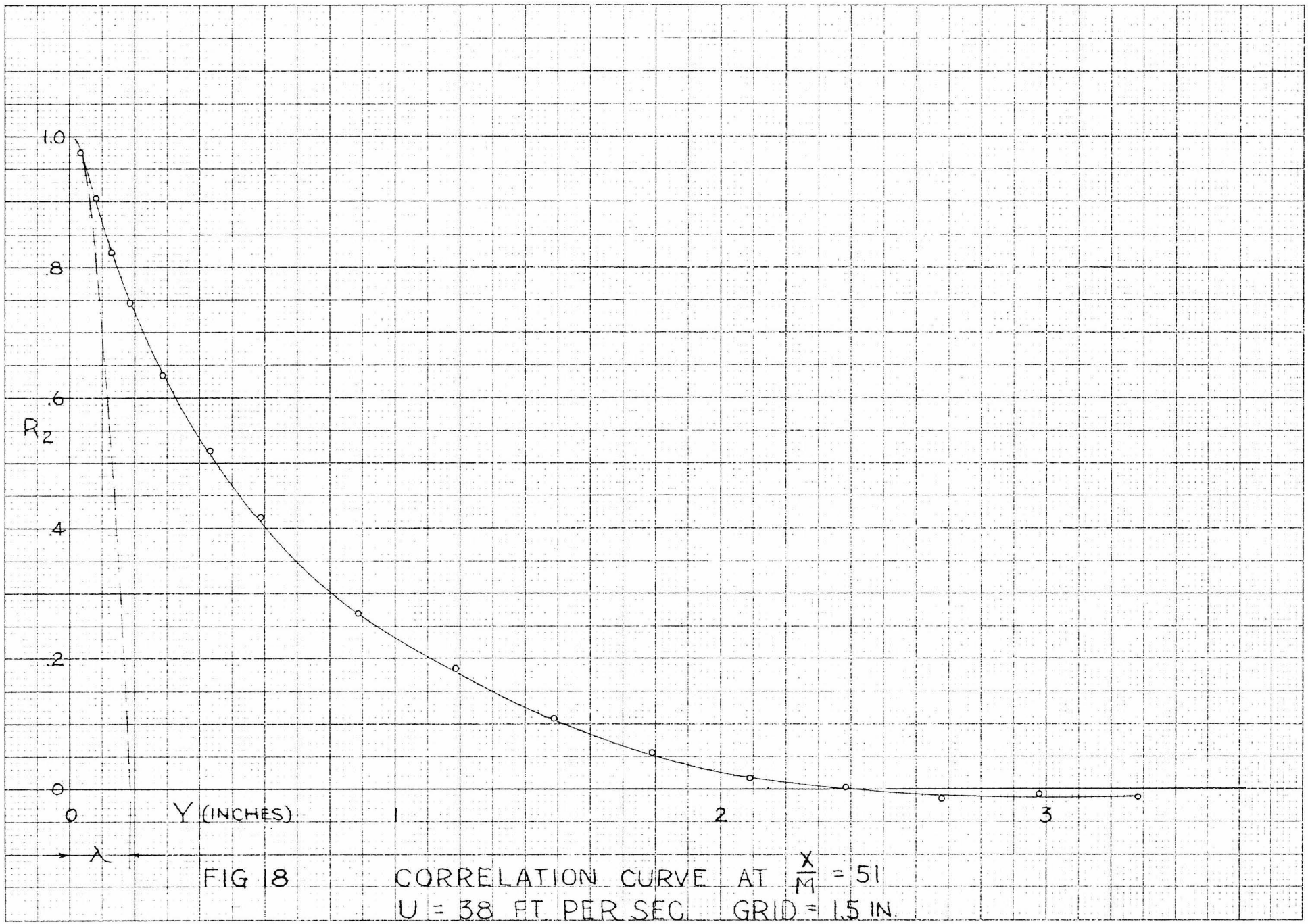

FIG 18 CORRELATION CURVE AT $\frac{X}{M} = 51$
U = 38 FT. PER SEC. GRID = 1.5 IN.

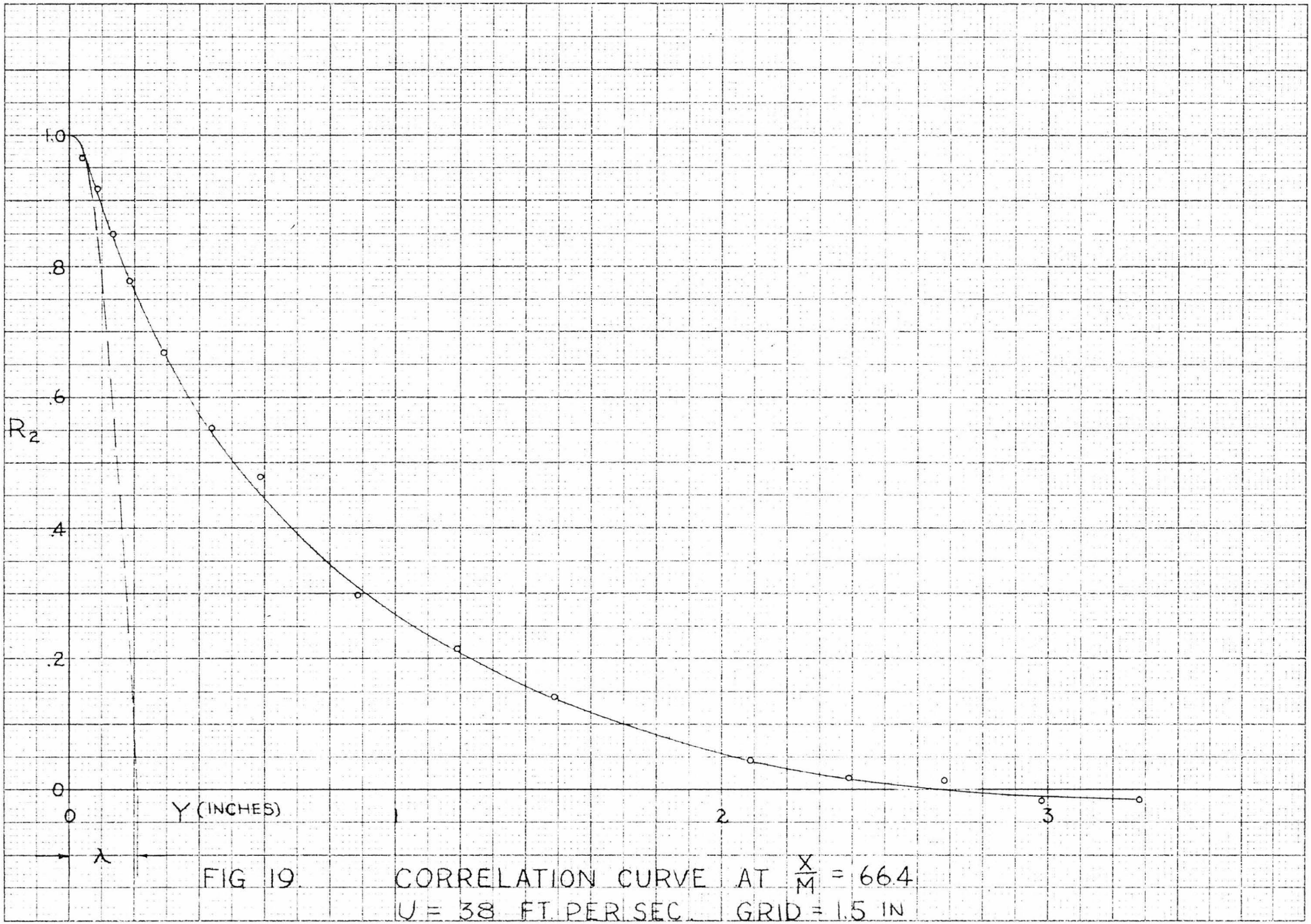

FIG 19. CORRELATION CURVE AT $\frac{X}{M} = 66.4$
U = 38 FT PER SEC. GRID = 1.5 IN

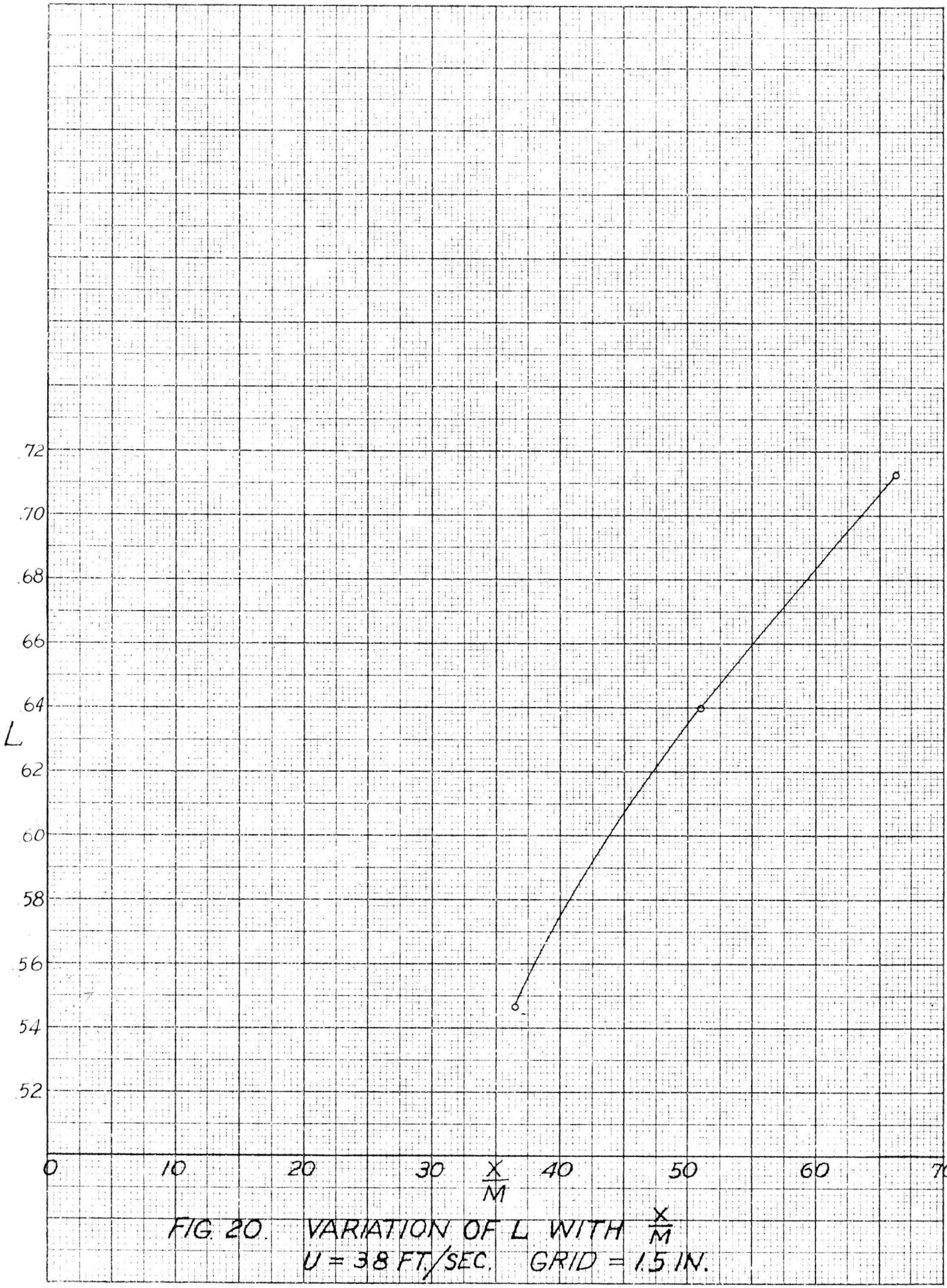

FIG. 20. VARIATION OF L WITH $\frac{X}{M}$
U = 38 FT/SEC. GRID = 1.5 IN.

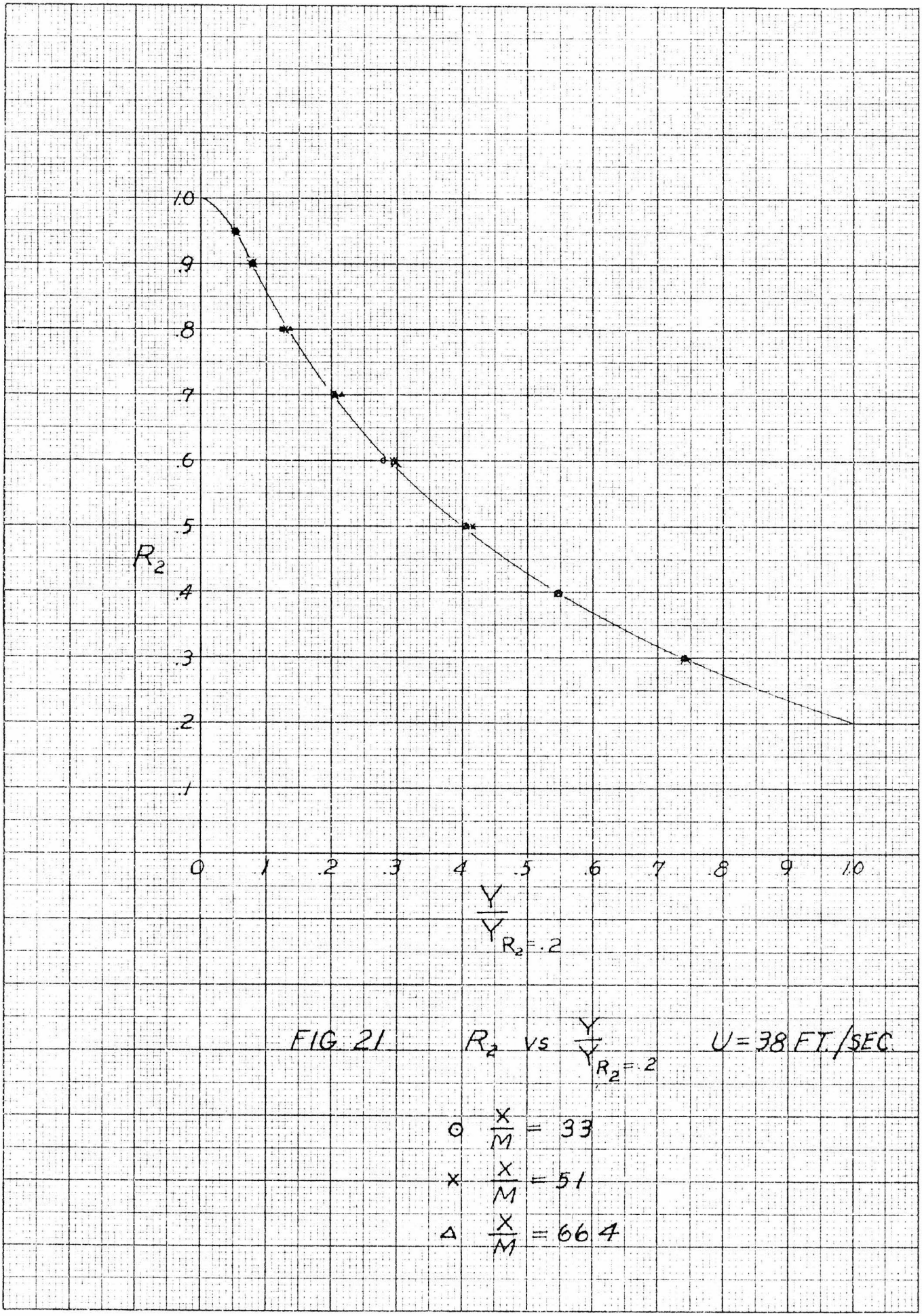

FIG. 21 R_2 vs $\frac{Y}{Y_{R_2=.2}}$ $U = 38$ FT./SEC

○ $\frac{X}{M} = 33$

× $\frac{X}{M} = 51$

△ $\frac{X}{M} = 664$

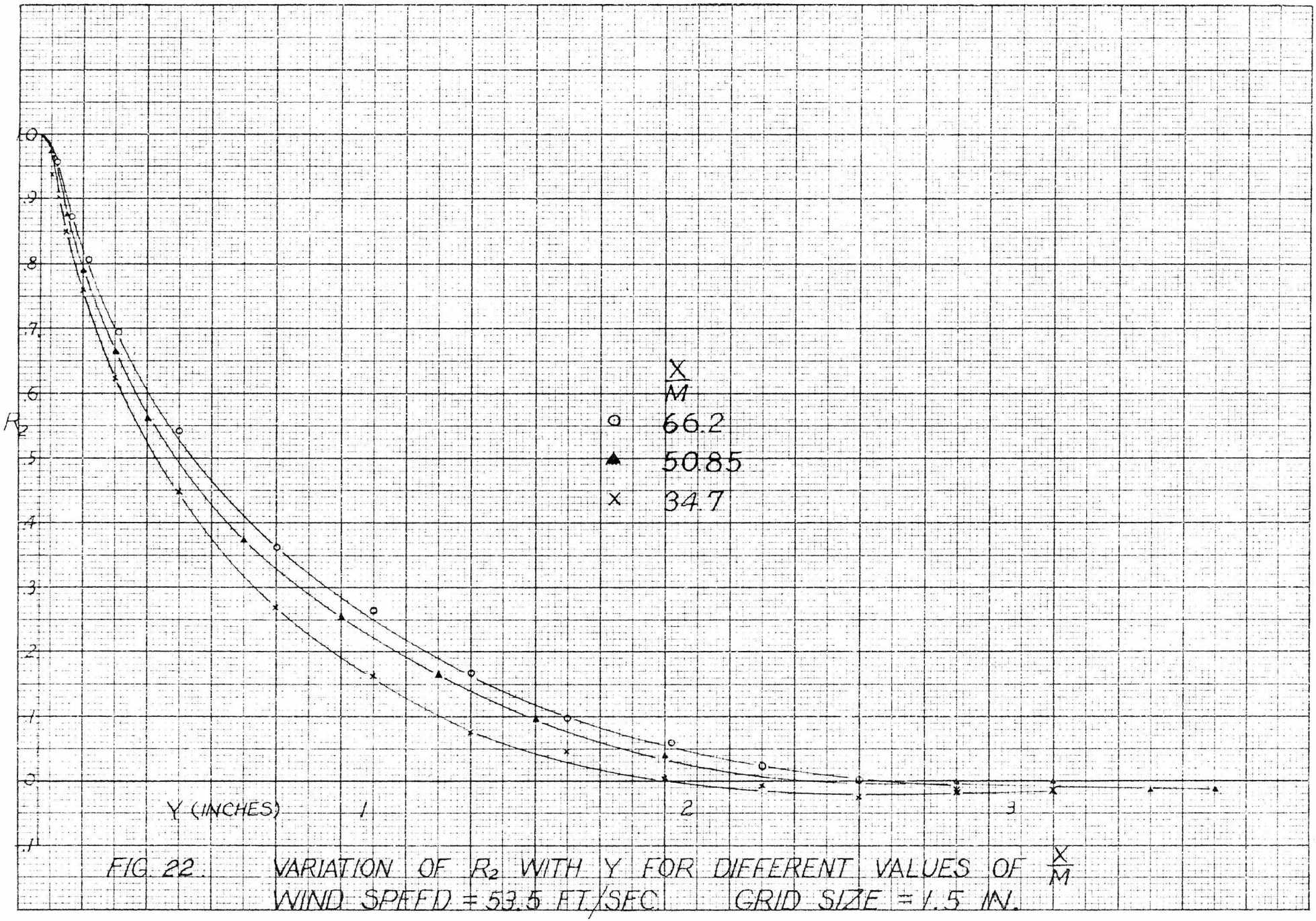

FIG 22. VARIATION OF R_2 WITH Y FOR DIFFERENT VALUES OF $\frac{X}{M}$
WIND SPEED = 53.5 FT./SEC. GRID SIZE = 1.5 IN.

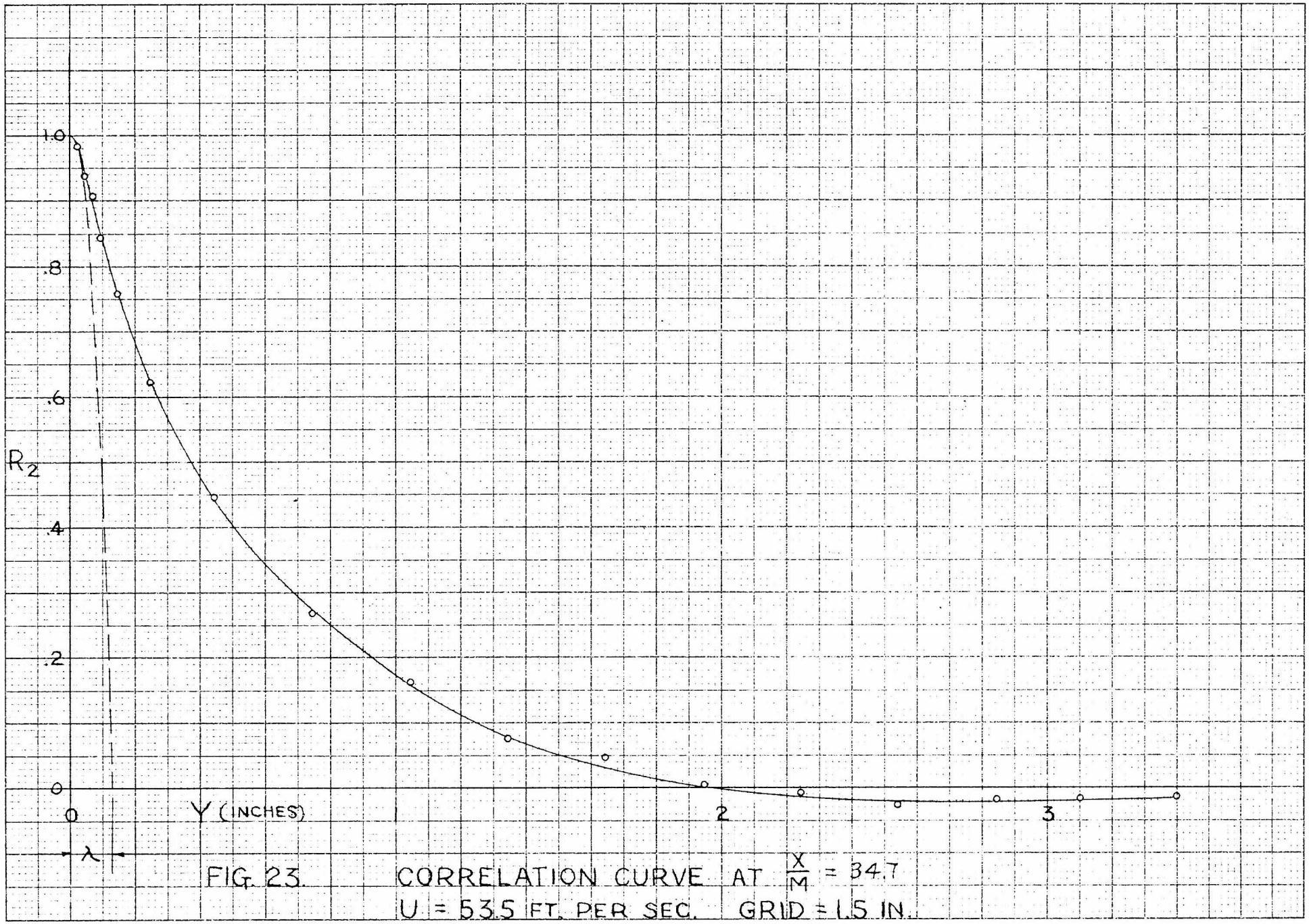

FIG. 23. CORRELATION CURVE AT $\frac{X}{M} = 34.7$
U = 53.5 FT. PER SEC. GRID = 1.5 IN.

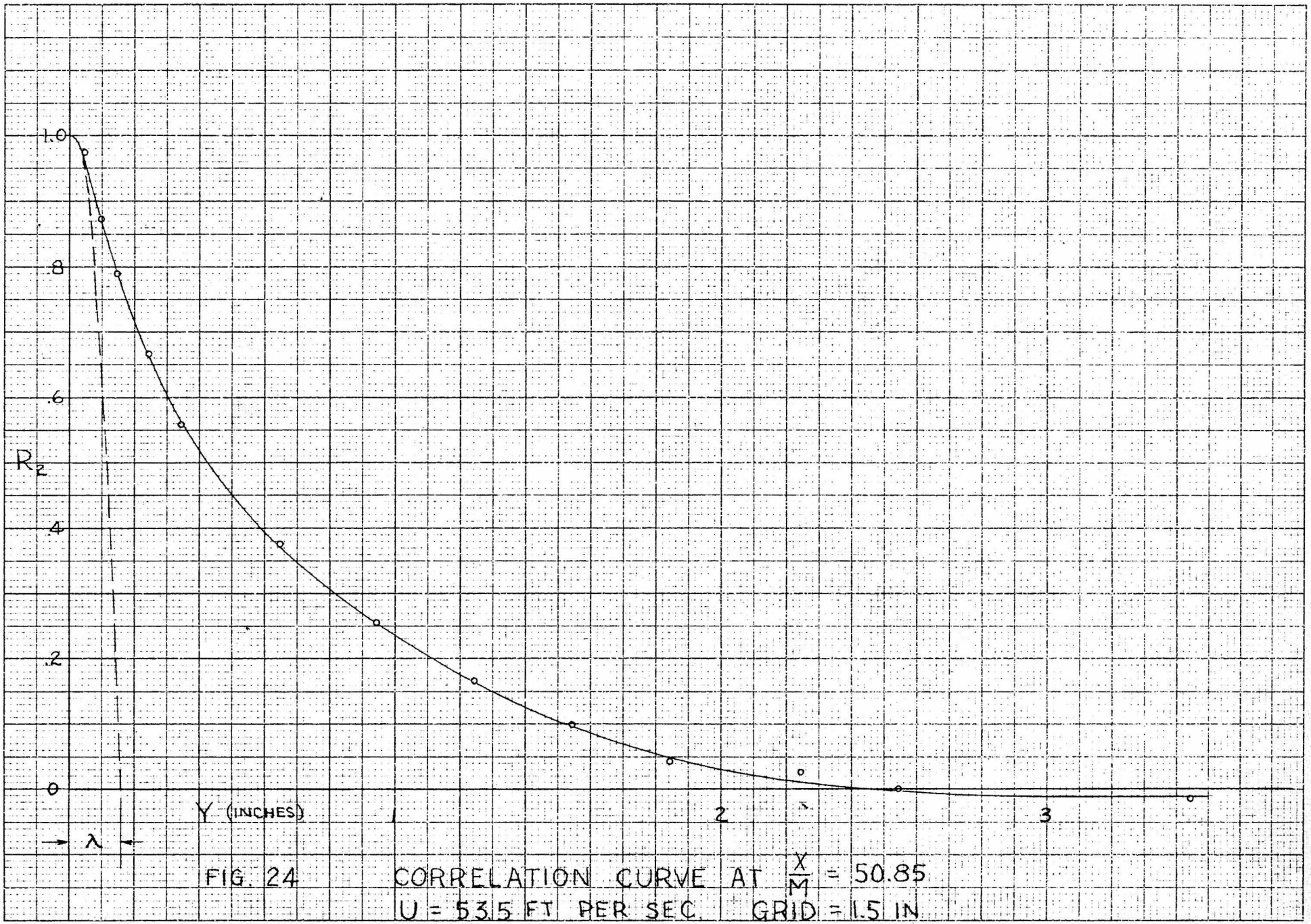

FIG. 24 CORRELATION CURVE AT $\frac{X}{M}$ = 50.85
U = 53.5 FT PER SEC. GRID = 1.5 IN

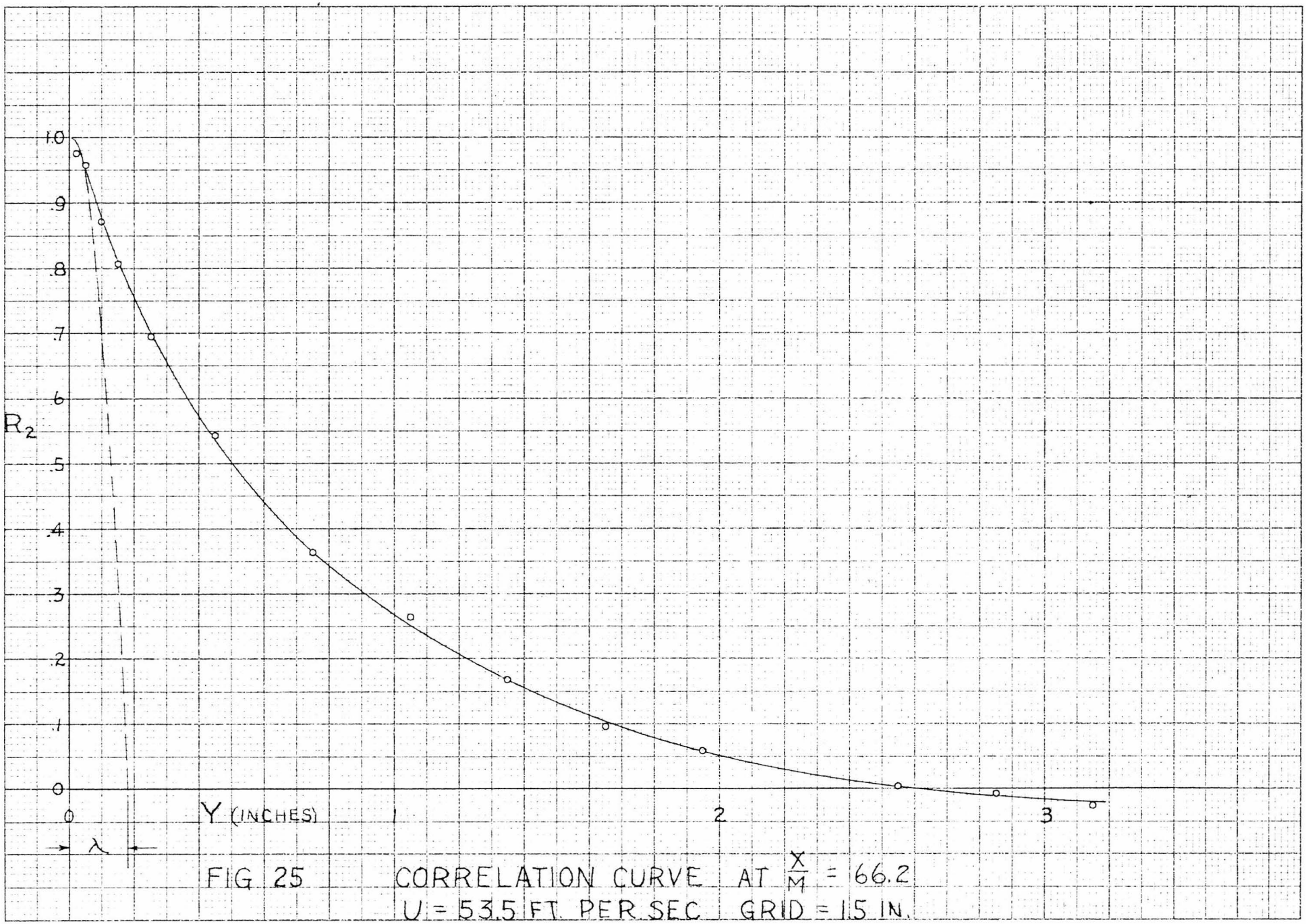

FIG. 25 CORRELATION CURVE AT $\frac{X}{M} = 66.2$
U = 53.5 FT. PER SEC. GRID = 1.5 IN.

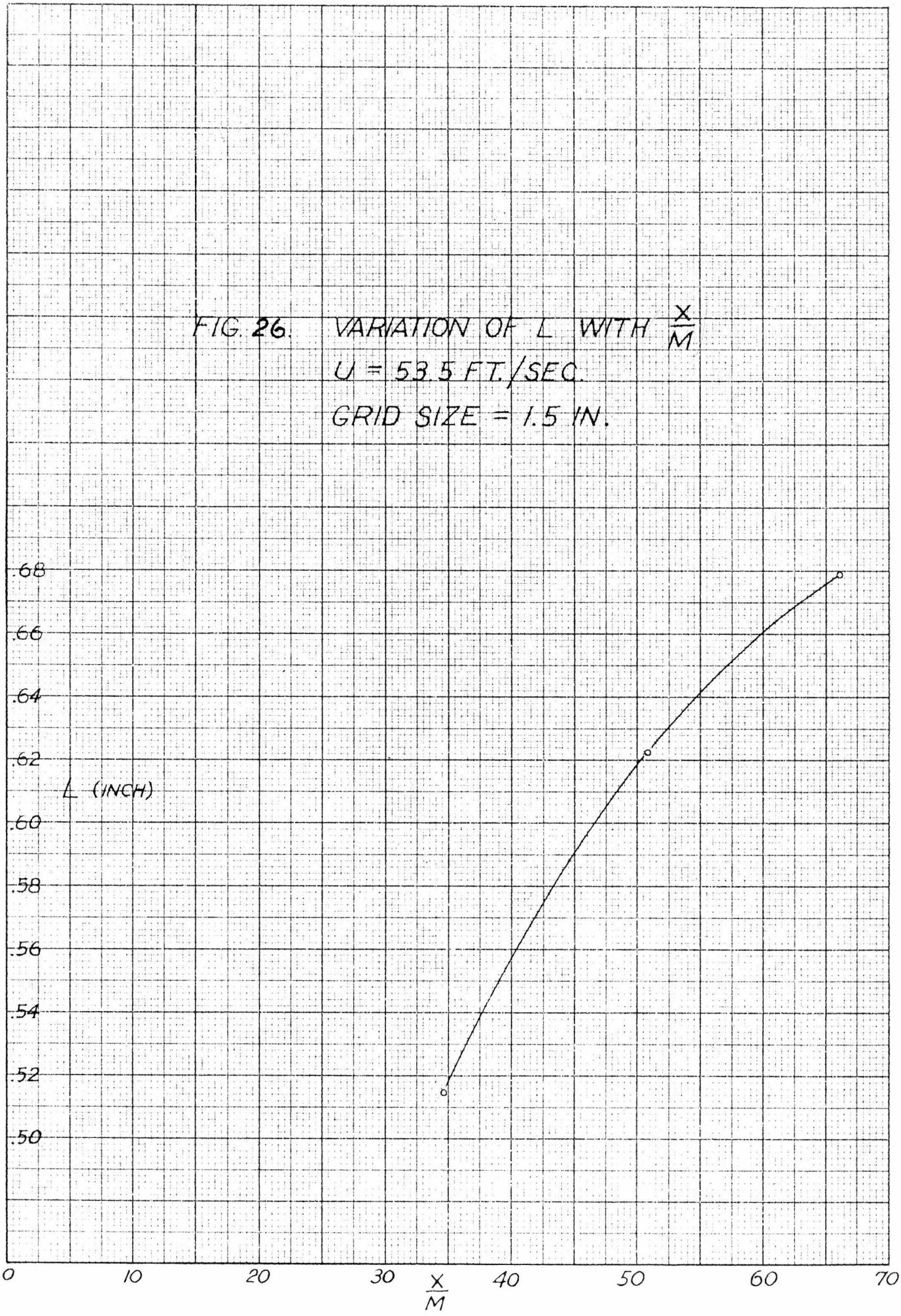

FIG. 26. VARIATION OF L WITH $\frac{X}{M}$
U = 53.5 FT./SEC.
GRID SIZE = 1.5 IN.

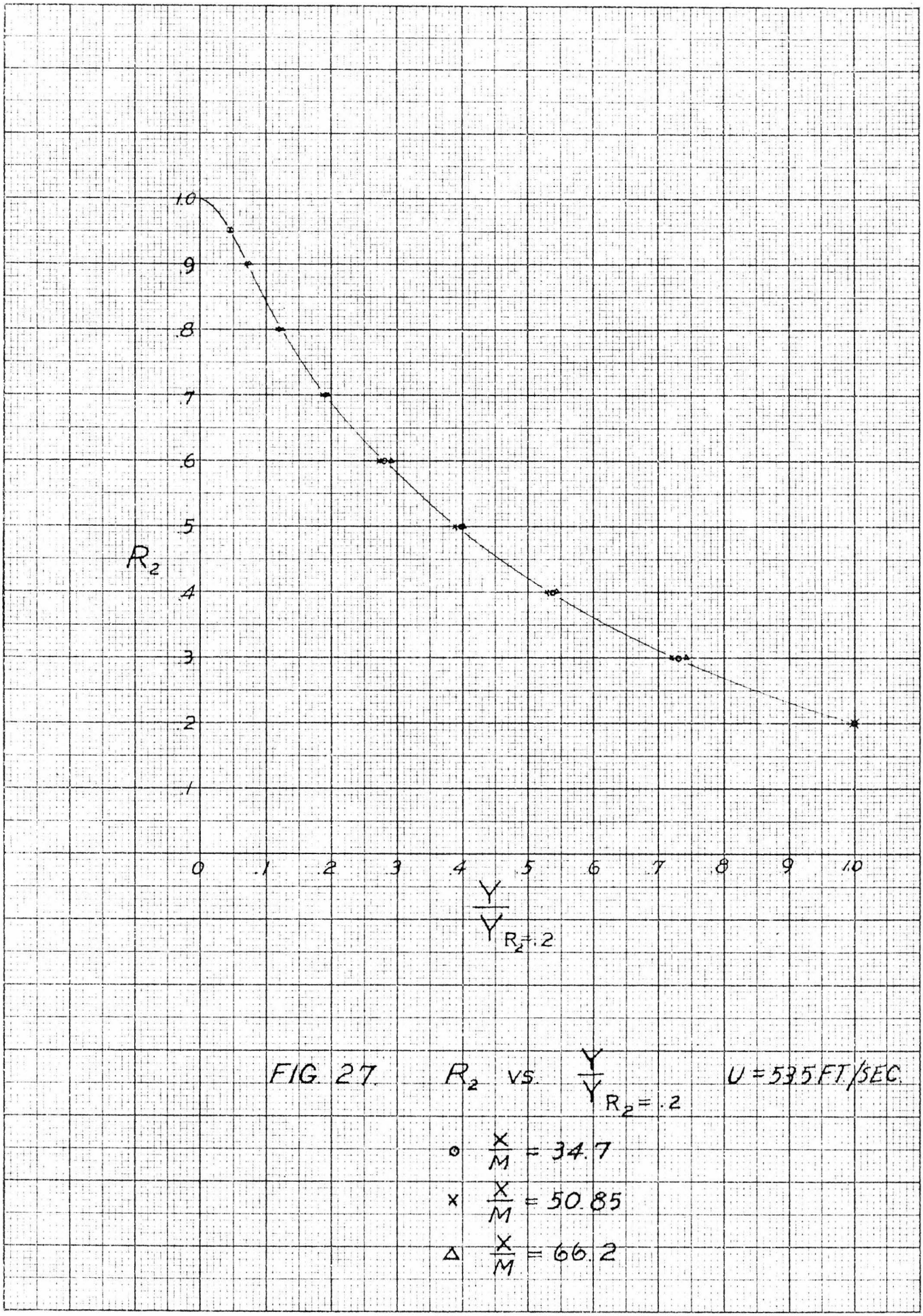

FIG. 27 R_2 vs. $\frac{Y}{Y_{R_2=.2}}$ $U = 535$ FT/SEC

- o $\frac{X}{M} = 34.7$
- x $\frac{X}{M} = 50.85$
- Δ $\frac{X}{M} = 66.2$

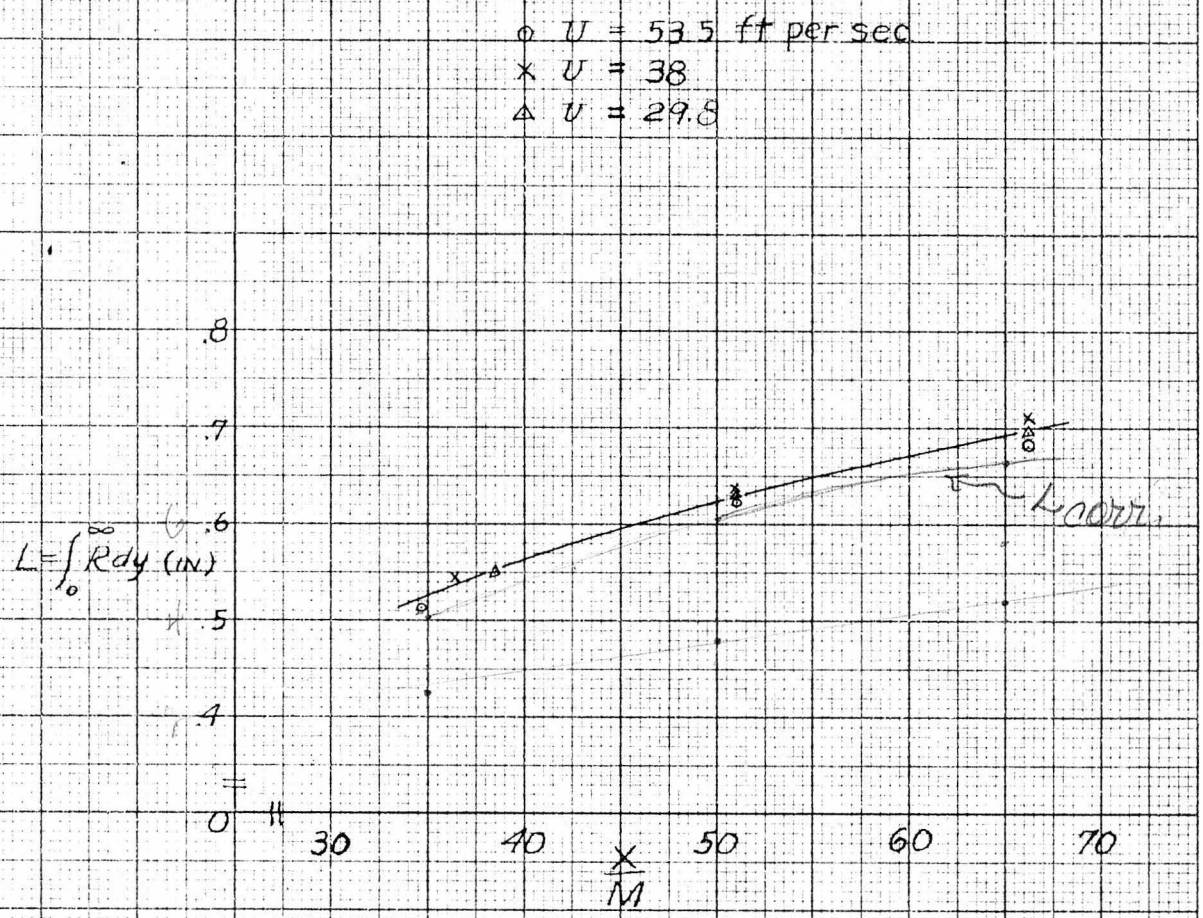

FIG 28. INCREASE OF THE SCALE OF TURBULENCE WITH $\frac{X}{M}$

GRID = 1.5 IN.

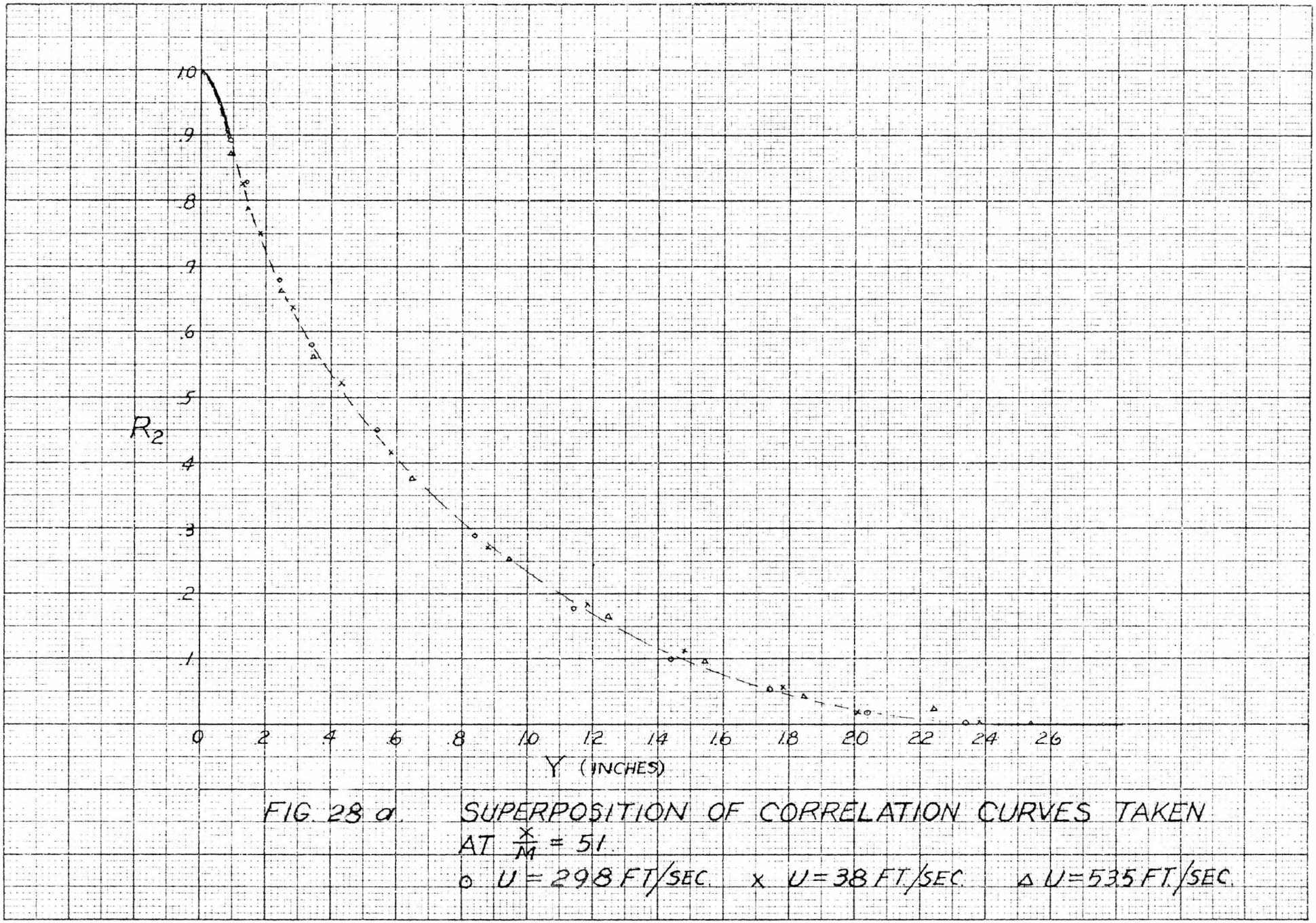

FIG. 28 a. SUPERPOSITION OF CORRELATION CURVES TAKEN AT $\frac{x}{M} = 51$

o $U = 298$ FT/SEC. x $U = 38$ FT/SEC. △ $U = 535$ FT/SEC.

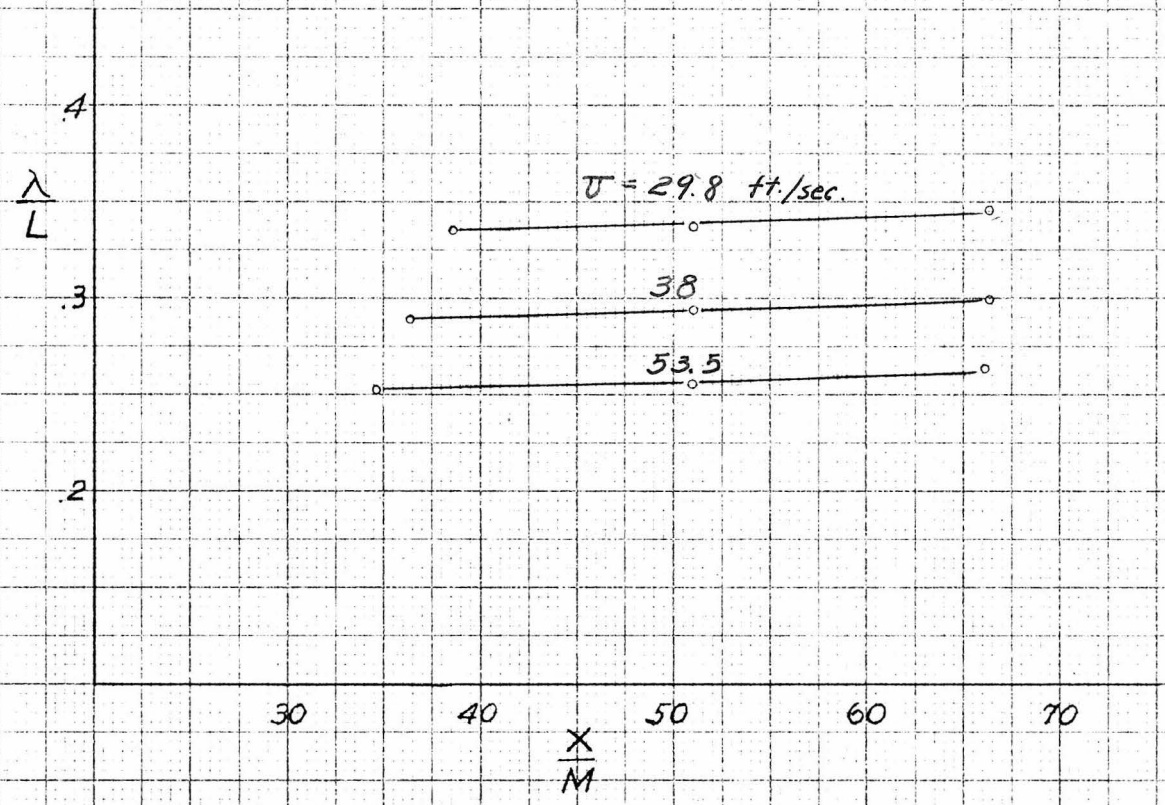

FIG. 29 VARIATION OF $\frac{\lambda}{L}$ WITH $\frac{X}{M}$

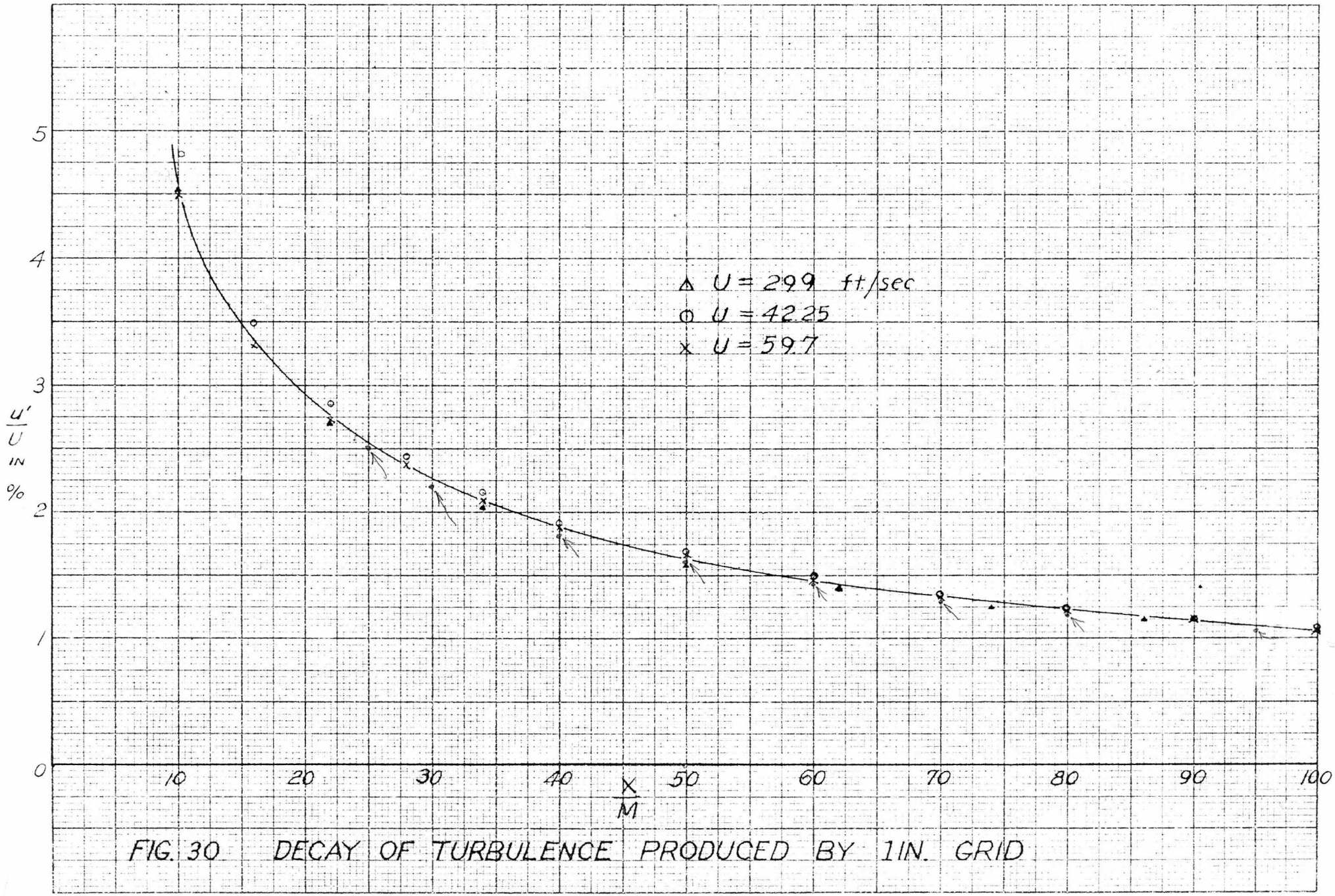

FIG. 30 DECAY OF TURBULENCE PRODUCED BY 1IN. GRID

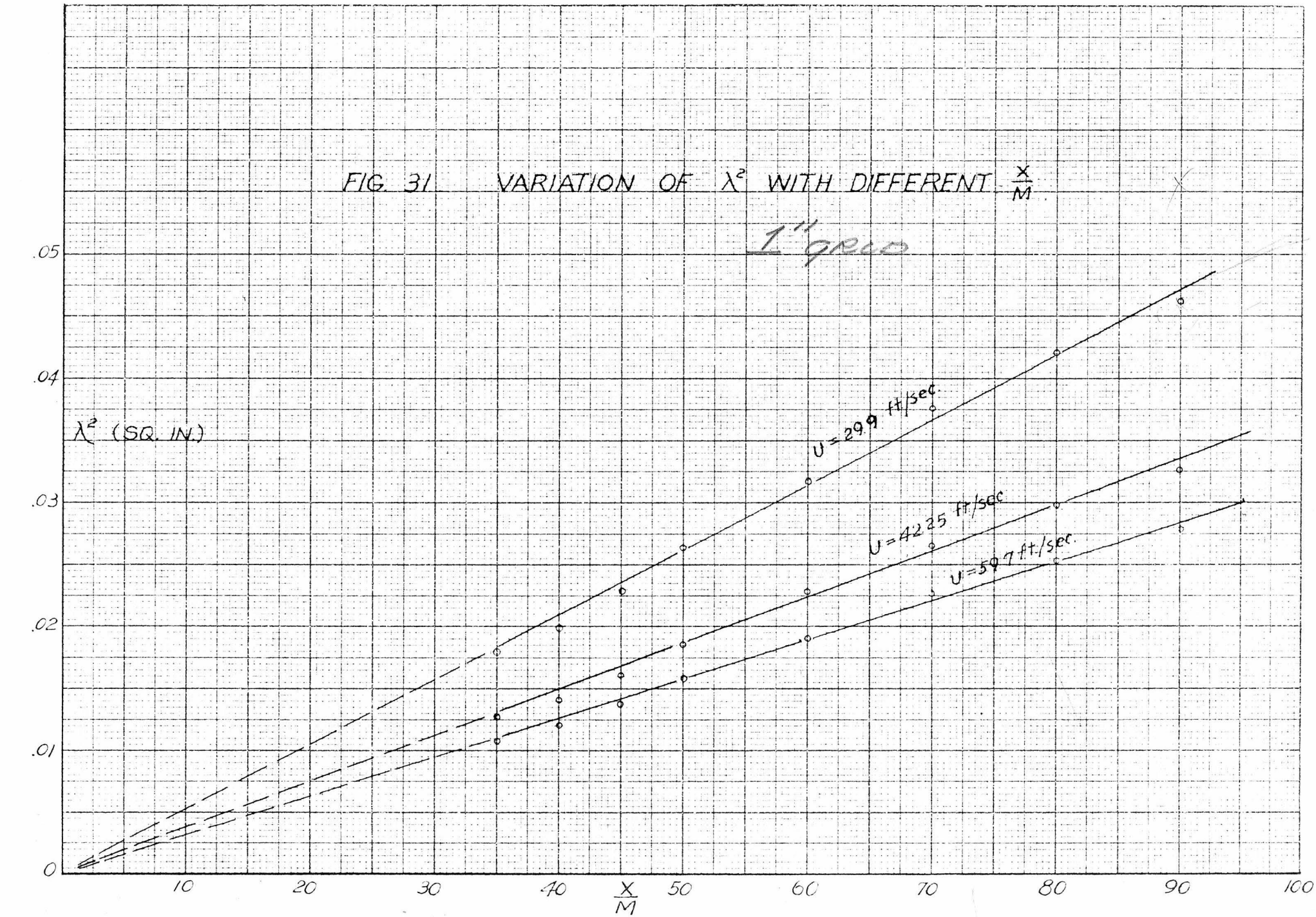
FIG. 31 VARIATION OF λ^2 WITH DIFFERENT $\frac{X}{M}$
1" grid
λ^2 (SQ. IN.)
.05
.04
.03
.02
.01
0
U = 29.9 ft/sec.
U = 42.25 ft/sec
U = 59.7 ft./sec.
10
20
30
40
50
60
70
80
90
100
$\frac{X}{M}$

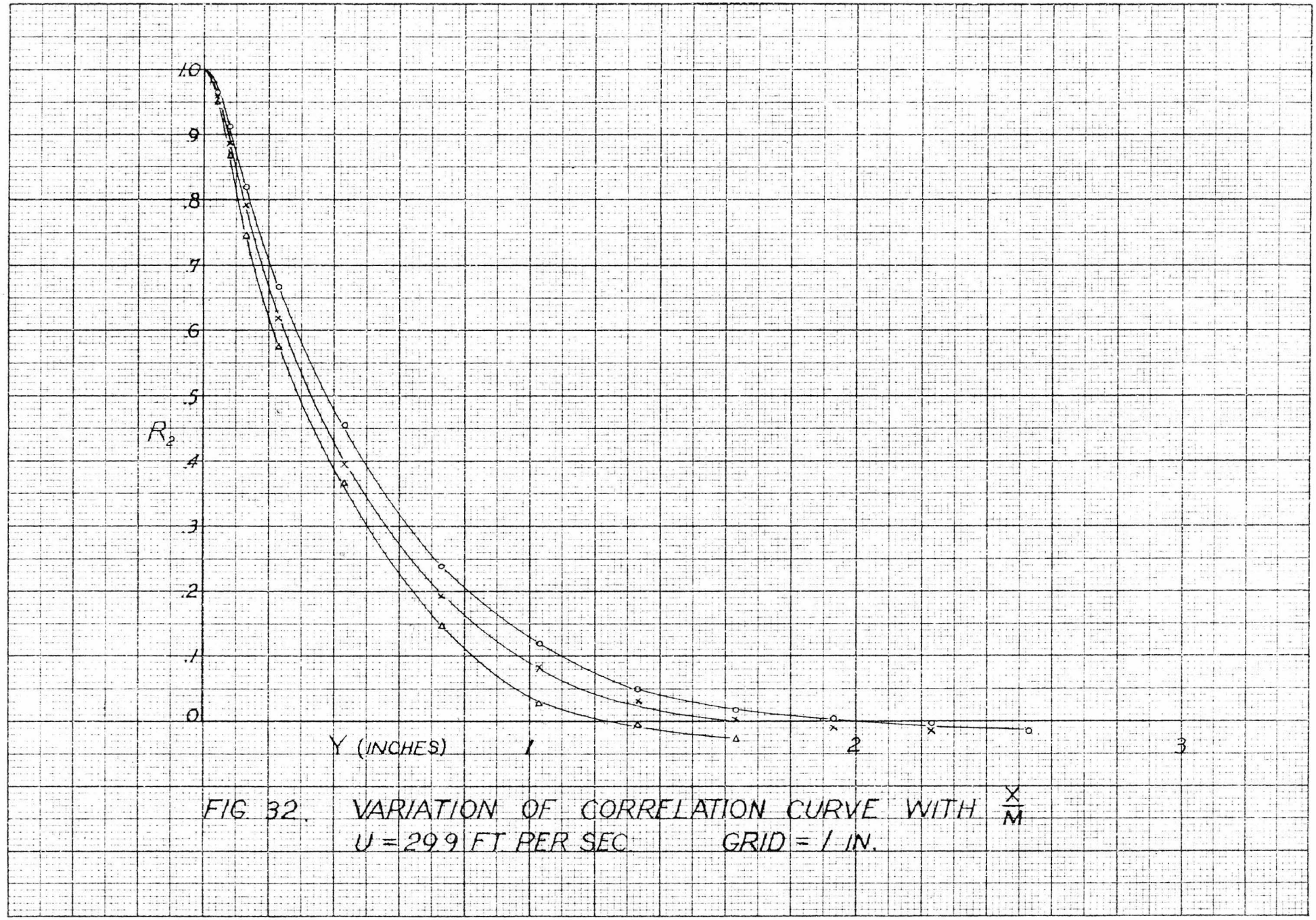

FIG 32. VARIATION OF CORRELATION CURVE WITH $\frac{X}{M}$
$U = 29.9$ FT PER SEC GRID = 1 IN.

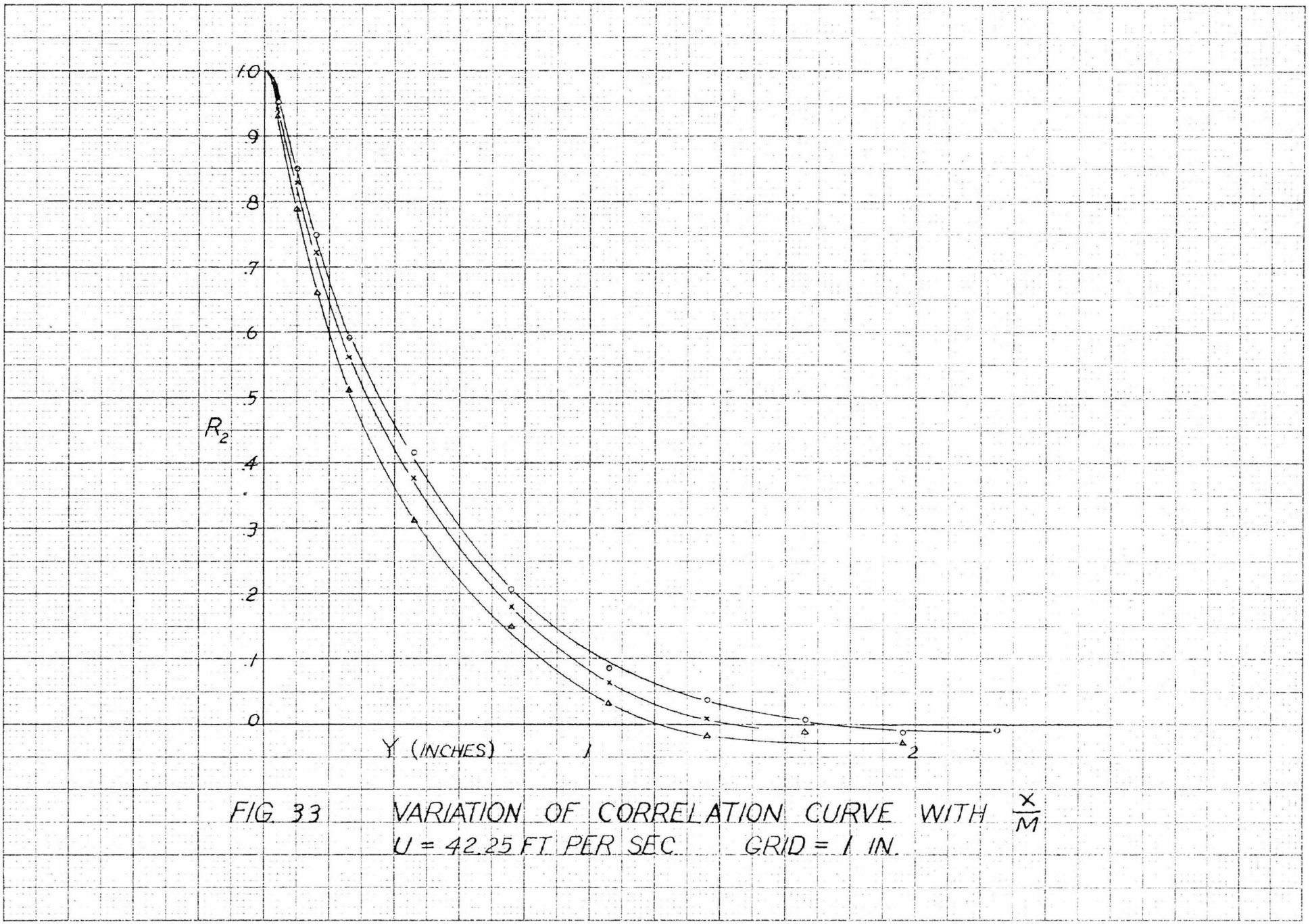

FIG. 33 VARIATION OF CORRELATION CURVE WITH $\frac{X}{M}$
U = 42.25 FT. PER SEC. GRID = 1 IN.

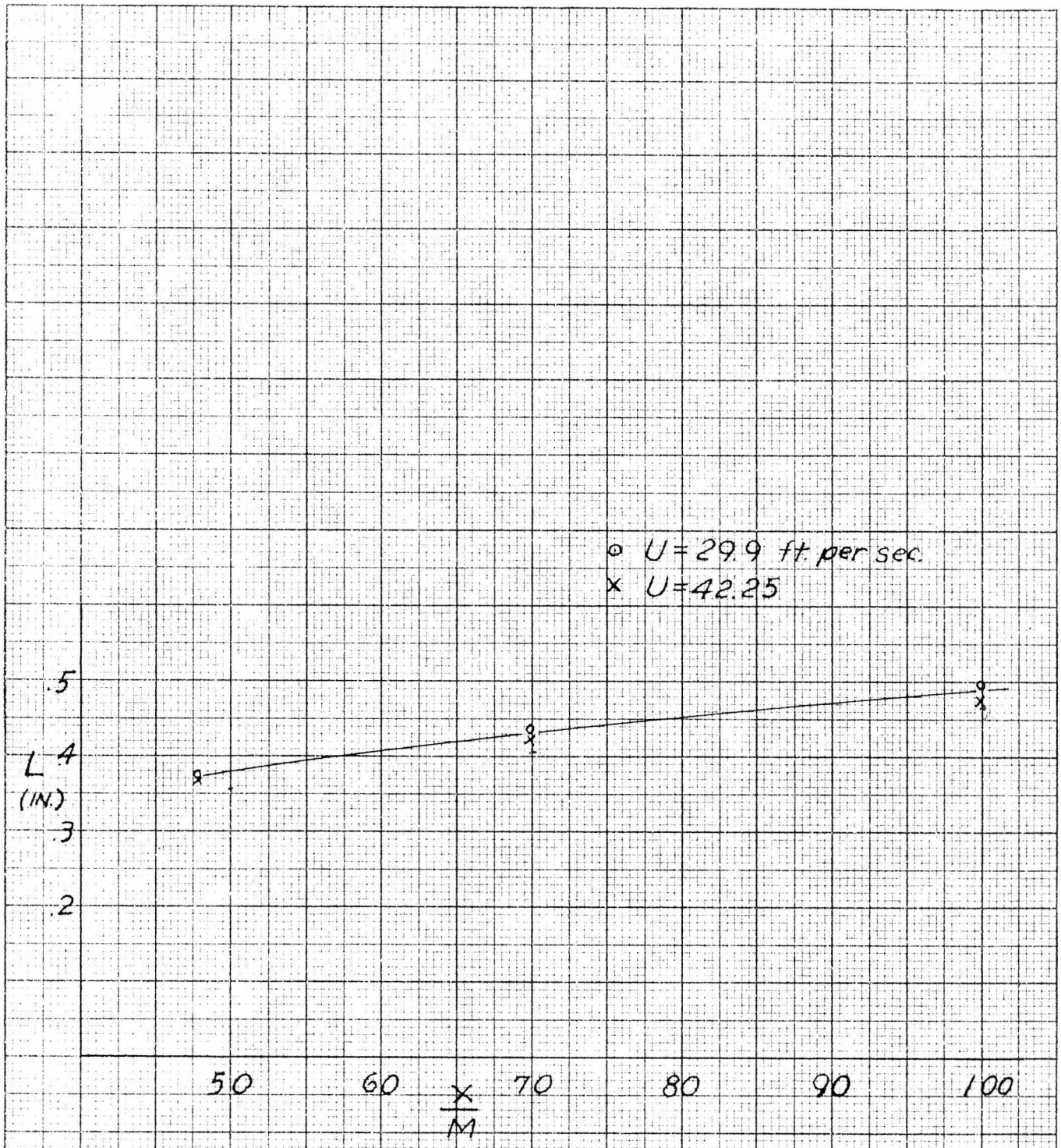

FIG 34 INCREASE OF THE SCALE OF TURBULENCE WITH $\frac{X}{M}$

GRID = 1 IN.

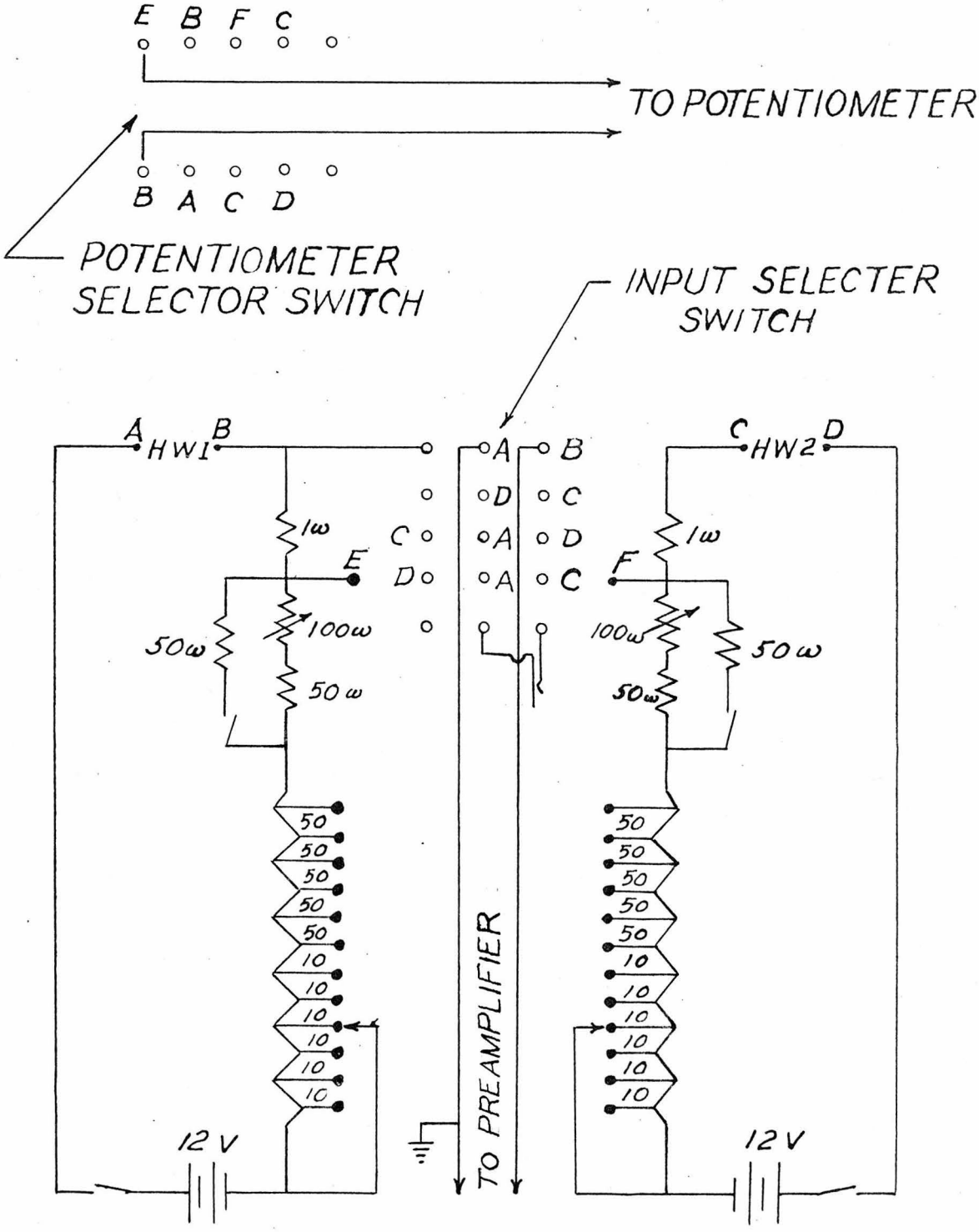

FIG. 35. INPUT CIRCUIT FOR CORRELATION AMPLIFIER

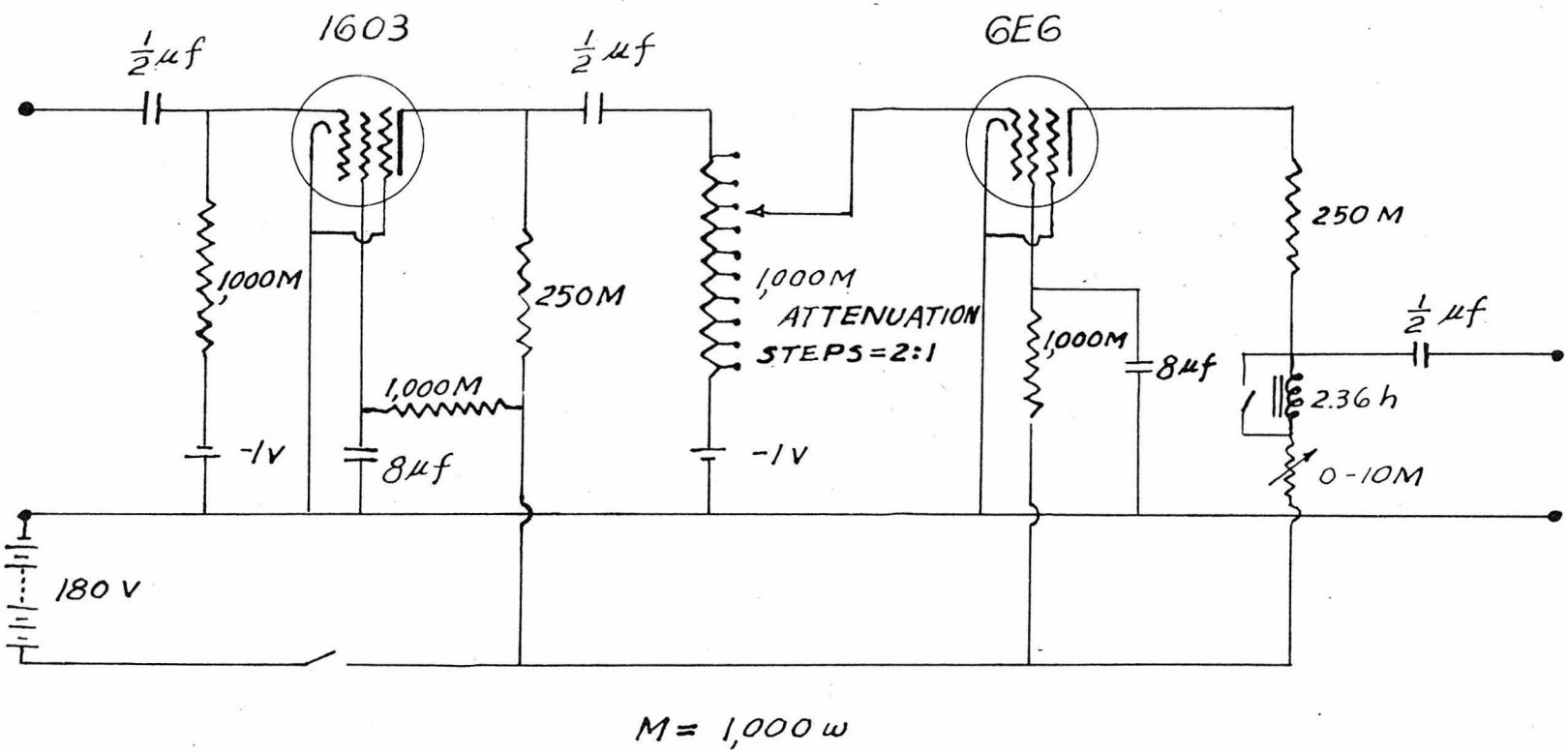

FIG. 36. PREAMPLIFIER - BATTERY OPERATED 6 VOLT FILAMENTS

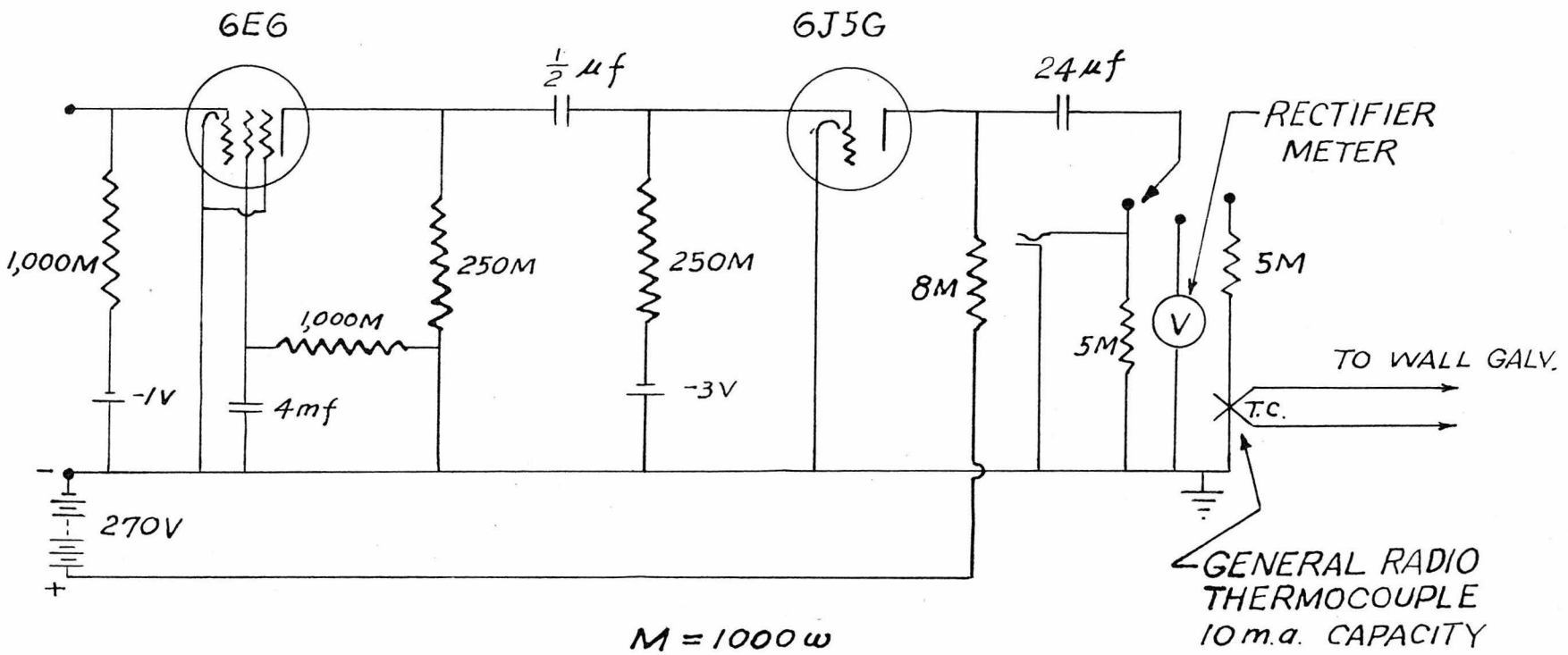

FIG. 37 POWER AMPLIFIER - BATTERY OPERATED
6 VOLT FILAMENTS

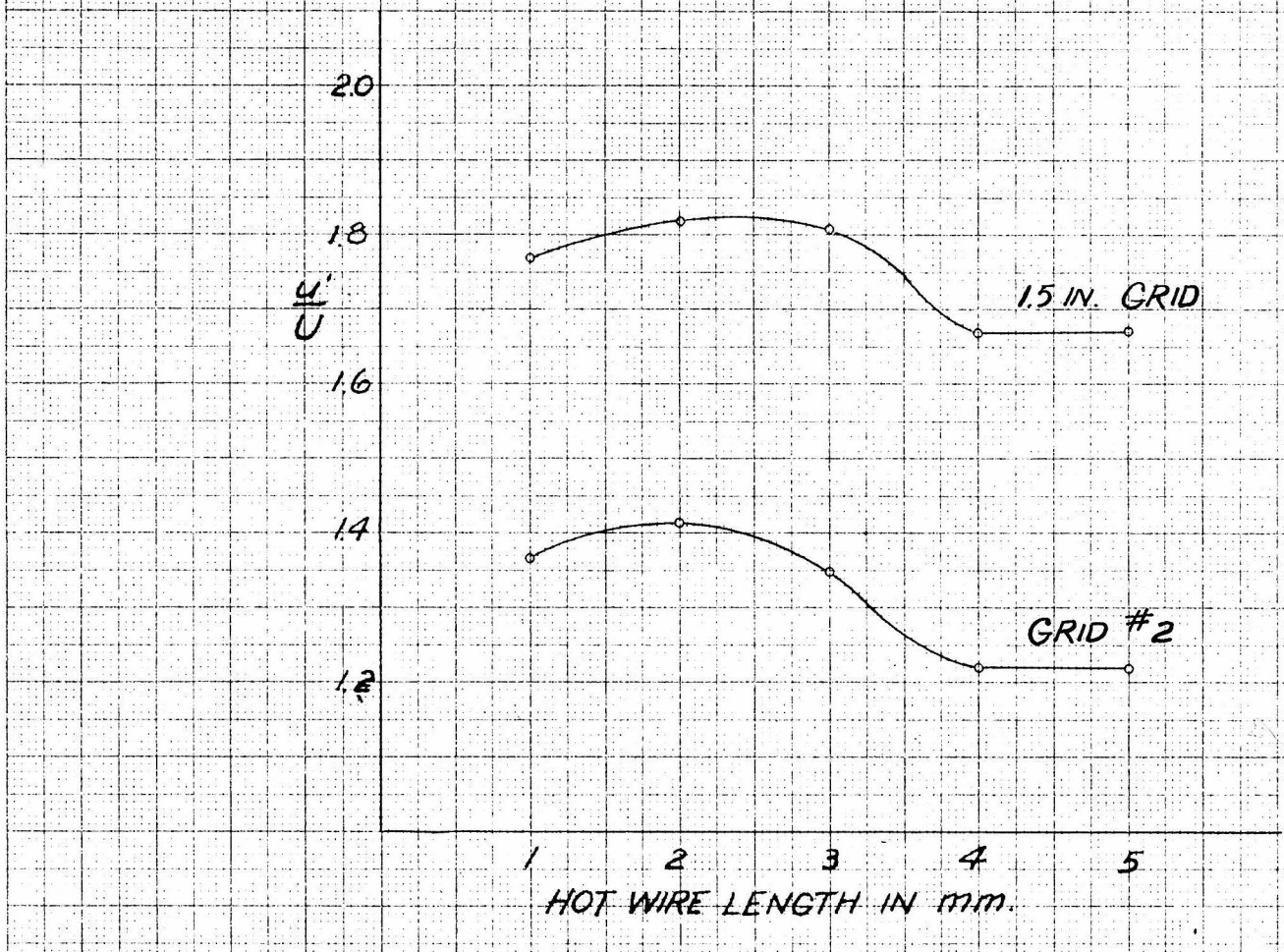

FIG. 38. EFFECT OF HOT WIRE LENGTH

TABLE 8

CALIBRATION OF HOT WIRE

U = 29.8 ft./sec. B.P. = 748 mm. T = 19 deg. C

δ = .805

f	Δ(mm.)	TAP	I^2	R_c	I
90	6	3	7	1150	2.66
180	3	3	7	1150	2.66

$$\frac{u'}{U} = \frac{2.22 \times 540 \times 10^{-3}}{9.085} = 13.22\% \quad \text{on tap 3,} \quad \text{on I = 2.66}$$

DECAY OF TURBULENCE

$\frac{X}{M}$	I_3	$\frac{u'}{U}$ (%)
10.50	1.225	6.1
13.37	.945	4.7
18.05	.795	3.95
22.10	.700	3.48
26.05	.636	3.16
30.05	.576	2.865
38.05	.500	2.49
46.10	.439	2.183
54.10	.404	2.01
62.10	.375	1.865
70.10	.351	1.745

TABLE 9

CALIBRATION OF HOT WIRE

U = 38 ft./sec. B.P. = 748.6mm. T = 21 deg. C.

ρ = .1196

f	(mm.)	TAP	I^2	R_c	I
90	6	2	6.75	1050	2.61
180	3	2	6.90	1050	

$\frac{u'}{U}$ = 10.4 % on I_2 = 2.61

DECAY OF TURBULENCE

(1.5 in. grid)

$\frac{X}{M}$	I_2	u'/U (percent)
10.80	1.55	6.17
14.085	1.2025	4.78
18.085	1.005	4.0
22.09	.876	3.49
26.09	.808	3.11
34.10	.684	2.72
42.10	.596	2.37
50.06	.552	2.20
58.10	.505	2.02
66.08	.471	1.875

TABLE 10

CALIBRATION OF HOT WIRE

U = 53.5 ft./sec. B.P. = 747.4 mm. T = 18.8 deg. C.

δ = .804 ρ = .1208

f	(mm.)	TAP	I^2	R_c	I
90	6	3	6.3	950	2.51
180	3	3	6.3	950	2.51

$\frac{u'}{U}$ = 7.37 % on I_3 = 2.51

DECAY OF TURBULENCE

(1.5 in. grid)

$\frac{X}{M}$	I_3	u'/U (percent)
10	2.096	6.15
12.76	1.815	5.325
16.65	1.47	4.32
20.70	1.279	3.76
24.65	1.192	3.5
28.65	1.06	3.11
32.65	1.00	2.93
39.3	.865	2.54
46	.813	2.39
52.6	.738	2.17
59.4	.7025	2.06
66.0	.68	1.99
72.7	.605	1.775

TABLE 11a

Correlation of turbulence produced by 1.5 in. grid

U = 29.8 ft./sec. $\frac{X}{M}$ = 38.6 B.P. = 748.2 mm.

T = 22 deg. C δ = .8055

Y (in.)	M_+	M_-	R_2
.02	20.30	0.185	.9825
.05	19.78	0.555	.947
.10	19.225	1.43	.862
.15	18.75	2.30	.781
.25	16.875	3.65	.645
.35	16.075	4.525	.560
.55	14.635	6.45	.388
.85	13.56	7.935	.2615
1.15	12.05	9.15	.1363
1.45	11.75	10.10	.0755
1.75	11.30	10.98	.01435
2.05	11.30	11.105	.0087
2.35	11.25	11.45	-.00882

TABLE 11b

Correlation of turbulence produced by 1.5 in. grid

U = 29.9 ft./sec. $\frac{X}{M}$ = 51 B.P. = 749.5 mm.

T = 17.5 deg. C. δ = .805

Y (in.)	M_+	M_-	R_2
.02	10.70	.12	.9775
.04	10.60	.20	.963
.09	10.20	.59	.891
.14	9.625	.98	.829
.24	9.10	1.725	.681
.34	8.275	2.20	.580
.54	7.725	2.925	.451
.84	6.75	3.725	.289
1.14	6.15	4.30	.177
1.44	5.80	4.75	.0995
1.74	5.60	5.025	.0542
2.04	5.35	5.15	.01905
2.34	5.475	5.45	.00275
2.64	5.30	5.40	-.00935
2.94	5.175	5.375	-.01895
3.24	5.075	5.25	-.01695

TABLE 11c

Correlation of turbulence produced by 1.5 grid

U = 29.9 ft./sec. $\frac{X}{M}$ = 66.4 B.P. = 749.5 mm.

T = 17.5°C δ = .805

Y (in.)	M_+	M_-	R_2
.02	7.8	.10	.975
.04	7.85	.16	.961
.09	7.825	.40	.903
.14	7.625	.70	.8235
.24	7.15	1.225	.703
.34	6.825	1.60	.620
.54	6.325	2.575	.422
.84	5.7	2.925	.322
1.14	5.45	3.40	.2315
1.44	5.125	3.80	.1485
1.74	4.85	4.10	.0878
2.04	4.70	4.55	.01623
2.34	4.60	4.55	.00547
2.64	4.60	4.70	.01095
2.94	4.55	4.725	.01886
3.24	4.60	4.775	.01867
3.54	4.675	4.775	.01058

TABLE 12a

Correlation of turbulence produced by 1.5 in. grid

U = 38 ft.sec. $\frac{X}{M}$ = 36.4 B.P. = 749 mm.

T = 21 deg. C. δ = .807

Y (in.)	M_+	M_-	R_2
.02	6.70	.05	.985
.04	6.65	.15	.956
.10	6.24	.55	.839
.15	6.00	.89	.742
.25	5.55	1.26	.630
.45	5.05	1.825	.469
.75	4.40	2.35	.304
1.05	4.10	2.875	.1755
1.35	3.875	3.20	.0955
1.65	3.45	3.275	.026
1.95	3.45	3.45	.000
2.25	3.45	3.50	-.0062
2.55	3.375	3.40	-.0037

TABLE 12b

Correlation of turbulence produced by 1.5 in. grid

U = 38 ft./sec $\frac{X}{M}$ = 51 B.P. = 748.3 mm.

T = 20°C δ = .806

Y (in.)	M_+	M_-	R_2
.022	8.37	.055	.987
.037	8.50	.100	.9775
.082	8.30	.400	.908
.132	7.94	.760	.826
.182	7.70	1.100	.750
.282	7.23	1.600	.638
.432	6.83	2.150	.522
.582	6.32	2.600	.4175
.882	5.70	3.270	.271
1.182	5.27	3.620	.1856
1.482	5.13	4.100	.1115
1.782	4.83	4.320	.05575
2.082	4.67	4.500	.01855
2.382	4.55	4.520	.00331
2.682	4.45	4.600	-.0166
2.982	4.52	4.55	-.0033
3.282	4.50	4.60	-.0110

TABLE 12c

Correlation of turbulence produced by 1.5 in. grid.

U = 38 ft./sec. $\frac{X}{M}$ = 66.4 B.P. = 750.4 mm.

T = 20 deg. C. δ = .806

Y (in.)	M_+	M_-	R_2
.022	6.38	.06	.970
.037	6.23	.10	.969
.082	6.10	.26	.919
.132	5.95	.475	.8525
.182	5.65	.700	.780
.282	5.40	1.070	.670
.432	5.10	1.450	.5575
.582	4.92	1.730	.480
.882	4.25	2.300	.298
1.182	4.00	2.570	.218
1.482	3.70	2.930	.116
1.782	3.60	3.130	.0698
2.082	3.55	3.220	.04875
2.382	3.40	3.250	.02255
2.682	3.40	3.300	.0149
2.982	14.00	14.330	-.0180
3.282	13.42	14.720	-.01655

TABLE 13a

Correlation of turbulence produced by 1.5 in. grid.

U = 53.5 ft. per sec. $\frac{X}{M}$ = 34.7 B.P. = 748.2 mm.

T = 19.5 deg. C. δ = .806 ρ = .12075

Y (in.)	R_2
.02	.982
.045	.938
.070	.907
.095	.849
.145	.759
.245	.623
.445	.4475
.745	.269
1.045	.1625
1.345	.07575
1.645	.0465
1.945	.00375
2.245	-.00833
2.545	-.0264
2.845	-.0201
3.100	-.0154
3.400	-.0124

TABLE 13b

Correlation of turbulence produced by 1.5 in. grid.

U = 53.5 ft. per sec. $\frac{X}{M}$ = 50.85 B.P. = 749.6 mm.

T = 19 deg. C. δ = .805

Y (in.)	R_2
.02	.997
.045	.973
.095	.874
.145	.789
.245	.663
.345	.56
.645	.375
.945	.255
1.245	.1665
1.545	.975
1.845	.414
2.245	.2695
2.545	0
3.445	-.01425
3.645	-.01434
3.945	-.0186

TABLE 13c

Correlation of turbulence produced by 1.5 in. grid.

U = 53.5 ft. per sec. $\frac{X}{M} = 66.2$ B.P.= 747.3 mm.

T = 20 deg. C.

Y (in.)	R_2
.02	.975
.045	.958
.095	.873
.145	.806
.245	.695
.445	.543
.745	.361
1.045	.262
1.345	.1686
1.645	.0978
1.945	.06025
2.545	.00346
2.845	-.00733
3.145	-.0281

TABLE 14

THE DECAY OF TURBULENCE PRODUCED BY 1 IN. GRID

($\frac{1}{4}$ IN. DOWEL)

B = 747.1 mm. T = 20 deg. C. δ = .805 ρ = .1204

Wollaston H.W. length ~ 2 mm. (.0005 in. diam.)

U = 29.9 ft. per sec.

X (in.)	u/U (percent)
10.25	4.5
16	3.32
22	2.725
28	2.363
34	2.09
40	1.885
50	1.665
60	1.464
70	1.336
80	1.244
90	1.15
100	1.05
110	1.013

TABLE 15

THE DECAY OF TURBULENCE PRODUCED BY 1 IN. GRID

($\frac{1}{4}$ IN. DOWEL)

B = 747.1 mm. T = 20 deg. C. β = .805 ρ = .1204

Wollaston H.W. length ~ 2 mm. (.0005 in. diam.)

U = 42.25 ft. per sec.

X (in.)	u'/U (percent)
10.25	4.82
16	3.5
22	2.86
28	2.45
34	2.16
40	1.924
50	1.692
60	1.495
70	1.353
80	1.243
90	1.15
100	1.08
110	1.02

TABLE 16

THE DECAY OF TURBULENCE PRODUCED BY 1 IN. GRID

($\frac{1}{4}$ IN. DOWEL)

B = 748.7 mm. T = 19 deg. C. δ = .805 ρ = .121

Wollaston H.W. length ~ 2 mm. (.0005 in. diam.)

U = 59.7 ft. per sec.

X (in.)	u'/U (percent)
10.25	4.53
22	2.71
34	2.025
50	1.575
62	1.395
74	1.24
86	1.145
100	1.06
110	.98

TABLE 17a

Correlation of turbulence produced by 1 in. grid.

U = 30 ft./sec. $\frac{X}{M} = 47.875$ B.P. = 747 mm.

T = 23 deg. C. $\rho = .119$

$\frac{X}{M}Y''$	M_+	M_-	R (percent)
.02	13.985	.15	98.00
.04	13.525	.35	95.00
.08	12.975	.925	86.75
.13	12.100	1.775	74.50
.23	11.300	3.075	57.50
.43	10.00	4.65	36.50
.73	8.220	6.125	14.65
1.03	7.075	6.70	2.72
1.33	6.925	7.00	-0.538
1.63	6.925	7.30	-2.735

TABLE 17b

Correlation of turbulence produced by 1 in. grid.

U = 30 ft./sec. $\frac{X}{M}$ = 69.875 mm. T = 22.2 deg. C.

ρ = .1195

Y (in.)	M_+	M_-	R (percent)
.02	7.225	.08	97.9
.04	7.50	.15	96.0
.08	7.00	.425	88.7
.13	6.925	.80	79.3
.23	6.15	1.45	61.9
.43	5.475	2.375	39.5
.73	4.50	3.05	19.2
1.03	4.25	3.600	8.25
1.33	3.95	3.70	3.27
1.63	3.80	3.825	0.328
1.93	3.725	3.85	-0.99
2.23	3.725	3.825	-1.325

TABLE 17c

Correlation fo turbulence produced by 1 in. grid.

U = 30 ft./sec. $\frac{X}{M}$ = 99.875 B.P. = 746.5 mm.

T = 22.2 deg. C. ρ = .1195

Y (in.)	M_+	M_-	R (percent)
.02	21.8	.2	98.25
.04	21.25	.375	96.50
.08	20.7	.95	91.25
.13	19.6	1.95	82.00
.23	18.05	3.75	65.65
.43	16.00	6.00	45.00
.73	13.725	8.40	24.05
1.03	12.30	9.65	12.06
1.33	11.25	10.30	4.40
1.63	10.85	10.50	1.64
2.23	10.275	10.35	-0.363
2.53	10.275	10.60	-1.555

Photo 1

Wind Tunnel

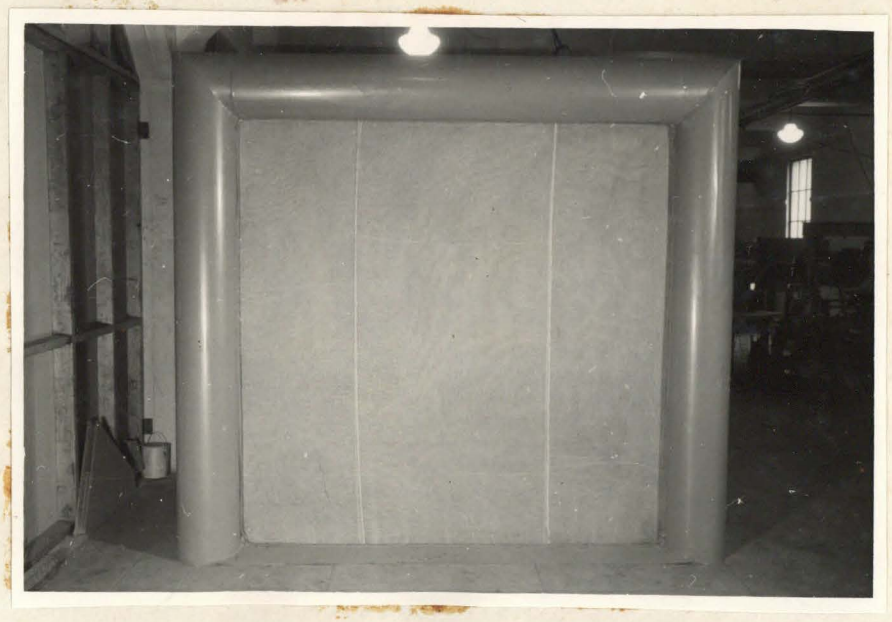

Photo 2

Front View of The Entrance

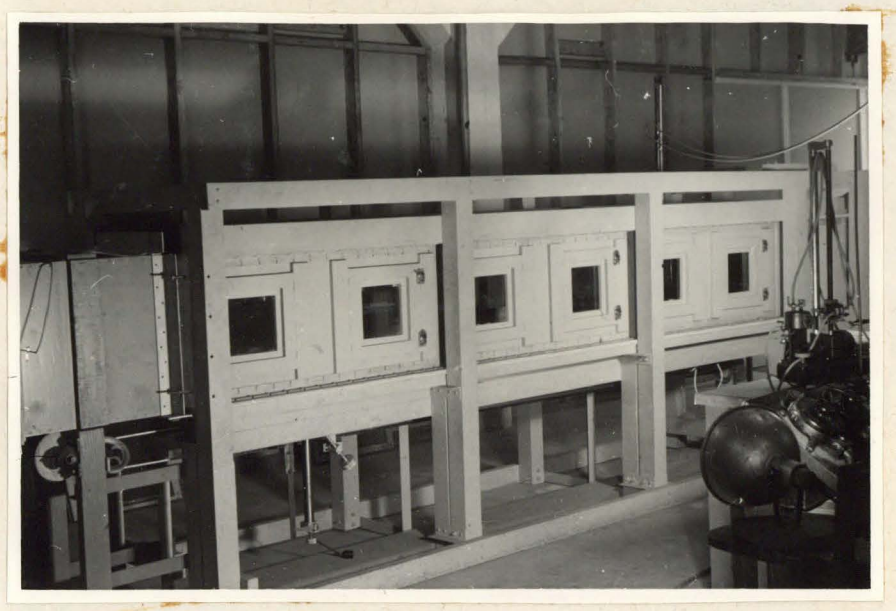

Photo 3

Working Section

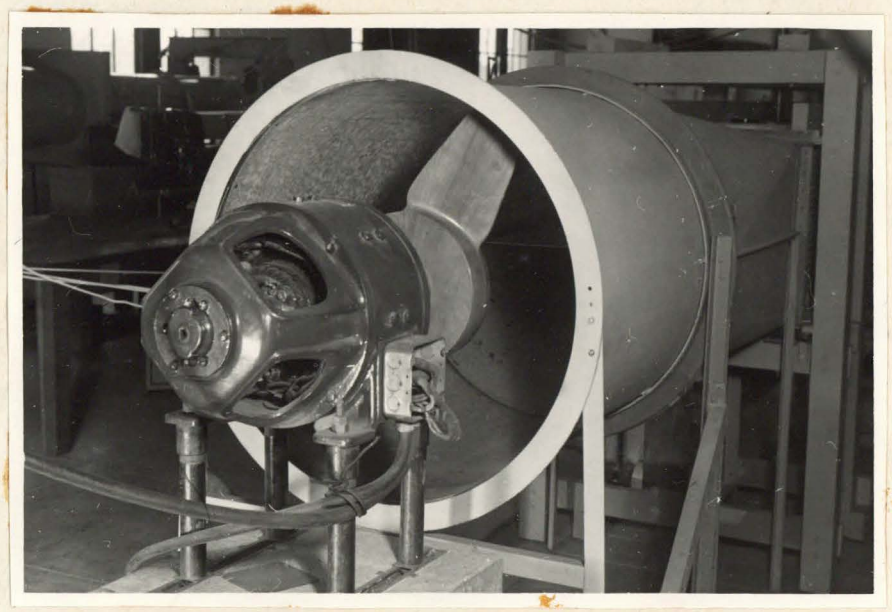

Photo 4

Diffuser and Propeller with Motor

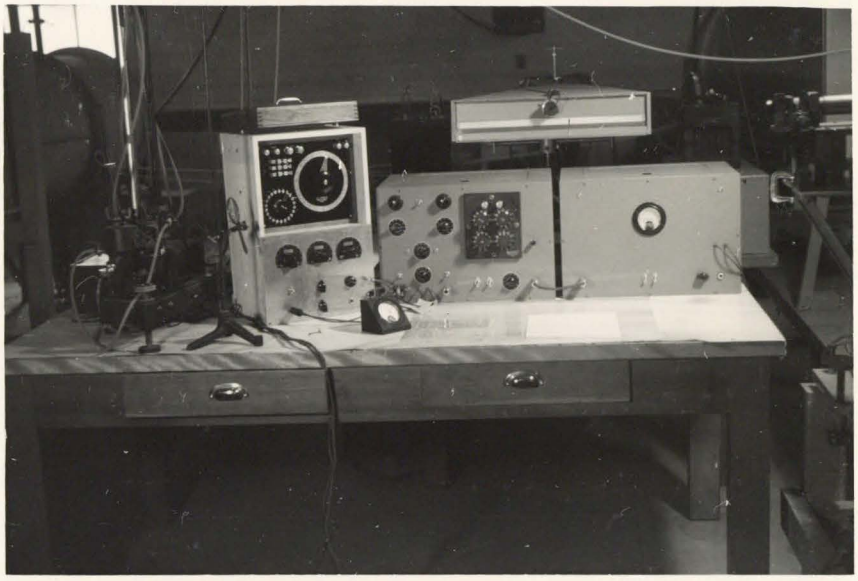

Photo 5

Potentiometer, Hot-Wire Amplifier, and Galvanometer

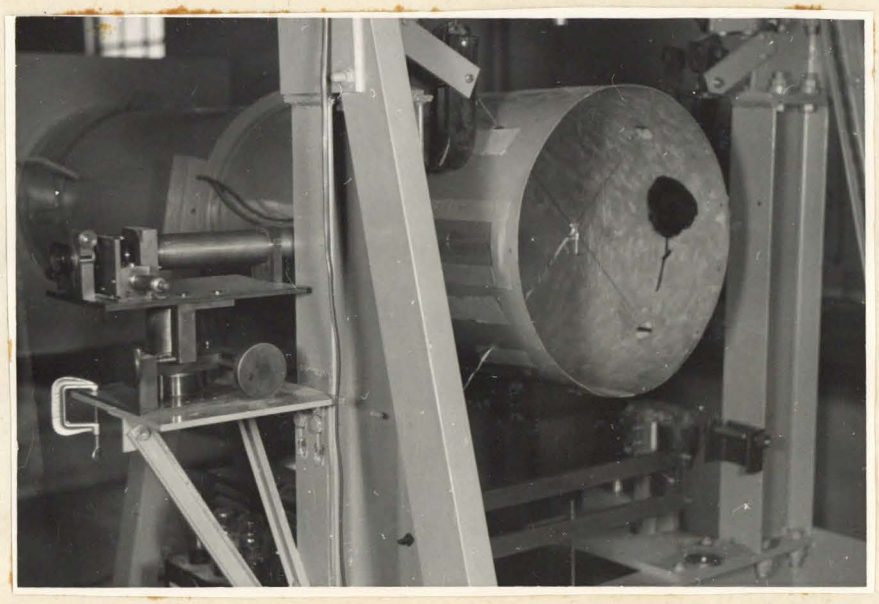

Photo 6

Calibrating Tunnel

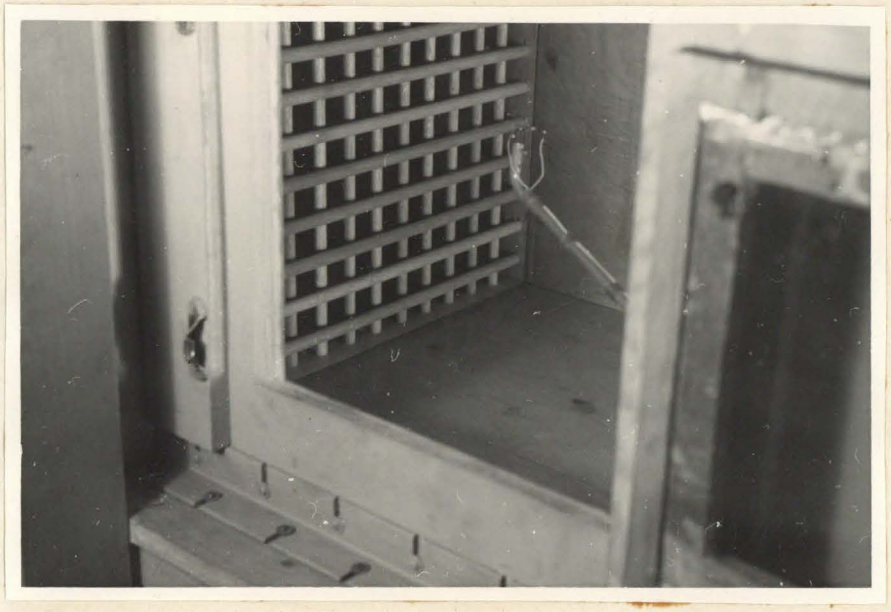

Photo 7

Hot Wire Behind The Turbulence Producing For The Measurements Of The Decay.

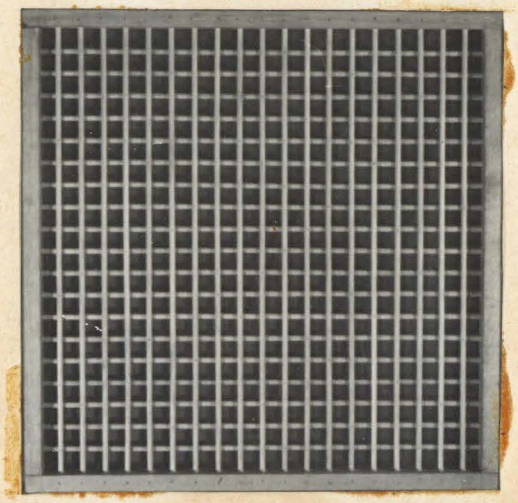

Photo 9. 1 in. Grid

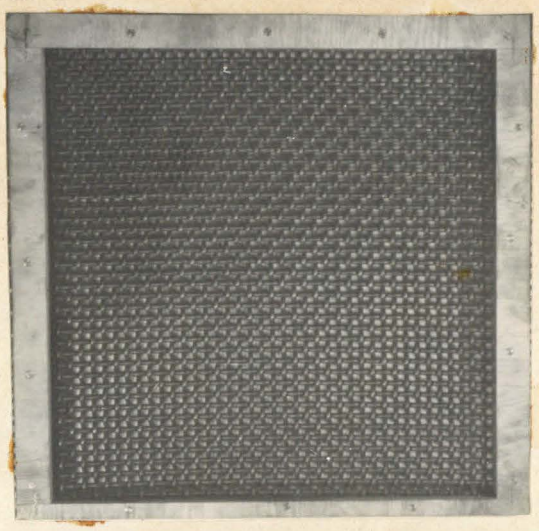

Photo 10. Grid No. 1

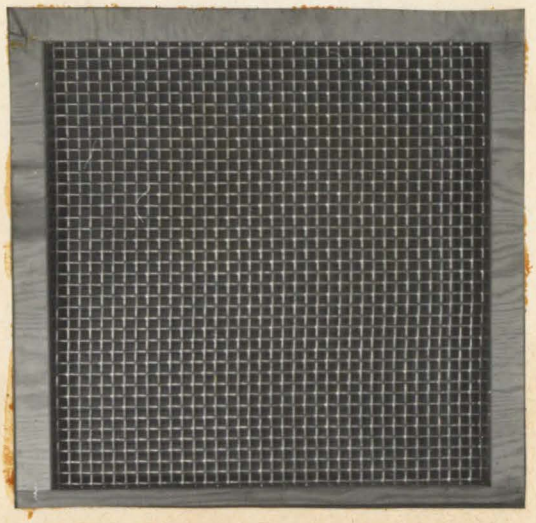

Photo 11 Grid No. 3

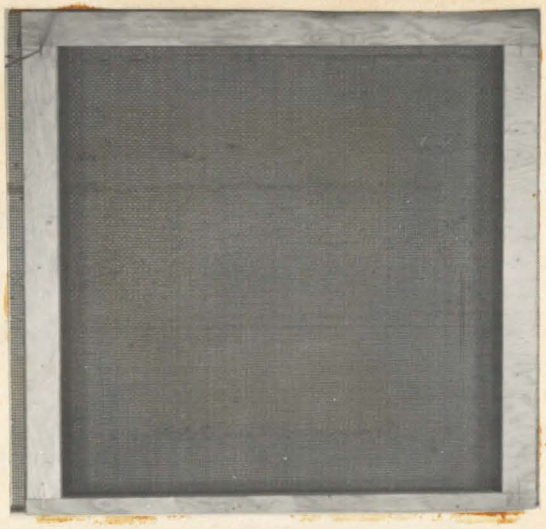

Photo 12. Grid No. 4

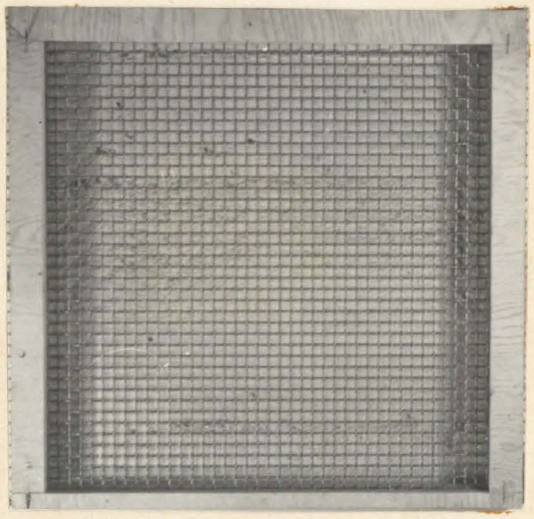

Photo 13. Grid No. 2